CHALMERS

Model Based Approach to Supervision of Fast Charging

Master of Science in Power Engineering

SHEMSEDIN NURSEBO

Department of Energy and Environment
Division of Power Engineering
CHALMERS UNIVERSITY OF TECHNOLOGY
Göteborg, Sweden, 2010

Model Based Approach to Supervision of Fast Charging

SHEMSEDIN NURSEBO

Performed at ABB Corporate Research

Examiner: Professor Torbjön Thiringer
Department of Energy and Environment
Division of Electric Power Engineering
Chalmers University of Technology

Supervisor: Dr. Hector Zelaya
ABB Corporate Research
Västerås, Sweden

Department of Energy and Environment
Division of Electric Power Engineering
CHALMERS UNIVERSITY OF TECHNOLOGY
Göteborg, Sweden, 2010

Model Based Approach to Supervision of Fast Charging

SHEMSEDIN NURSEBO
Department of Energy and Environment
Division of Electric Power Engineering
Chalmers University of Technology

Abstract

Due to various economic, political and environmental reasons, the introduction of electric vehicles (EVs) into the streets is probable. Their introduction will require extra facilities such as the charging stations. In order for EVs to be able to penetrate the market their recharging/ refueling time should be comparable to conventional once. This results in charging stations supplying hundreds of amps to EV batteries. The usual trend in charging EV batteries is that the BMS (Battery Management System) gives various orders and information signals and the charger acts as a slave in the system. But this could result in a dangerous situation if the BMS happens to fail for some reason. Thus in this report a supervisory algorithm is investigated. It is based on modeling the important characteristic of the battery and then identifying suitable model parameters. Then these models are effectively used during decision making in the battery charging process.

The results of this report show that:

- Model based approach to supervision of battery fast charging provides a satisfactory result
- Battery voltage monitoring through prediction could be used to avoid overvoltage on battery terminals. While SOC models could be used to predict the SOC steps ahead but its use is not that important. Similarly temperature prediction in normal situation is less important as the rate of change of temperature in very low. But temperature prediction could be valuable when the rate of temperature rise is high for some reason.
- Temperature and state of charge models can effectively be used to validate the corresponding readings from the BMS.
- At the present state the algorithm is relatively prone to noise levels in the working environment which could be improved in future works.

Acknowledgement

After all the supports I get from the peoples around me to make this thesis a success, it is my pleasure to use this opportunity to acknowledge their valuable inputs. First of all, I am highly grateful to my supervisor Hector for his interest in me to work on this thesis and for his constant guidance during the whole project. It is also worthy of mentioning the efforts of other staffs in ABB corporate research to make my stay at ABB enjoyable. It will be unfair not to mention the positive response, valuable information and guidance provided by Jens Groots on batteries.

It is my pleasure to value the supports provided by my friends Mebratu, Thinley, Jemal, Khalid and Bereket among many others during my stay at Chalmers. They really have made my stay possible as well as enjoyable. Of course, the overall Chalmers community deserves my gratitude for its well coordinated system. And I am always indebted to my family for their unconditional support. Thank you God for all blessings you have bestowed on me.

Last but not least, I highly appreciate the guidance and feedback provided by my examiner Torbjön.

Shemsedin Nursebo

List of abbreviations

BMS	Battery Management System
HEV	Hybrid Electric vehicle
EV	Electric vehicle
PHEV	Plug-in Hybrid Vehicle
xEV	Hybrid ,plug-in hybrid and Electric vehicle,
USABC	U.S. Advanced Battery Consortium
EPRI	Electric Power Research Institute
MIT	Sloan automotive Laboratory at Massachusetts Institute of Technology
NiMH	Nickel metal Hydride
NiCd	Nickel Cadmium
Li-ion	Lithium ion
CC/CV	Constant current/Constant voltage
LM	Levenberg-Marquardt
AC	Alternating current
DC	Direct current
THD	Total Harmonic Distortion
CCM	Continuous conduction mode
DCM	Discontinuous conduction mode
VSC	Voltage source converter
PWM	Pulse width Modulation
DSP	Digital signal processor
V-I	Voltage-current
RCGR	Reference Current generating Routine
MCGR	Minimum Current Generating Routine
TMR	Temperature monitoring Routine
SOCMR	State of Charge Monitoring Routine
BVMR	Battery Voltage Monitoring Routine
MPIR	Model Parameter Identification Routine
SA	Supervisory Algorithm

TABLE OF CONTENTS

1 INTRODUCTION

1.1 Purpose

Owing to different political, economic and environmental reasons the introduction of electric vehicles (EVs) into the streets is unavoidable. Parallel to their introduction the infrastructure that supports them needs considerable attention. One of the main components of this infrastructure besides the grid is the charging station.

In order for EVs to be considered as an alternative their refueling/recharging time should match or be near to their IC engine counter parts. This demands fast charging stations which provide, depending on the vehicle type, hundreds of amps to vehicle batteries. Table 1.1 below shows the power requirements in different fast charging approaches for different vehicle types.

Table 1.1 different fast charging power requirements **[1]**

Type of Charging	*Charging duration*	*Charges up to (SOC)*	***Charger Power Level. kW***		
			Heavy Duty	**SUV/Sedan**	**Small Sedan**
Fast Charge	10 minutes	100%	**500**	**250**	**125**
Rapid Charge.	15 minutes	60%	**250**	**125**	**60**
Quick Charge.	60 minutes	70%	**75**	**35**	**20**
Plug-In Hybrid.	30 Minutes		**40**	**20**	**10**

As can be seen from the table the power demand is very high which needs special consideration both in charging system and in safety issues. To this end, there are a couple of companies working on charging infrastructure. Table 1**.2** provides the ratings of the charging station a few of these companies are providing (taken from their respective sites).

Table 1.2 charging station ratings as provided by their respective providers

Company	AC charging output	DC charging
ABB	-	50-250KW
Aerovironment	208VAC to 240VAC @ 30A	30-250KW @480V 3-ph lines
Aker wade	16A, 32A and 63A	36 kW and 50 kW
Coulomb Technologies	230V/16A(level I) 230V/32A (3 phase)(Level II)	-
Elektromotive	240V/20Amps	-

The usual trend in off-board battery chargers, however, is a master-slave approach where the BMS demands a current and the charger supplies the current. The BMS has of course better knowledge and information about the battery, than for instance an off-board charger. However if the BMS happens to malfunction for any reason, considering the sensitivity of the batteries to overcharging, there will be a disaster that nobody wants to undertake.

Thus the purpose of this thesis is adding intelligence to the battery chargers which insures safe charging even if the BMS happens to malfunction. It will also act as a supervisory system to warn or avoid accidents. These tasks require

- A tangible way of finding if the BMS is working inappropriately
- An internal algorithm that calculates the safe charging current and the duration of charging if the BMS is not working properly.
- Also the supervisory algorithm needs to interact with the converter controller; hence it is important to understand how it works. Thus some discussion on the converter is included.

1.2 Scope

This report describes the modeling and identification the battery system based on which a supervisory algorithm is developed. The supervisory algorithm developed for the battery charging system works only under the assumptions described thought the report in different places.

1.3 Structure

The report has the following structure:

Section 1: Introduction (this section) describes the purpose and scope for this report.

In section 2 a brief discussion of the battery types which could be used in EVs as well as plug in hybrid vehicles (PHEVs) are provided. The main concern there is

- How large batteries are required for each vehicle type?
- What is the state of art batteries for EVs?
- What is their characteristic in terms of charging? What is the charging strategy recommended by their respective manufacturers?
- Which are the charge monitoring techniques that are recommended for each battery type?

Answering these questions will clear the way for decisions to be taken in the algorithm to be developed!

The core of any algorithm development is decision making. The approach used in this thesis for decision making is model based approach. Thus in section 3 various models which facilitate decision making are discussed. These include:

- Simplified battery model for predicting battery terminal voltage steps ahead
- State of charge reading validating and predicting model
- Temperature reading validating and predicting model

These models will, however, be committed to their responsibility only when they are equipped with the correct parameters. Otherwise only general information is available about batteries. This information is far way behind to equip the model parameters with correct values beforehand. Hence section 4 is devoted to an investigation of identification algorithms which will be executed on line for each battery to be charged. The identification algorithm used in the thesis is bounded Levenberg-Marquardt method.

Section 5 is added for sake of understanding how the converter is working in order to have a clear idea how it may affect the proposed algorithm. Hence, there a typical battery charger circuit is discussed; some analysis of a three phase AC/DC converter and buck-boost DC/DC converter is provided.

Section 6 describes

- The charge monitoring algorithm
- The assumptions in selection of the algorithm
- Implementation issues related with algorithm

Section 7 provides the result and analysis of the proposed algorithm in Matlab simulation

Section 8 provides the conclusion the report.

Section 9 lists future works that could be done based on this work.

Section 10 is appendix

Section 11 references specifies source material and further reading.

2 BATTERY TECHNOLOGIES

When we consider an intelligent charger, or charging in general, understanding the characteristic of the batteries to be charged is indispensable. Knowing the capacity of the batteries to be charged also needs considerable attention. However there are comparatively only few such cars on the road. Thus finding any tangible information on this topic is not easy. Thus we need to find an alternative solution. To that end there are three most noticeable bodies working on EV related issues. These are USABC[1], EPRI[2] and MIT[3]. Accordingly these bodies have specifications on the battery requirements for different xEVs type as shown in **Fel! Hittar inte referenskälla.**. Based on this it is possible to evaluate currently available battery types for possible xEV use. Of course, the same is provided by them.

Table 2.1 Battery goals for different PHEVs [2]

Vehicle assumption	units	USABC			MIT	EPRI		
		PHEV	PHEV	EV[7]	PHEV	PHEV	PHEV	EVs[3]
CD[4] range	miles	10	40		30	20	60	
CD Operation		All electric	All electric		blended	All electric	All electric	
Depth of discharge (DoD)	percent	70%	70%	80%	70%	80%	80%	
Body type		Cross. SUV	Mid. car		Mid. car	Mid. car	Mid. car	
Battery goals								
Peak power	kW	50	46		44	54	99	75-100
Peak power density (2sec pulse)	kW/kg	830	380	300(30 sec)	730	340	330	300-400
Total energy capacity	kWh	6	17	40	8	6	18	25-40
energy density	kWh/kg	100	140	150(@ C/3 discharge rate)	130	40	60	100-140

[1] U.S. Advanced Battery Consortium (USABC)
[2] Electric Power Research Institute
[3] Sloan Automotive Laboratory at MIT
[4] Charge depletion

From the table, EPRI's analysis suggests the performance goals for an *all-electric* PHEV-20 is achievable by current NiMH technology, the goals of the USABC and MIT are beyond even current Li-Ion technology capabilities. In any case, it is clear that lead acid, nickel-Cadmium (Ni-Cd) and sodium-nickel chloride (ZEBRA) technologies are not likely to achieve goals for even the less ambitious PHEVs. In contrast, Li-Ion battery technologies hold promise for achieving much higher power and energy density goals [2].

Thus, it appears that while NiMH could be used for lower performance PHEV designs (e.g. *blended* operation with lower CD range); only a chemistry with the energy and power density capabilities of Li-Ion can meet USABC goals for PHEVs with *all-electric* range [2]. Thus in this thesis focus is given only to Li-ion and NiMH batteries. In the following sections we will briefly look at the state of the art NiMH and Li-ion batteries and charging related issues.

2.1 Nickel-Metal Hydride cell (NiMH)

Compared to other battery chemistries, the primary advantage of NiMH is its proven longevity in calendar and cycle life, and overall history of safety. However, the primary drawbacks of NiMH are limitations in energy and power density, and low prospects for future cost reductions. As it has reached its maturity there is little room left for improvement in power and energy density or cost. Thus NiMH batteries could play an interim role in less demanding blended-mode designs, but it seems likely that falling Li-Ion battery prices may preclude even this role [2].

2.1.1 State of the art NiMH batteries

As with any battery type, NiMH batteries are either energy or power optimized. Most of high power NiMH batteries are intended for application in full and moderate to mild HEVs [3]. They are not our concern here and we will focus on high energy and medium energy/power NiMH batteries. Table 2.2 provides state of the art high energy and medium energy/power NiMH batteries.

Table 2.2 Characteristics of currently available NiMH batteries (high energy and medium energy/power design cells and modules) **[3]**

manufacturer	SAFT	COBASYS		VARTA	
Cell capacity(Ah)	100[5]	85[5]	43[6]	45[6]	25[6]
Module voltage(V)	12	12	12	5(4.8)	5(4.8)
Specific energy(Wh/kg)	69	60	45	50	35
Specific power(W/Kg)	160[7]	200[7](250)[8]	605[7]	400	700[7]

[5] High energy design
[6] Medium energy/power design
[7] At 80% DOD
[8] At 50% DOD

The high energy NiMH battery design of COBASYS has specific energy and specific power characteristics which do not meet the requirements shown in **Fel! Hittar inte referenskälla.** for a midsize EV.

The medium energy/power designs of COBASYS and VARTA were developed to have much higher specific power levels, now meeting PHEV specific power requirements. Their specific energies of around 45 Wh/kg are close to meeting minimum requirements for PHEVs, implying only small (COBASYS) or modest (VARTA) weight penalties for PHEV batteries of the required storage capacities.

Data detail on SAFT's product sheet indicates a high probability for substantially longer cycle life. After 1500 discharges, battery storage capacity is shown to have declined by less than 2%, and the internal resistance (essentially the inverse of specific power) increased by only 15% [3].

2.1.2 Charging performance

Figure 2-1 shows how voltage, temperature and pressure vary as charging progresses. The voltage spike up on initial charging then continues to rise gradually through charging until full charge is achieved. Then as the cell reaches overcharge, the voltage peaks and then gradually trends down.

Since the charge process is exothermic, heat is being released throughout charging giving a positive slope to the temperature curve. When the cell reaches overcharge, where the bulk of the electrical energy input to the cell is converted to heat, the cell temperature increases dramatically.

Cell pressure, which increases somewhat during the charge process, also rises dramatically in overcharge as greater quantities of gas are generated at the **C** rate than the cell can recombine. Without a safety vent, uncontrolled charging at this rate could result in physical damage to the cell [4].

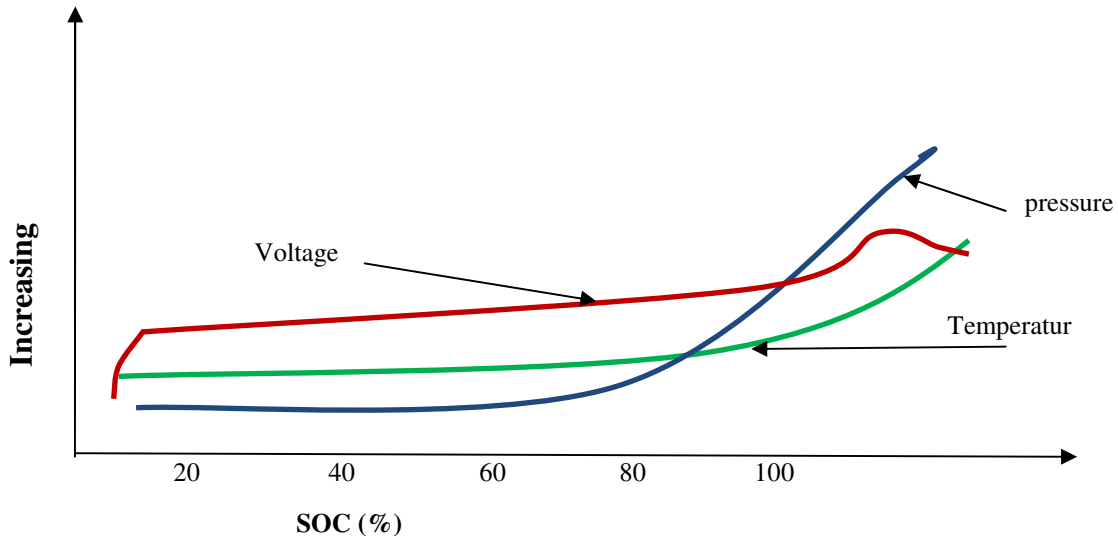

Figure 2-1 NiMH cell charging characteristic [4]

The charging performance of a NiMH cell is affected by charging temperature and rate. Specifically charge acceptance in NiMH cell decreases monotonically with rising temperature. It begins below 20°C and continues through the upper limits of normal cell operation [5]. More over the voltage profile moves down for higher charging temperature.

2.1.3 Charging methods

Unlike, the lead acid battery where voltage level is closely monitored, here current level should be controlled. Whereas the voltage level, or change in voltage level or temperature are used as a feedback signals.

The preferred charging method for NiMH batteries is fast charging. Fast charging is preferred since it reduces crystalline formation. Moreover, fast-charge rates serve to accentuate the slope changes used to trigger both the temperature and voltage-related charge terminations [4].

Depending on the battery type, fast charge restores almost all of the discharged capacity. However for some this phase is followed by an intermediate timed charge which completes the charge and restores the full capacity. The fast charge (with currents in the 1**C** range) is typically switched to the intermediate charge using a temperature sensing technique, which triggers at the onset of overcharge. The intermediate charge normally consists of a 0.1**C** charge for a timed duration selected based on battery pack configuration.

But some time if the battery is excessively discharged allowing a high current may make it impossible to sufficiently restore the battery capacity. In this case the battery is first trickle charged at the rate of 0.2C~0.3C to the appropriate voltage level (usually 0.8V per cell) [5]. Then it is followed by the same charging steps described above.

Because of the sensitivity of cell life to overcharge history and the greater subtlety of some of the overcharge transitions, charge termination redundancy in charger design is recommended. This applies to both built-in redundant charge control techniques and fail-safe charge termination techniques such as thermal fusing [4].

2.1.3.1 Overcharge Detection

Primary charge control schemes typically depend on sensing either the dramatic rise in cell temperature or the peak in voltage. Charge control based on temperature sensing is the most reliable approach to determining appropriate amounts of charge for the nickel-metal hydride cell [4]. Temperature-based techniques are thus recommended over voltage-sensing control techniques for the primary charge control mechanism.

Some overcharge of the battery is vital to ensure that all cells are fully charged and balanced, but maintenance of full charge currents for extended periods once the cell has reached full charge can reduce life.

2.1.3.1.1 Temperature-Based Charge Control

Use of charge control based on the temperature rise accompanying the transition of the cell to overcharge is generally recommended because of its reliability (when compared to voltage peak sensing techniques) in sensing overcharge. The exothermic nature of the nickel-metal hydride charge process results in increasing temperature throughout the charging process. There are three ways we can use temperature sensing for overcharge detection [4]:

- Based on absolute temperature rise: this approach is subjected to change with weather condition and is not reliable. Thus this approach should only be used as a fail-safe strategy to avoid destructive heating in case of failure of the primary switching strategy.
- Based on relative temperature rise: this is the simple form of temperature based switching where the battery temperature increment, say 20^0c, from the start of charging is monitored. The chosen ΔT has to account for both normal temperature gain during charge and the spike at overcharge. Selection of the proper temperature increment can be greatly influenced by the environment surrounding the cell.
- Based on slope change in temperature profile: charge switching based on the change in slope of the temperature profile eliminates much of the influence of the external environment and can be a very effective technique for early detection of overcharge.

2.1.3.1.2 Voltage-Based Charge Control

Voltage –based charge control can only be used as backups to temperature-based control. This is due to the fact that the voltage peak typically occurs later in the overcharge process, the voltage overcharge is not as distinct as that seen with temperature and the voltage behavior may change with cycling.

Similar to the temperature based control, the voltage-based control cab be approached in three ways [4]:

- Based on absolute maximum (~1.8V/cell): is relatively imprecise.
- Based absolute voltage rise: can be useful if the initial charging state is known.
- Based on change in voltage profile: can provide detection of early entry to over-charge region.

Moreover, since the voltage does peak during overcharge, switching on the voltage de-crease (5 to 10mV/cell) is feasible. This eliminates the concerns faced in both voltage and temperature increment methods about determining the increment that ensures charge re-turn without excessive overcharge.

2.1.3.2 Environmental Influences on Charging Strategy [4]

The discussions above are most pertinent for devices operating in the room-ambient range. The following subsection provides the general information in extreme temperature environment under the batteries operating range.

2.1.3.2.1 High Temperature (40 to 55^0c)

At higher temperatures, the charge acceptance of nickel-based batteries is drastically re-duced. Charging of nickel-metal hydride cells in high-temperature environments requires careful attention for two reasons: (1) the selection of set points, for both temperature and voltage-sensing systems, can be affected if the cells are already at elevated temperatures prior to starting charge; and (2) charge duration may have to be extended due to the charge acceptance inefficiencies.

2.1.3.2.2 Low Temperature

The charge time increases at lower temperatures so charge durations must be carefully considered to provide adequate low-temperature charging while avoiding excessive charge at normal temperatures. Charge rates must also be reduced at low temperatures. An upper limit of 0.1C is recommended below 15°C. Charging below 0°C is not advisa-ble.

As a concluding remark here is that unlike lead acid batteries where it is enough to moni-tor voltage only, charging NiMH is a complex monitoring process where voltage and temperature feedback signals play a major role.

2.2 Li-Ion battery technology

In contrast to NiMH, Li-Ion technology has the potential to meet the requirements of a broader variety of PHEVs and EVs. Lithium is said to be very attractive for high energy

batteries due to its lightweight nature and potential for high voltage, allowing Li-Ion batteries to have higher power and energy density than NiMH batteries. Also a reduction in Li-Ion cost relative to NiMH is anticipated [2]. However, Li-Ion batteries face drawbacks in longevity and safety which still need to be addressed for automotive applications.

2.2.1 State of the art Li-ion batteries

Unlike "NiMH", which specifies particular battery chemistry, the term "Li-Ion" refers to a family of battery chemistries, each of which has its own characteristics with respect to the categories of energy, power, cost, lifetime, and safety. Specific battery chemistries are typically named according to the material used for the positive electrode (cathode), although the negative electrode (anode) material can also be a distinguishing factor.

Table provides state of the art Li-ion batteries which are likely to be used for xEVs application.

Table 2.3 the performance characteristics of lithium-ion cells of different chemistries from various battery developers **[6]**

manufacturer	Technology type	Ah	Voltage range	Wh/Kg (@300W/kg)	$(W/Kg)_{90\%eff}$ 50% SOC	charging temperature
K2	Iron phosphate	2.4	3.65-2	86	667	
EIG	Iron phosphate	10.5	3.65-2	83	708	
A123	Iron phosphate	2.1	3.6-2.5	88	1146	-30~60^{0}c
Lishen	Iron phosphate	10.2	3.65-2	82	161	0~45^{0}c
EIG	Graphite/NiCoMnO2	18	4.2-3.0	140	895	
GAIA	Graphite/LiNiCoO2	42	4.1-3.0	94	174@70%SOC)	0~40^{0}c
Quallion	Graphite/Mn spinel	1.8	4.2-3	144	491(@60%SOC)	
		2.3	4.2-3.0	170	379(@60%SOC)	
Altairnano	Lithium Titanate	11	2.8-1.5	70	684	-40~55^{0}c
		52	2.8-1.5	57	340	
EIG	Lithium Titanate	12	2.7-1.5	43	584	

2.2.2 Charging method

In general Li-ion, batteries are charged using constant current/constant voltage. But the charge rate and the voltage limit differ for different batteries from different manufacturer as shown in the Table 2.3 above.

As for the charge rate it can vary from 0.3C to 6C or more depending on the model type. A typical constant current/constant voltage (CC/CV) is shown in Figure 2-2.

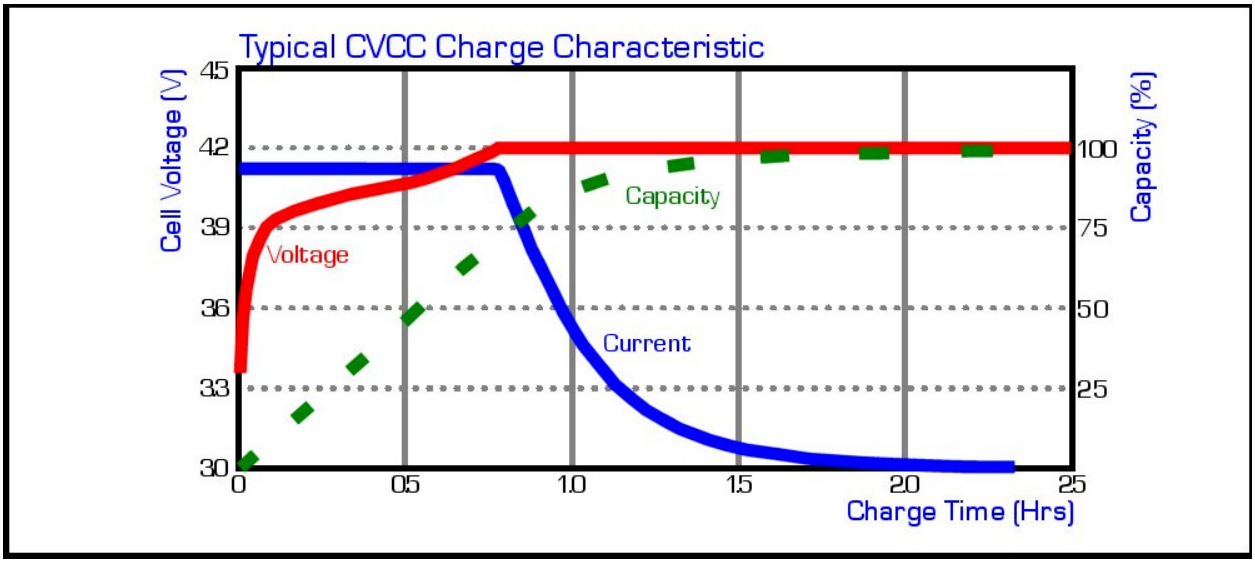

Figure 2-2 a typical constant current/constant voltage charging of Li-Ion battery [8]

2.2.2.1 Effect of temperature on charging performance

In general Li-ion batteries exhibit a good charge acceptance in wide temperature range. But the actual charging temperature range differs with in different battery chemistries as shown in Table 2.3 above. Some of the points mentioned in the discussion of NiMH batteries concerning temperature in relation to monitoring equally apply here.

2.3 Summary on batteries

Finally as a concluding remark to this section, battery type most likely to be used for EVs and high range PHEVs is Li-ion battery while NiMH could be used for lower performance PHEV designs.

From the charger point of view the range of battery capacities that are likely to be charged is between (6-40 kWh) or more. The charging current depends on the battery type and capacity. The fast charging strategy most likely to be used is constant current/constant voltage. Charge monitoring is done by using voltage and temperature. While change in temperature slope could be used to trigger charge termination in NiMH, this is not the case in Li-ions. Moreover, since in fast charging strategy batteries are not charged fully this may not be necessary at all. However temperature increase and absolute temperature limits can be used to insure safe charging. Charge termination will be facilitated by SOC measurement from the BMS.

3 REVIEW OF BATTERY MODELS

The charging process can be facilitated if the battery system is well defined and understood. For this reason it is essential that the battery is modeled into a system whose physical response can be simulated and analyzed. Thus in this section different battery models discussed in literatures are reviewed and suitable models for the job at hand are selected. The modeling is approached in two ways: electrical modeling and thermal Modeling. Much of the discussion is devoted to electrical modeling while a brief discussion is given on thermal modeling towards the end.

3.1 Modeling tips

In order to better understand modeling, it necessary that we have some basic understanding of the underlying processes. In this subsection some basics of the underlying process are discussed.

3.1.1 Charge, discharge, recovery, resistive effect

In every battery, there are two electrodes: positive and negative. Each electrode, in general, involves an electronic (metallic) and an ionic conductor in contact. At the surface of separation between the metal and the solution there exists a difference in electrical potential, called the electrode potential. The electromotive force (e.m.f.) of the cell is then equal to the algebraic sum of the two electrode potentials.

In equilibrium (no load), the species are uniformly distributed in the electrolyte. Once the external flow of electrons is established, the electrochemical reaction results in reduction of the number of species near the electrode. Thus, a nonzero concentration gradient is created across the electrolyte. If a load is switched off, then the concentration near the electrode surface will start to increase, or recover, due to diffusion, and eventually, the concentration gradient will become zero again. In other words, electro-active species will become uniformly distributed in the electrolyte, but their concentration level will be smaller than the initial value. The above processes help us understand where open circuit voltage dependence on SOC comes from. It also explains the increase in resistance at higher discharge rate.

More resistive effect is encountered due to finite conductivities of electrodes, electrolyte, and separators, from concentration gradients of ionic species near the electrodes and from limited reaction rates (kinetics) at the electrode surfaces [9].

Once the concentration of near the cathode drops below a certain level, the cathode reaction can no longer be sustained. Similarly, once the concentration of near the anode drops below a certain level, the anode reaction can no longer be sustained.

3.1.2 Capacitive effects

Generally, mass transfer arises either from differences in electrical or chemical potential, or from the movement of a volume element of the solution. The transfer of charge across the electrode surface causes a charge separation. The excess of charge on the electrode

surface is counterbalanced by the accumulation of ions, of opposite charge, on the solution side of the interface. The layer across which this charge separation occurs is called the electrical double layer, and is extremely thin compared with the width of the electrolyte and electrodes [10].

In its simplest form the double layer is described by the Helmholtz model, which describes the double layer as a parallel plate capacitor with a small plate separation (see **Figure 3-1**). This layer is referred to as the Helmholtz layer and can be described by a constant capacitance Cdl. These differences are only expected close to the electrode surface, since we assume electro-neutrality in the bulk of the solution.

More capacitive effect is introduced due to pure electrical polarization and from diffusion limited space charges (pseudo-capacitance). Both double layer capacitance and diffusion capacitance (pseudo capacitance) influence the transient response of the battery, especially when the rates of reactions are high [9].

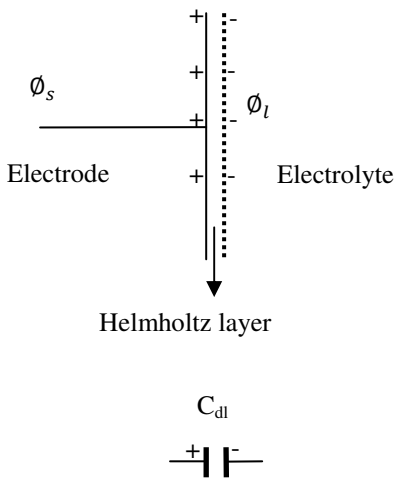

Figure 3-1 Electrical double layer as a parallel plate capacitor with capacitance Cdl; the electrode is assumed to be positively charged [**9**]

3.2 Battery Model Revision

The main aim of this section is to highlight the complexities involved in battery modeling and based on this study conclude on a recommended battery model for the supervision outlined before.

There are a wide range of battery models out there in various literatures. These battery models can be categorized in the following groups:-

- Electrochemical or physical battery models
- Electrical models
- Mathematical models

3.2.1 Electrochemical or physical battery models

Electrochemical models are the most accurate and mainly used to optimize the physical design aspects of batteries, characterize the fundamental mechanisms of power generation. They can relate battery design parameters with macroscopic (e.g., battery voltage and current) and microscopic (e.g., concentration distribution) information. However, they are complex and time consuming because they involve a system of coupled time-variant spatial partial differential equations a solution for which requires days of simulation time, complex numerical algorithms, and battery-specific information that is difficult to obtain, because of the proprietary nature of the technology [11]. Thus they will not be discussed here.

3.2.2 Mathematical models

Mathematical models use stochastic approaches or empirical equations which can predict runtime, efficiency, and capacity. However, these models are inaccurate (5-20% error) and have no direct relation between model parameters and the I-V characteristics of batteries. As a result, they have limited value in circuit simulation software [11]. The simplest and popular one is Peukert's law.

3.2.2.1 Peukert's law

The simplest model for predicting battery lifetimes that takes into account part of the non-linear properties of the battery is Peukert's law. It captures the non-linear relationship between the lifetime of the battery and the rate of discharge, but without modeling the recovery effect [12]. According to Peukert's law, the battery lifetime (L) can be approximated by:

$$L = a/I^b \qquad \textbf{3-1}$$

Where I is the discharge current, and 'a' and 'b' are constants which are obtained from experiments. Ideally, 'a' would be equal to the battery capacity and b would be equal to 1. However, in practice 'a' has a value close to the battery's capacity, and 'b' is a number greater than one. For most batteries the value of b lies between 1.2 and 1.7 [12].

The Peukert relationship can be written to relate the discharge current at one discharge rate to another combination of current and discharge rate:

$C_1=C_2\ (I_2/I_1)^{(n-1)}$

Where

- C = capacity of the battery
- Subscripts 1 and 2 refer different discharge-rate states

Peukert's formula shows an average error of 14% and a maximum error of 43%. Peukert's formula works well for light loads, but the errors will become very large at heavy loads [12].

Another more complex model for life time determining is the R V W's analytical battery model [13]. However its discussion here is unnecessary as far as our aim is concerned.

3.2.3 Electrical models

For electrical engineers, electrical models are more intuitive, useful, and easy to handle, especially when they can be used in circuit simulators and alongside application circuits. This group uses a combination of capacitors, resistors and voltage sources or current sources to model behavior of a battery. A wide variety of them have been proposed in various literatures for one or more battery chemistries. Only a few of them are discussed below:

The simplest model is composed of a voltage source and an internal resistance as shown in Figure 3-2

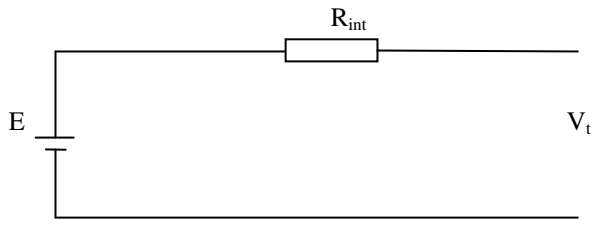

Figure 3-2 Simplest battery model

V_t can be obtained from the open circuit measurement and R_{int} can be obtained from both the open circuit measurement and one extra measurement with load connected at the terminal when the battery is fully charged. This model does not take into account the varying characteristic of the internal impedance of the battery with the varying state of charge.

In [14] an improved representation, which takes the variation of R_{int} with SOC in to account, is used while the constant voltage source is kept as it is.

$$R_{int} = \frac{R_0}{S^k} \qquad \textbf{3-2}$$

Where

- $S = 1 - \frac{\sum Ah}{C_{10}}$, state of charge(SOC)
- Ro is the initial internal resistance R_{int} with the battery fully charged. This value varies as the battery ages.
- C10 is the ten-hour capacity (Ah) at the reference temperature. This value also varies as the battery ages.

- k is a coefficient that is a function of the discharge rate

In [11] a model capable of predicting runtime and I-V characteristic is provided. This model has been verified to work for both NiMH and Li-Ion cells [11]. The equivalent circuit is given as below

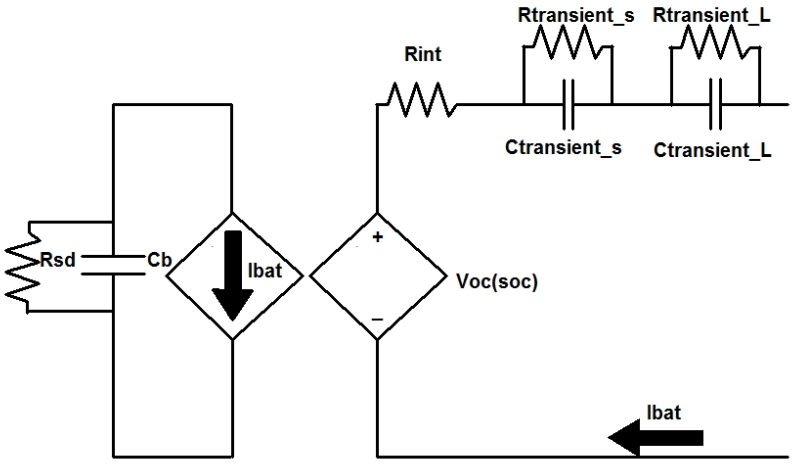

Figure 3-3 a generic runtime battery model [**11**]

On the left, a capacitor (C_b) and a current-controlled current source, model the capacity, SOC, and runtime of the battery. The RC network simulates the transient response. To bridge the SOC to open-circuit voltage, a voltage-controlled voltage source is used.

Usable capacity

The usable capacity, which is represented by C_b, declines as cycle number, discharge current, and/or storage time (self-discharge) increases, and/or as temperature decreases. The voltage across C_b varies between 0 and 1 depending on SOC. Thus voltage across C_b represents SOC of the battery.

Self-discharge resistor R_{Sd} is used to characterize the self-discharge energy loss when batteries are stored for a long time. Theoretically, R_{Sd} is a function of SOC, temperature, and, frequently, cycle number. Practically, it can be simplified as a large resistor, or even ignored [11].

Open circuit voltage

The nonlinear relation between the open-circuit voltage (VOC) and SOC is important to be included in the model. Thus, voltage-controlled voltage source VOC (V_{SOC}) is used to represent this relation. The open circuit voltage is normally measured as the steady-state open circuit terminal voltage at various SOC points. However, for each SOC point, this measurement can take days as the different processes inside the cell have longer time constant [11].

Transient response

In a step load current event, the battery voltage responds slowly. Its response curve usually includes instantaneous and curve-dependant voltage drops. Therefore, the transient response is characterized by the two parallel RC branches in Figure 3-3 above. The series resistor R_{int} is responsible for the instantaneous voltage drop of the step response. $R_{Transient\_s}$, $C_{Transient\_s}$, $R_{Transient\_L}$, and $C_{Transient\_L}$ are responsible for short- and long-time constants of the step response. Using two RC time constants, instead of one or three, is the best tradeoff between accuracy and complexity because two RC time constants keep errors to within 1 mV for all voltage curve fittings [11].

Model extraction [11]

Theoretically, all the parameters in the proposed model are multivariable functions of SOC, current, temperature, and cycle number. These functions make the model extraction complex and the test process long. However, within certain error tolerance, some parameters can be simplified to be independent or linear functions of some variables for specific batteries. Thus the different parameters can be made only SOC dependent and give overall good result provided that it is in isothermal environment. This was of course done for Li-polymer cell and may not hold for lead acid or other battery chemistries. As some battery chemistries depend significantly on discharge and charge rate.

The model extraction is done by curve fitting the behavior (V vs. SOC) of the battery which is the most representative of the group. All the extracted RC parameters are approximately constant over 20%–100% SOC and change exponentially within 0%–20% SOC caused by the electrochemical reaction inside the battery. Just to have some insight into the problem, the following equations are the curve fit results for different parameters of the Li-polymer cell used in [11].

$$VOC\,(SOC) = -1.031e^{-35SOC} + 3.685 + 0.2156SOC - 0.1178SOC^2 + 0.3201SOC^3$$

$$R_{Series}\,(SOC) = 0.1562e^{-24.37SOC} + 0.07446$$

$$R_{Transient\,S}\,(SOC) = 0.3208e^{-29.14SOC} + 0.04669$$

$$C_{Transient\,S}\,(SOC) = -752.9e^{-13.51SOC} + 703.6$$

$$R_{Transient\,L}\,(SOC) = 6.603e^{-155.2SOC} + 0.04984$$

$$C_{Transient\,L}(SOC) = -6056e^{-27.12SOC} + 4475.$$

3-3

In reference [15] an extension of [11] is provided where the transient response is composed of three time constants in seconds, minutes, hours; also a rate factor is included to model the effect of discharge rate.

Ref. [9] presents a model based on curve fitting experimentally available voltage vs. SOD curve for various temperature and current level. The battery output voltage can be calculated due to the battery open circuit voltage, voltage drop resulting from the battery equivalent internal impedance and the temperature correction of the battery potential. Accordingly, the battery output voltage may be expressed as

Vbat =VOC - ibat * Zeq + ΔE(T)

3-4

In reference [16] a model having the form in Figure 3-4 is proposed

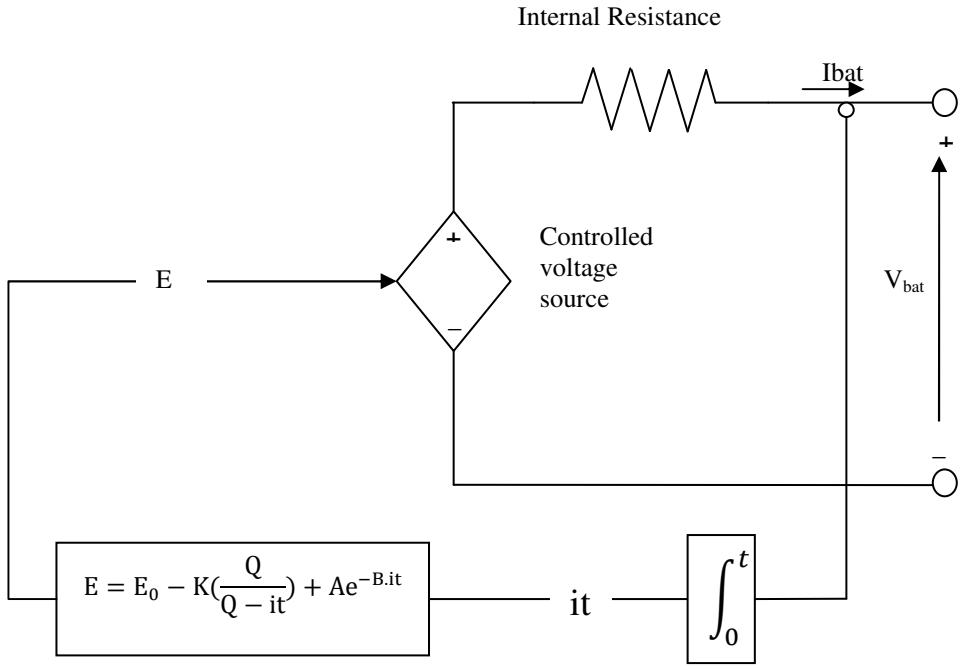

Figure 3-4 non linear battery model [16]

$$E = E_0 - K(\frac{Q}{Q - q}) + Ae^{-Bq}$$

3-5

Where:

$\boldsymbol{i = \frac{dq}{dt}}$	*A = exponential zone amplitude (V)*
$\boldsymbol{V_{batt} = E - (Ri)}$	*B = exponential zone time constant inverse (Ah)* $^{-1}$
$\boldsymbol{powerlosses = i^2R}$	*Vbatt = battery voltage (V)*
E = no-load voltage (V)	*R = internal resistance (Ω)*
E0 = battery constant voltage (V)	*i = battery current (A)*
K = polarization voltage (V)	***Q = battery capacity (Ah)***
	q= current charge level in battery (Ah)

Model assumptions:

- The internal resistance is supposed constant during the charge and discharge cycles and does not vary with the amplitude of the current.

- The model's parameters are deduced from the discharge characteristics and assumed to be the same for charging.
- The capacity of the battery does not change with the amplitude of the current (No Peukert effect).
- The temperature does not affect the model's behavior.
- The self-discharge of the battery is not represented.
- The battery has no memory effect

Model limitations:

- The minimum no-load battery voltage is 0 V and the maximum battery voltage is not limited.
- The minimum capacity of the battery is 0 Ah and the maximum capacity is not limited. Therefore, the maxi-mum SOC can be greater than 100% if the battery is overcharged.

What is good about this modeling approach is the model parameters can easily be extracted from the manufacturers' datasheet. The interested reader can refer to [16] for model parameter extraction procedure.

This is actually the model which is used in Matlab to represent the battery and is available in SimPowerSystems toolbox. Since there are no interface to real battery this model has been used as a battery in analyzing the algorithm.

While (3-5) gives the steady state open circuit voltage for a given state of charge, it does not model the transient behavior of the battery. Thus, in the Matlab, the equations below (3-6 & 3-7) are used to include the transient behavior of batteries. Moreover different models are used for charging and discharging as well as for different battery chemistries such as Li-ion, lead acid and NiMH/NiCd batteries. The equations below show only the charging model for Li-ion and NiMH. More information is available on the Matlab help file for the battery model.

The charging mode for Li-ion is

$$E = E_0 - K\left(\frac{Q}{0.1Q + q}\right)i^* - K\left(\frac{Q}{Q - q}\right)q + Ae^{-Bq} \qquad \textbf{3-6}$$

And for NiMH is

$$E = E_0 - K\left(\frac{Q}{0.1Q + |q|}\right)i^* - K\left(\frac{Q}{Q - q}\right)q + \text{Laplace}^{-1}\left(\frac{\exp(s)}{\text{sel}(s)}.\frac{1}{s}\right) \qquad \textbf{3-7}$$

Where

i^* the low frequency current dynamics found by lowpass filtering i

And i<0 for charging

As a general conclusion on battery model revision, the battery models are usually optimized for a given application. For example the one in [16] is optimized for HEV, or function such as determining life time [12 & 13], or available capacity. There are others which can be used to determine V-I characteristic. But what is common for all is that the accuracy of the model depends on the detail knowledge of the battery chemistry, which is normally only available to battery manufacturers.

3.3 Electrical Models used in the optimization algorithm

The discussion above indicates that most models in literature are interested in capturing the whole V-I characteristic of the battery i.e. from lowest SOC to highest. Even for a given battery type it is difficult, if not impossible, to find a single equation which works at different temperature and state of health (SOH).

Consequently, it is very difficult and time consuming for an on-line implementation. But what we can do, based on our prior information about batteries is

Use the current and voltage measurement to build a model which can predict the voltage of the battery steps ahead.

Use the simple knowledge we have about sate of charge and current relation to validate the reading from the BMS; and if the measurements are found to be accurate, use it to predict SOC steps ahead.

As long as our aim is safe and reliable charging it works perfectly. Thus what follows is the discussion of two simple models for tasks just described.

3.3.1 Model for voltage prediction

Of course we do not need a model that predicts the voltage–current relation for the whole range of SOC. However, what we need is a model that can predict the battery terminal voltage accurately a minute or so ahead. This is enough as the model parameters are updated every 10 sec or so by the optimization algorithm. Moreover the model should not be battery chemistry specific.

Thus based on this understanding and the discussions we have in battery model revision the following circuit is well suited for the job at hand.

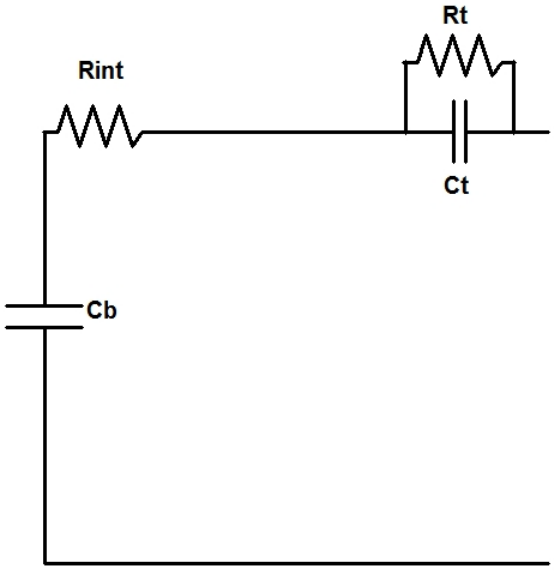

Figure 3-5 simple battery circuit model

Here:

- R_{int} -internal resistance: takes care of the instantaneous voltage boost whenever a current step is applied. Its value for a given battery cell is usually in a mOhm range.
- R_tC_t-RC circuit branch: will be responsible for the transient responses occurring in a battery with time constants in a minute range. It exact value differs from battery to battery. Considering the low Value resistance involved in RC branch the capacitance Ct is in kF (kilo farad range).
- The voltage over Cb: can be taken as the open circuit voltage of the battery. However it is not exactly the open circuit voltage as longer dynamics of the battery is included in it. Actually it doesn't matter as long as we can accurately predict the terminal voltage of the battery 10 sec or so ahead.

  There is no one value range for capacitance Cb; it is value greatly varies even for single battery because it is not related to any single physical process in the above model. But generally its starting value in the optimization algorithm in section IV can be made way above Ct.

In the model formulation, we need to know the initial voltage of the different capacitors. Considering the model formulation above it is reasonable to assume the voltage on transient RC branch to be zero and the voltage over Cb to be equal to the open circuit voltage of the battery. That is just before charging starts.

The model equations in state space form are given as:

$$\begin{bmatrix} \dot{x1} \\ \dot{x2} \end{bmatrix} = \begin{bmatrix} \dot{V}cs \\ \dot{V}cb \end{bmatrix} = \begin{bmatrix} -1/RtCs & 0 \\ 0 & 0 \end{bmatrix} \begin{bmatrix} x1 \\ x2 \end{bmatrix} + \begin{bmatrix} 1/Cs \\ 1/Cb \end{bmatrix} Iin + Ke$$

$$y = v0 = [1\ 1]\begin{bmatrix} x1 \\ x2 \end{bmatrix} + [R_i]Iin + e$$

3-8

Where

- e is stands for any error that results from measurement and modeling
- K is the Kalman gain

3.3.2 Model for SOC measurement validation and prediction

If the SOC measurement from BMS is taken at different time as charging progresses, it is possible to calculate the capacity of the battery and any columbic inefficiency associated with it using the following simple relation.

$$\frac{dsoc}{dt} = \frac{\eta}{C_b} I_{bat}$$

3-9

And in discrete form

$$soc_{k+1} = soc_k + \frac{\eta t_s}{C_b} I_{bat}$$

3-10

Where η is the coulumbic efficiency

C_b the battery capcity

t_s the samping time

Once the model parameters are identified they can be used to validate the next SOC reading. Once the SOC reading is found to be consistent the model can be used to predict the SOC steps ahead.

3.4 Battery Thermal models

When consider of thermal model we have to able to answer the following questions:

How much does the temperature rise for a given charging current and a given cooling power? What does the trajectory of this temperature rise looks like. This answer to this question is determinant in understanding and validating the temperature reading from the BMS. Moreover we need to include a thermal model in our simulation to take into account the temperature rise during the charging process.

How is the charge acceptance affected for a given charging current at different temperature? This is the same as asking, how much does the capacity of the battery vary with temperature?

For a given state of charge, how much does the open circuit voltage of the battery vary with temperature?

The last two questions required only to build our simulation model. That is once we have decided how much the temperature rise is for a given charging current we need to know how this affects charge acceptance of the battery and the battery terminal voltage. This is how ultimately the battery thermal model is included. If we know how much the temperature rises and but if it does not affect the characteristic of the battery. There is no need to include the thermal model. Reference [9] provides a way on how this can be answered from manufacturers' data sheet.

The next subsection discusses the answer for the first question and the subsequent section will answer the rest.

3.4.1 Battery thermal model for predicting temperature rise

Conservation of energy for a battery cell with lumped thermal capacity balances accumulation, convective heat dissipation, and heat generation terms as [17]

$$\frac{d(\rho c_p T)}{dt} = hAs(T - T_\infty) + \left(q_r + q_j + q_c\right)A$$

3-11

Where

- ρ density
- c_p specific heat capacity
- T cell temperature
- h the heat transfer coefficient for forced convection from each cell,
- A_s is the cell surface area exposed to the convective cooling medium (typically air)
- T_∞ is the free stream temperature of the cooling medium.
- A electrode plate area (cm2)
- q_c ohmic heat generation rate due to contact resistance (W)
- q_j ohmic (joule) heat generation rate of solid and electrolyte phases(W)
- q_r heat generation rate of electrochemical reaction (W)

The above equation however does not suit our problem as it contains battery specific parameters. It also considers the change in heat capacity and density of the battery with temperature [18]. An alternative is to ignore the change in heat capacity and density with temperature and have the following circuit friendly approach for thermal model [9].

$$mC_p \frac{d(T)}{dt} = i^2 R_{int} + \sum \frac{{V_{tr}}^2}{R_{tr}} + hAs(T - T_\infty)$$

3-12

However, we have no idea what value h and 'As' would be for a given vehicle. Thus it is reasonable to assume 'hAs' to be constant for a given charging period; where, off course, 'As' is constant and then we assume constant cooling power.

$\sum \frac{V_{tr}{}^2}{R_{tr}}$ is composed off voltage transients having time constants of different duration. Thus, to simplify calculation, we can assume it to be constant based the following reasoning.

Voltage transients with long time constants vary slowly and they can be considered constant compared to the 10 seconds time window chosen for the algorithm

Voltage transients with short time constants can be assumed constant as they will reach a constant value after an initial transient.

The calculation results for V_{tr} and R_{tr} are less critical in giving the thermal generation equivalent of the transient voltage drops.

Once again for constant charging current $i^2 R_{int}$ is also constant for reasonably longer period of time. Consequently, (3-12) can be reduced to

$$a\frac{dT}{dt} + bT = P$$

3-13

Where

- P represents any thermal generation or cooling system and initial thermal state, as represented by T_∞.

Now, (3-13) can be solved as:

$$T = T0exp(-dt) + Q\big(1 - exp(-dt)\big), d = \frac{b}{a} \quad Q = \frac{P}{b}$$

3-14

Thus given a short period of time, it is expected the temperature measurements have to fit to this equation. Once the model parameters that fit to a given measurement data are identified, the same model can be used for validating the subsequent data up to a given time like 10sec. This time span could be chosen based on our understanding of parameter variation and the computational power of the DSP.

3.4.2 Modeling effect of temperature on charge acceptance and open circuit voltage

When the temperature of a battery rises it affects the battery capacity and the open circuit voltage. Generally for lithium ion batteries charge acceptance increase with temperature [9] while for NIMH [4] the charge acceptance is optimum at room temperature and decrease more with decrease in temperature than with increase. As for the open circuit voltage at a given SOC, it increases for Li-ion batteries with increase in temperature. However, NiMH batteries have higher voltage at room temperature and decreases with temperature both ways; but relatively the decrease with increase in temperature is negligible.

It is apparent that the two chemistries have different characteristic and will result in a different models. Since this model is required only for simulation, we have provided the modeling for Li-ion batteries only.

According to [9] two parameters are enough to model the two temperature effects: temperature factor β (T) and the temperature-dependent potential-correction term ΔE (T). When these two terms are included the SOC equation from (3-9) and open circuit voltage are adjusted as follows.

$$\frac{dsoc}{dt} = \frac{\eta\beta(T)}{C_b} I_{bat} \qquad \textbf{3-15}$$

$$E = E_0(SOC, i) + \Delta E(T) \qquad \textbf{3-16}$$

Where

- E0 is the open circuit voltage at reference temperature for reference discharge rate
- Cb and η are the capacity and columbic efficiency of the battery at reference temperature. Note that, in Matlab battery model mentioned above Cb and η doesn't change with discharge rate.
- β(T) is the factor responsible for the change in charge acceptance due to temperature. It is one at reference temperature

The way this two parameters are calculated in reference [9] results in a piecewise linear curves.

Finally in our overall simulation model the following are true

- The battery capacity and columbic efficiency doesn't vary with discharge rate
- The open circuit voltage varies both with temperature and discharge rate
- The charge acceptance or capacity of the battery varies with temperature

4 BATTERY SYSTEM IDENTIFICATION

4.1 Introduction

There are different types of systems: linear, nonlinear, time invariant, time varying. These systems can be modeled in different model types: transfer function models, state space … etc. Nonlinear systems have specialized model types such as Wiener and Hammerstein, and neural network models [19].

However modeling is not the subject this chapter, it is mentioned here only to stress the link between the model type and the identification procedure we use. Battery system modeling is provided in chapter three. In this chapter our mission is to identify model parameters.

Model parameter identification can be approached in different ways depending system model type. The most popular identification methods in literature are prediction error method and sub space identification method. While the former is usually used for transfer function models the later is used for state space models. However the basic principle is the same in either case: minimizing the prediction error. Moreover in each method there are various ways to solve the problem; hence various algorithms are developed by different authors and can be found in [19, 20, 21, 22, 23].

Generally, these methods are used for black box identification. Black box identification refers to an identification procedure where the detailed knowledge of the system is not required. The system model is built from input output data alone. Knowledge of the system order will be appreciated but not necessary. Whenever this knowledge is not available, there are ready made identification tools, like Matlab identification toolbox, which can decide the best model order and the model parameters based input-output data provided.

However in black box identification there is no relation between identified parameters and the system. Besides, there is no single solution to the problem. This is clearly visible in state space models where the similarity transform will result in the same input-output relation with different state values and model parameters. The same is provided below in (4-1& 4-2):

$$\hat{x}(t) = \hat{A}\hat{x}(t) + \hat{B}u(t)$$
$$y(t) = \hat{C}\hat{x}(t) + Du(t) \qquad \textbf{4-1}$$

$$\hat{A} = TAT^{-1} \qquad \hat{B} = TB \qquad \hat{C} = CT^{-1} \qquad \textbf{4-2}$$

The concept of system identification mentioned above is an offline one. However it is also possible to find their online counterparts which are well adapted to online where the computation complexity should be reduced. They are usually discussed in literature under recursive Identification methods [22, 24, 25]

In this thesis, however, a different approach than highlighted above is followed. This is because

Considerable information about the system (battery system) has already been gathered.

The model parameters are required to provide some meaningful information about the battery, such as the internal resistance of the battery, capacity of the battery

As opposed to recursive identification methods there is no need to update model parameters during each sampling interval.

The approach used in this report is usually stated as white box identification in literature. The subsequent sections will provide detailed information about this identification procedure.

4.2 System Identification based on Optimization approach

There are a wide variety of optimization algorithms, also known as non-linear least square methods, which could be possible choices for the job at hand. They are generally iterative processes. Some of them are: Gauss-Newton, Levenberg-Marquardt (LM) and Powell's Dog led method [26]. These non-linear least square methods are instrumental in finding the minima of a given nonlinear function. In optimization problems this function is known as objective or cost function.

So how does this relate to our problem? Well, given a model, our problem is finding the parameters of the model that result in the minimum error between the observed and predicted data. Thus the error function between the observed and predicted data will be our objective function. To clarify this Idea more the following subsection provide how the objective functions are developed for each model discussed in section III.

4.2.1 Model Objective functions

Objective function for battery voltage prediction

We have specified in section III that the model in **Figure 3-5**, provided that it has the correct parameter values, can correctly predict the battery voltage in the time range we are working on. The same battery model in **Figure 3-5** can be represented by the following system of equation (refer to (3-8)).

$$\begin{bmatrix} \dot{x1} \\ \dot{x2} \end{bmatrix} = \begin{bmatrix} \dot{V}cs \\ \dot{V}cb \end{bmatrix} = \begin{bmatrix} \theta_1 & 0 \\ 0 & 0 \end{bmatrix} \begin{bmatrix} x1 \\ x2 \end{bmatrix} + \begin{bmatrix} \theta_2 \\ \theta_3 \end{bmatrix} Iin$$

$$\hat{y}_1(t_k|\theta) = v(t_k) = [1\ 1] \begin{bmatrix} x1 \\ x2 \end{bmatrix} + [\theta_4] Iin(t_k)$$

4-3

Now the question remains how we can get the correct parameter for each battery model. For this we have two tools. One is best initial guess for each parameter as it is highlighted in section III. The second tool is the voltage measurement we have from the BMS or the sensors in charger itself. The philosophy is that the calculated voltage using battery current as input to the model should be equal to the measured voltage. Of course the initial parameter values are too erroneous to result in a correct voltage prediction. Thu we need a way to reduce this error between the measured out voltage and predicted output voltage.

That is we have to minimize our objective function. Mathematically our objective function is

$$f_1(\theta) = y_1(t_k) - \hat{y}_1(t_k|\theta)$$

4-4

Where $y_1(t_k)$ is the measured voltage and $\hat{y}_1(t_k|\theta)$ is the predicted voltage as shown in (*4-3*).

The same reasoning applies for other model objective functions and they are given in (4-5 and 4-6). While the objective function for the first two cases relay on input-output relation but the objective function for the temperature monitoring is different. It is based on knowing the present value of temperature and predicting its future value based on the thermal model of the battery.

Objective function for soc monitoring (refer to (3-10))

$$\hat{y}_2(t_k|\theta) = soc_k = soc_0 + \frac{\theta_1 t_s}{\theta_2}\sum_{i=0}^{k} I_{bat}(t_i)$$

$$f_2(\theta) = y_2(t_k) - \hat{y}_2(t_k|\theta)$$

4-5

However since this is a linear model we will use simple linear solvers to identify the parameters and there is no need to go for iterative ones. Moreover, from numerical point of view there is no way to distinguish the two model parameters therefore we will fix the efficiency at 100% as we calculate for the capacity of the battery.

Objective function for Thermal model (refer to (3-14))

$$\hat{y}_3(t_k|\theta) = T_k = T0exp(-\theta_1 t_k) + \theta_2\big(1 - exp(-\theta_1 t_k)\big)$$

$$f_3(\theta) = y_3(t_k) - \hat{y}_3(t_k|\theta)$$

4-6

Since one input-output data can't give us any better result than our original parameters thus we need a couple of data to work with. The larger the data the better but it is also computational intensive. Besides for time varying systems like battery the older data are less important. Thus choice of sampling time and sample data length should take these things into account. One way or another, at the end the objective function is a vector with length equal to the sample data length selected.

Once we know what our objective function looks like the next question is 'how we set about to minimize our objective function?' The next section discusses this issue.

4.2.2 Model Parameter Identification Routine

Now that the objective functions are discussed along with approximate initial parameter values we are left with how to adjust the parameter values. They have to be adjusted so as to result in the parameters values which minimize our objective function. Mathematically

given our objective function f: $R^n \rightarrow R^m \, with \, m \geq n$, where n is number of unknown model parameters and m sample data length, we want to minimize ||f(θ) ||. In nonlinear methods mentioned above this minimization is done by minimizing the square of the objective function as given below:

$$\theta^* = argmin_\theta\{F(\theta)\},$$

4-7

Where

$$F(\theta) = \frac{1}{2}\sum_{i=1}^{m}(f_i(\theta))^2 = \frac{1}{2}||f(\theta)||^2 = \frac{1}{2}f(\theta)^T f(\theta)$$

4-8

The index i represents a given sampling time

Adjusting the initial parameter values require to make a step vector h on the parameter vector θ such that the following holds

$$F(\theta + h) < F(\theta)$$

That is the each step taken should result in a decent direction. The main purpose of a given nonlinear least method is thus finding h that result in reduction of the objective function faster. Mainly, that is where the different nonlinear least square methods differ.

Thus, in this thesis, the Levenberg-Marquardt method is used. For it combines the benefit of both the steepest decent and the Gauss-Newton method. The steepest decent is good when the solution is far from the final solution while the Gauss-Newton method works well when we are in the neighborhood of the solution. In the next section we see some important points related to the Levenberg-Marquardt method. But before that we need to clarify two important terms which are common in nonlinear square methods and without which we can't move an inch.

Jacobean, $J \in R^{mxn}$, is a matrix containing the derivative of the original objective function with respect to each unknown parameters along its row and for each index i:

$$(J(\theta))_{ij} = \frac{\partial f_i}{\partial \theta_j}(\theta)$$

4-9

Gradient, g, the derivative of the square of objective function (see Eq. 4-8) by each unknown model parameter as:

$$g = F'(\theta) = \begin{bmatrix} \frac{\partial F}{\partial \theta_1}(\theta) \\ \vdots \\ \frac{\partial F}{\partial \theta_n}(\theta) \end{bmatrix} = J(\theta)^T f(\theta)$$

4-10

4.2.3 The Levenberg-Marquardt (LM) method

In the previous section it is stressed that the main difference between different nonlinear square methods is the way h is calculated. In LM this step h is given as [26]

$$(J^T J + \mu I) h_{lm} = -g \quad with \quad g = J^T f \; and \; \mu \geq 0$$

Where

hlm= is the step h to be taken in the LM method

J is the Jacobean of the objective function

I is an identity matrix

μ is the damping term

g is the gradient

4-11

Now we can manipulate the damping term μ to switch between steepest decent and gauss-Newton method depending on how far we are from the final solution. For large values of μ we get

$$h_{lm} = \frac{-g}{\mu} = \frac{-F'(x)}{\mu}$$

4-12

This is a short step in the steepest descent direction. This is good if the current iterate is far from the solution. If μ is very small, then

$$h_{lm} = \frac{-g}{J^T J}$$

4-13

This is the gauss-Newton step and is good if we are close to the final solution as mentioned above.

Now the question remains: How do we select the initial value of μ? How do we know how far from the final solution we are? And then how is μ it updated? How is the iteration stopped? Since these issues are more mathematically involved, interested reader can refer to appendix A. However, the following sections are understandable without these answers in mind.

4.2.4 A Secant Version of the LM Method

In (4-99) the Jacobean is calculated using the derivative of the cost function with respect to each model parameters. This approach requires a function vector where the row members are the derivative of the cost function with respect to each model parameters. During the work it is found that providing this function vector for each model and whenever a model changed is time consuming; specially for state space model. However a numerical approximation of the derivatives provides as satisfactory result as the actual derivate. Moreover a single function handles the Jacobean calculation for all model involved given the cost function for each model. The secant version of LM is, thus, a version of LM method where the derivates in Jacobean is approximated numerically by finite difference approximation as:

$$(J(x))_{ij} = \frac{\partial f_i}{\partial x_j}(x) \cong \frac{f_i(x + \delta e_j) - f_i(x)}{\delta}$$

4-14

Where 'e_j' is the unit vector in the jth coordinate direction and δ is an appropriately small real number.

4.2.5 Constrained optimization

What is common for all nonlinear optimization algorithms is that they are relatively prone, depending on the parameter set up of the cost function, to initial model parameters. This will sometimes result in unacceptable values. For example, during simulation, it is observed that, depending on the initial values given, the resulting model parameter contain negative values. This parameters being capacitances and resistances, it is not acceptable.

Moreover there can be several local minima for the objective function. And depending on where the initial parameter values are, the solution will have different values. Therefore for better result it is an utmost importance that the approximate values of the parameters are known. In addition, if the bounds of these parameters are specified, better results will be attained.

There are various approaches to solving constrained optimization problems. One way of doing it is by using penalty function or another way can be saturating the parameter when the limit is reach. But these methods are found to be not helpful. Yet another way could be defining the parameter in square root or log, however this is not tried.

However in this thesis it is found that the 'lsqlin' Matlab optimization tool along with Levenberg-Marquardt (LM) method, discussed above, works well.

4.2.5.1 The 'lsqlin' optimization tool

The' lsqlin' function solves the problem of the form in (4-15) with the given bounds. However we are only interested at the simple bound that is $lb \leq x \leq ub$

$$\min_x \frac{1}{2}\left|\left|C.x - d\right|\right|_2^2 \text{ such that } \begin{Bmatrix} A.x \leq b, \\ Aeq.x = beq, \\ lb \leq x \leq ub \end{Bmatrix} \quad \textbf{4-15}$$

Called as (Since we are not interested in the terms in bracket, we skip them)

$$x = lsqlin(C, d, [\ ], [\ ], [\ ], [], lb, ub, x0, options)$$

Where

C is a data matrix

X0 is vector of parameter whose value is to be calculated

d is a data vector

More insight into these parameters is given in the following subsection.

4.2.5.2 Levenberg-Marquardt (LM) method and 'lsqlin'

The trick in combining the two (LM and 'lsqlin') is modifying the way h_{lm} is calculated. (4-11) can be rewritten as:

$$(J^T J + \delta^2 I)h_{lm} = -J^T f, \text{where } \delta^2 = \mu \quad \textbf{4-16}$$

This can equally be defined as [27]:

$$\min_x \frac{1}{2}\left|\left|\begin{bmatrix} J \\ \delta I \end{bmatrix} h_{lm} - \begin{bmatrix} f \\ 0 \end{bmatrix}\right|\right|_2^2 \quad \textbf{4-17}$$

Now it is easy to 'lsqlin' function, as it is clear from the formulation (C= $\begin{bmatrix} J \\ \delta I \end{bmatrix}$, x=$h_{lm}$, d=$\begin{bmatrix} f \\ 0 \end{bmatrix}$). Yet another trick is bounding the step h_{lm}. The bounds for h_{lm} can be adapted from [27]:

$$xlb < xk + h_{lm} < xub$$

4-18

Since the actual computation results in

$h_{lm} = -lsqlin(...)$

$$xlb < xk - h_{lm} < xub$$

$$xk - xub < h_{lm} < xk - xlb$$

4-19

Now what is changed? Well, in the unbounded LM method we used to calculated h_{lm} using (4-11) where there is no limit on the actual h_{lm} calculated. However now we are calculating h_{lm} using the 'lsqlin' with upper and lower bound as necessary. But the rest including Jacobean calculation, μ selection and updating, iteration stopping mechanisms are intact as in LM method.

This finalizes the solution for the optimization problem and the resulting parameters are strictly bounded.

4.3 Auxiliary input to the identification algorithm

Executing the optimization algorithm during each sample interval is costly as well as unnecessary. Considering the potential variability of the battery parameters and computational complexity of the routine, the optimization routine will be executed after every 10sec. However, due to modeling inadequacy and measurement noises, there will be errors between measured and predicted values in the mean time. To keep the model up to date and reliable we have to take advantage of the data from each sampling interval. This could successfully be done by using Kalman filter. Then what is Kalman filter?

4.3.1 Kalman filter

The Kalman filter is a set of mathematical equations that provides an efficient computational (recursive) means to estimate the state of a process, in a way that minimizes the mean of the squared error [28].

The Kalman filter addresses the general problem of trying to estimate the state $x \in \Re^n$ of a discrete-time controlled process that is governed by the linear stochastic difference equation

$$x_k = Ax_{k-1} + Bu_{k-1} + w_{k-1}$$

4-20

With measurement $z \in \Re^m$ that is

$$z_k = C\, x_k + v_k$$

4-21

In our case

$$z_k = yk - Du_k$$

The random variables w_k *and* v_k and represent the system disturbance additive vector and model disturbance additive vector respectively [20]. They are assumed to be independent (of each other), white, and with normal probability distributions:

$$P(w) = N(0, Q)$$

$$P(v) = N(0, R)$$

4-22

Where Q and R are their respective covariance matrices, whose values are chosen based on our knowledge of the system.

4.3.2 Kalman filter calculation

As highlighted above during each sampling interval we need to get the best estimation of the states. These states will provide the basis for the correct prediction of the terminal voltage (see (4-21)). Now how is this accomplished?

In setting up the solution for the Kalman filter, we begin with the goal of finding an equation that computes an a posteriori state estimate $\hat{x}$ as a linear combination of a priori state estimate and a weighted difference between an actual measurement z_k and a measurement prediction $C\hat{x}^-$ as shown below in (4-23)

$$\hat{x} = \hat{x}^- + K(z_k - C\hat{x}^-)$$

4-23

The priori state estimate is the state estimated at time step k-1 as

$$\hat{x}^-{}_k = A\hat{x}_{k-1} + Bu_{k-1}$$

4-24

The actual derivation of the Kalman gain 'K' is beyond the scope of this report; interested reader can consult [28]. A typical expression for Kalman gain calculation is given in (4-25) [20, 28]

$$K = \frac{P_k^- C^T}{CP_k^- C^T + R}$$

4-25

The overall recursive implementation of Kalman filter is given in Figure 4-1 below [20, 28]

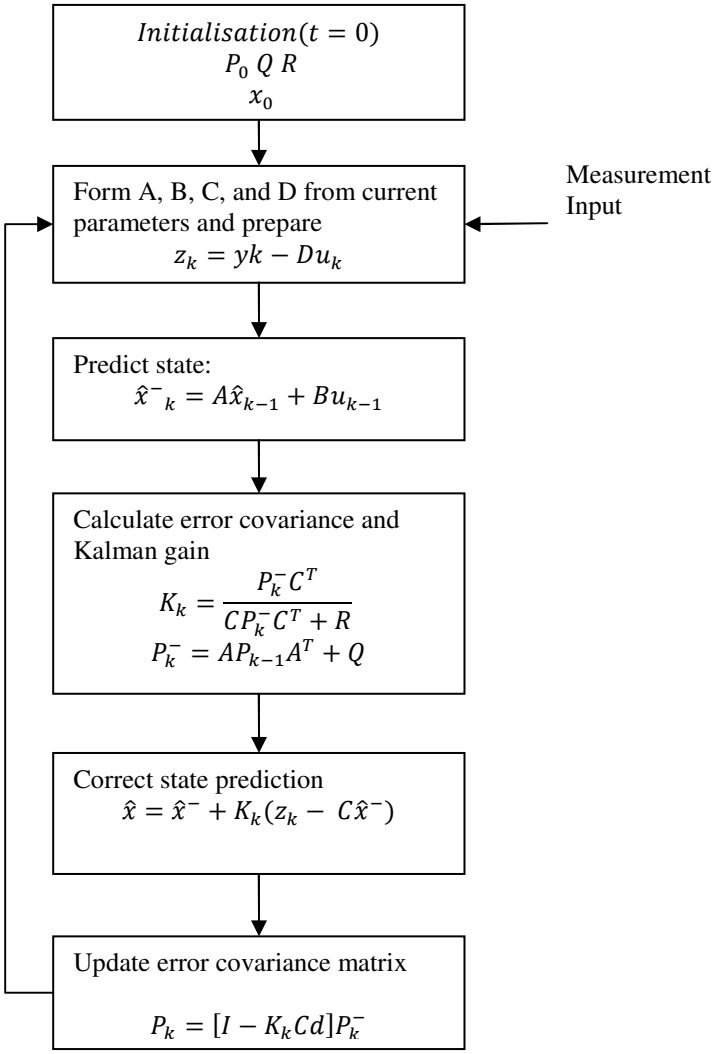

Figure 4-1 the recursive Kalman filter implementation

5 THE CONVERTER

In this section issues related to the converter are discussed. Since the aim the thesis is not to design a converter, here only a general information and operating characteristic will be presented. Interested reader can refer to the corresponding references for issues related to designing the converter and the control system.

5.1 Topology

There are a wide variety of converter topologies which could be used for battery charger application. To begin with the battery charger for EVs has two parts: the AC/DC and DC /DC converters. Mainly in the AC/DC side we have a variety of options to choose from; ranging from single phase [29] to three phases [30-34]. On the other hand the three phase converters can also be soft switched [30, 32] or hard switched [30, 31, 34]; or two levels [30, 31, 34] or three level [32, 33].

Choice of the best converter is a tradeoff between overall costs, efficiency, and quality of charging as well as the simplicity of the control circuit. However, the power level requirement for fast charging demands a three phase power source.

In this report, the battery charger shown in Figure 5-1 will be investigated [31].

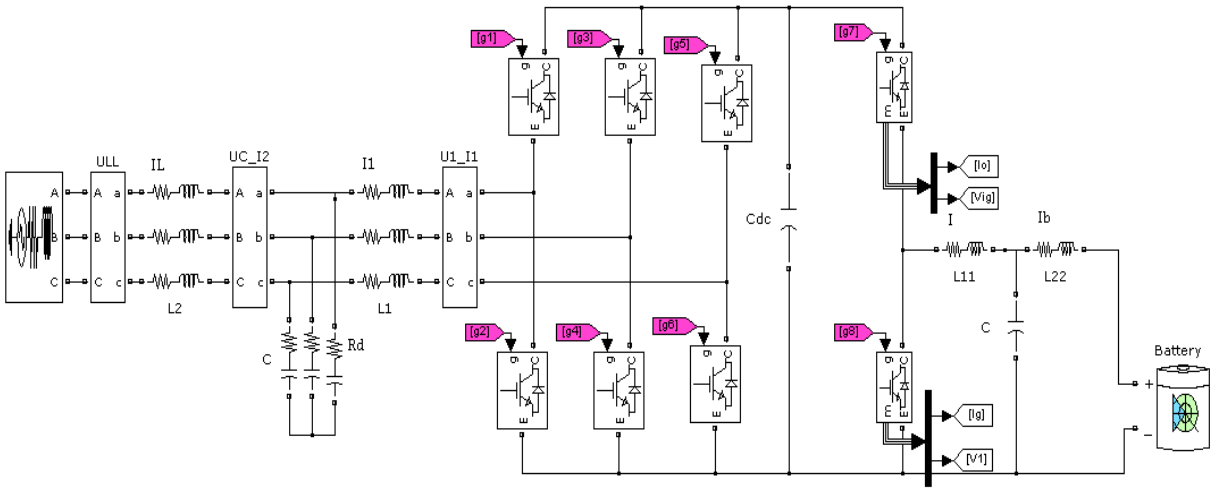

Figure 5-1 the charger power circuit Simulink diagram

The charger circuit consists of a hard switched three phase AC/DC converter preceded by LCL filters, and followed by a DC/DC two quadrant buck/boost converter with LCL filters. LCL filters chosen for their better filtering performance and lower inductance requirement compared to first order filter (L-filter) [31].

The charger which is going to be investigated has the ratings or operating conditions shown in Table 5.1.

Table 5.1charger rating

parameter	symbol	rating
Rated power	S	50KVA
Grid voltage	ULL	400V±10%
Grid frequency	f	50±5%
Battery voltage	Vbat	96 to 600
Charging current	Ibat	±150A
Dc link voltage	Vdc	700V
Switching frequency	f_{sw}	5kHz

5.2 Converter Parameter Values

Given the operating conditions as in Table 5.1, let us now focus on the values of the different components. The AC/DC converter has the values given in Table 5.2 for components involved. The LCL parameters are selected based on the procedure described in [37]. Valuable information on setting the DC link voltage can be found in [36] and [41] provides a simple expression on selecting the value of the DC link capacitor.

Table 5.2 AC/DC converter component values

Parameter	Value
DC link voltage	-
Inductor (L2)	250μH
Inductor (L1)	500μH
Capacitor(C)	33μF
Capacitor(Cdc)	6800μF
Damping resistor(Rd)	0.75Ω
Equivalent resistance of the inductors	1mΩ

Figure 5-2 shows the DC/DC Buck-Boost converter used in the charger. The corresponding component values are given in Table 5.3. The equivalent resistance has not been calculated; it is just chosen, its actual value could be different. The LCL filters for the DC/DC converter are selected following the same procedure as in [41].

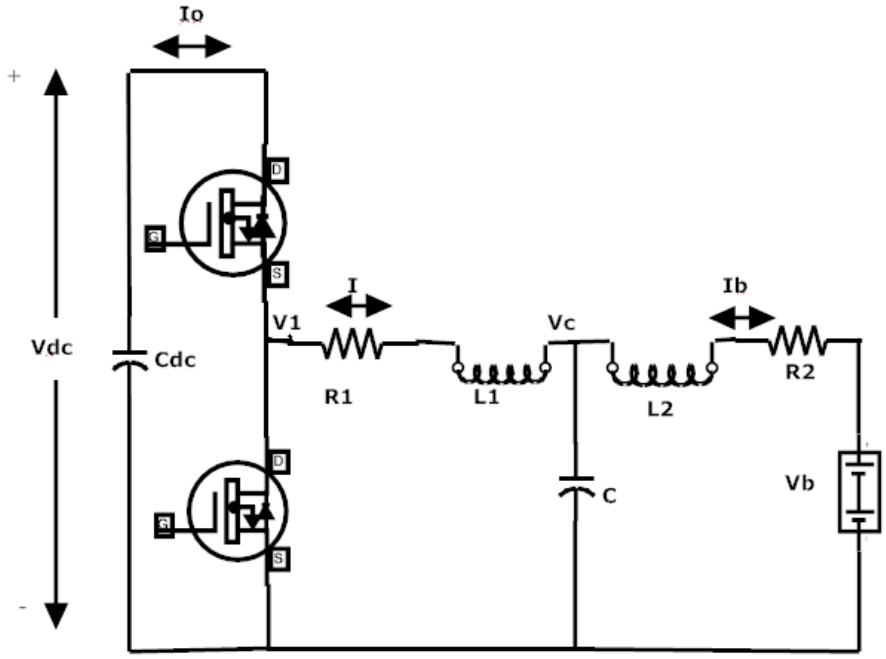

Figure 5-2 DC/DC buck-boost converter

Table 5.3 component values/Ratings for DC/DC converter

Parameter	value
C	33μF
L1	3.3mH
L2	120μH
f_{res}	2.55KHz
Equivalent resistance of the inductors(R1,R2)	1mΩ

5.3 The Control system

5.3.1 Control of AC/DC VSC

There are various literatures dealing with control of front end voltage source converter (VSC) [31, 34, 38, 39,40]. Some of them [31, 38, 39] discuss VSC control with LCL filter. Here the simple control strategy which makes use of the usual PI controls in synchronous frame is adopted [34, 38,40]. The synchronous frame is often used to obtain fast current control dynamic response [37].

Moreover the dq-coordinate can be aligned either to the grid voltage (ULL) or to the voltage over the capacitor bank (Uc). Here we are dealing with a control system where the dq-coordinate is aligned to Uc. The approach used to make sure the required reactive power is drawn from the grid is discussed at the end of this section.

The overall control diagram of the AC/DC voltage source converter (VSC) is shown in Figure 5-3.

To get the reference angle the three phase voltage over the capacitor bank are used. They are first transformed from 3 phase to stationary coordinate (alpha-beta). Then they are low pass filtered at cutoff frequency of 50Hz twice to filter out noise. After which they are normalized to get the cosine and sine of the transformation angle; mind you, they are shifted 90 degrees while filtering.

As mentioned above, the controller is a cascaded PI controller. The values of proportional and integral gain for the current controller and voltage regulator are given in **Table 5.4** and **Table 5.5** respectively. The controller also includes active damping resistor (Ra), decoupling, feed forward, saturation blocks and anti- windup terms. The active damping resistor is used to rule out the uncertainty in equivalent resistance of the inner inductor (L1). The appropriate manipulation of the PI output to accommodate the converter gain is also provided.

Here the modulation technique used is pulse width modulation (PWM) with triangular carrier wave.

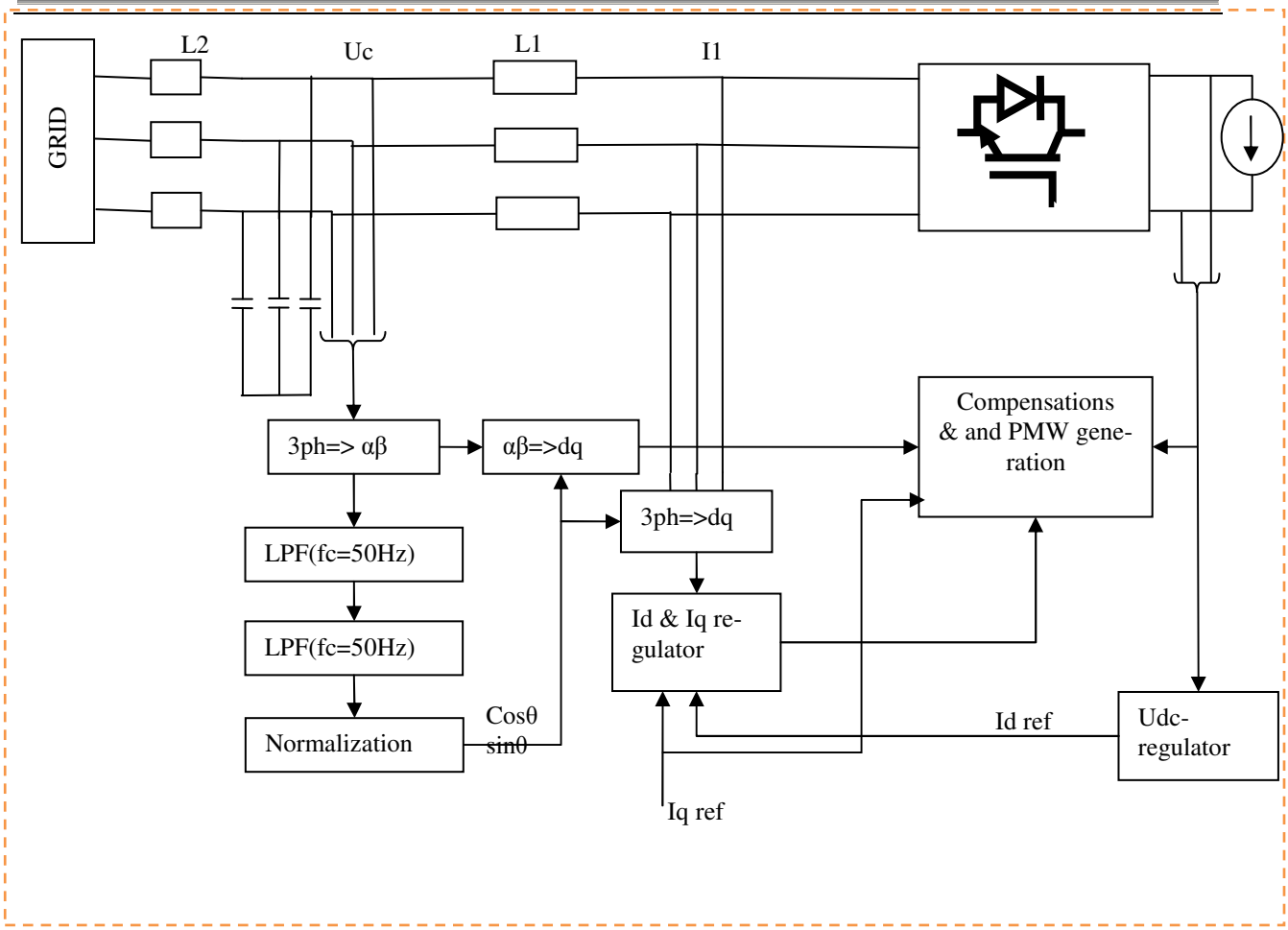

Figure 5-3 the overall diagram the VSC system

Table 5.4 Parameter values in the current control loop

parameter	value
Carrier wave amplitude(Vc)	1
Active damping resistor (Ra)	0.03Ω
Proportional gain(Kp)	2.5
Integral gain(Ki)	155
Sampling time(Ts)	1e-4
Converter gain(G)	350

Table 5.5 Voltage regulator parameters

parameter	value
Proportion gain(Kp)	10
Integral gain(Ki)	500

5.4 Control of the DC/DC converter

The overall control layout of the DC/DC converter is shown in **Fel! Hittar inte referenskälla.** and it is a cascaded PI controller as in the AC/DC case above. Similarly, the feed forward loop trough Ra is included to remove uncertainties due to the resistance R1. Other feed forward terms as shown in **Fel! Hittar inte referenskälla.** are also used. Not shown are the saturation blocks and the anti-windup loops. Some parameter, like the sampling time and switching frequency, are similar the AC/DC converter case. Here even though the modulation technique is PMW the carrier wave is saw tooth.

The proportional and integral gain values for the three PI controllers shown in **Fel! Hittar inte referenskälla.** are given in Table 5.6.

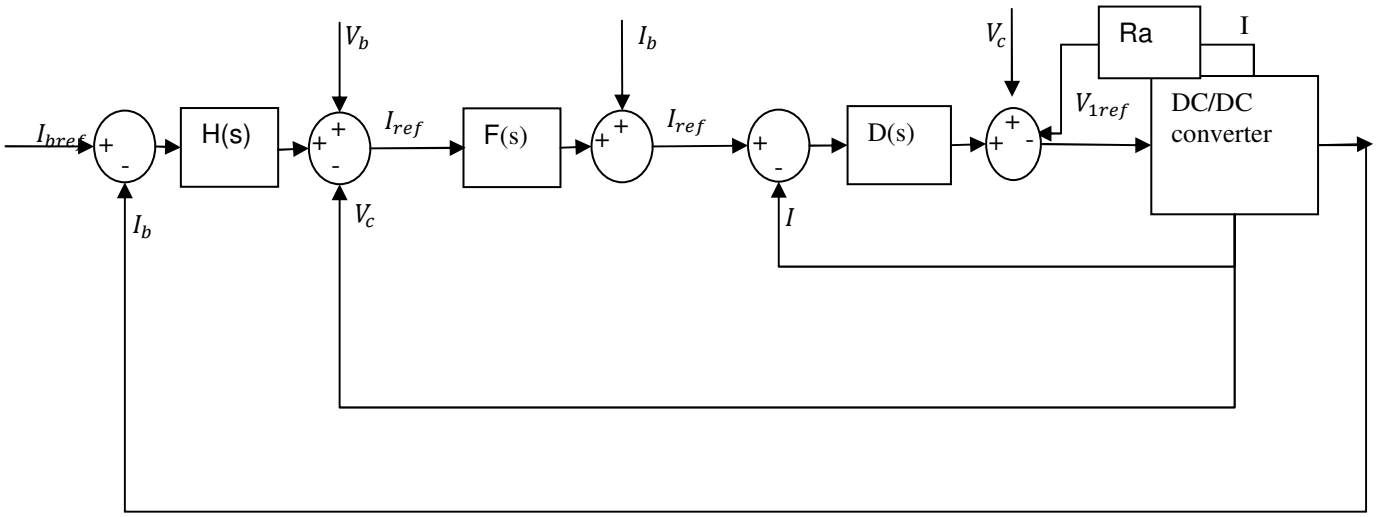

Figure 5-4 General block diagram the DC/DC converter control loop

Table 5.6 DC/DC converter controller parameters

parameter	value
Carrier wave amplitude(Vc)	1
Kp_D	16.5
KI_D	155
Kp_F	0.25
KI_F	5
Kp_H	0.75
KI_H	3
Ra	0.03

5.5 Results and analysis

The charger is intended to work on a constant DC link voltage of 700v while the battery voltage and current varies considerably. We have to also make sure that unacceptable voltage overshoots does not occur in the system. And the current drawn from the grid should be maintained below within the rating of the various components. Most importantly, the current delivered to the battery should be limited to the charge acceptance level of the battery as demanded by the BMS (battery management system).

The simulation is set up under the assumption, the DC link capacitor is pre-charged to the DC link voltage and the filter capacitors are pre-charged to the battery voltage. Pre-charging of the capacitors is important as will be discussed later. In the first 0.1 sec the controller locks in with the AC side filter capacitor voltage to generate the reference angle. Then the charger starts to provide power for the battery as set by the reference current. The battery model (Li-ion) available in Matlab SimPowerSystems toolbox is used for the analysis.

5.5.1 Low pass filter of the battery reference current

In attempt to run smoothly the two control circuits (the AC/DC and DC/DC converter control circuits) the battery reference current is low pass filtered. This step is crucial for the required performance of the battery charger to be met. This is due to the fact that the two control circuits are designed separately and it happened so that one control circuit is either slower or faster than the other. When this happens there will be over voltage or under voltage on the DC link. This results in overshoot on the grid and battery current. The larger the step change the worse the problem is; noticeably in the beginning. Figures (Figure 5-6,Figure 5-7, Figure 5-8) below show what happens.

As can be seen it is a disastrous situation for both the battery and the grid current, especially in the beginning. For the same step changes in battery reference current (100A) at 0.1sec and 0.5 the circuit works much worse in the beginning. Except for the small overshoots in the Dc link voltage, however, the circuit works well in the remaining part of the simulation.

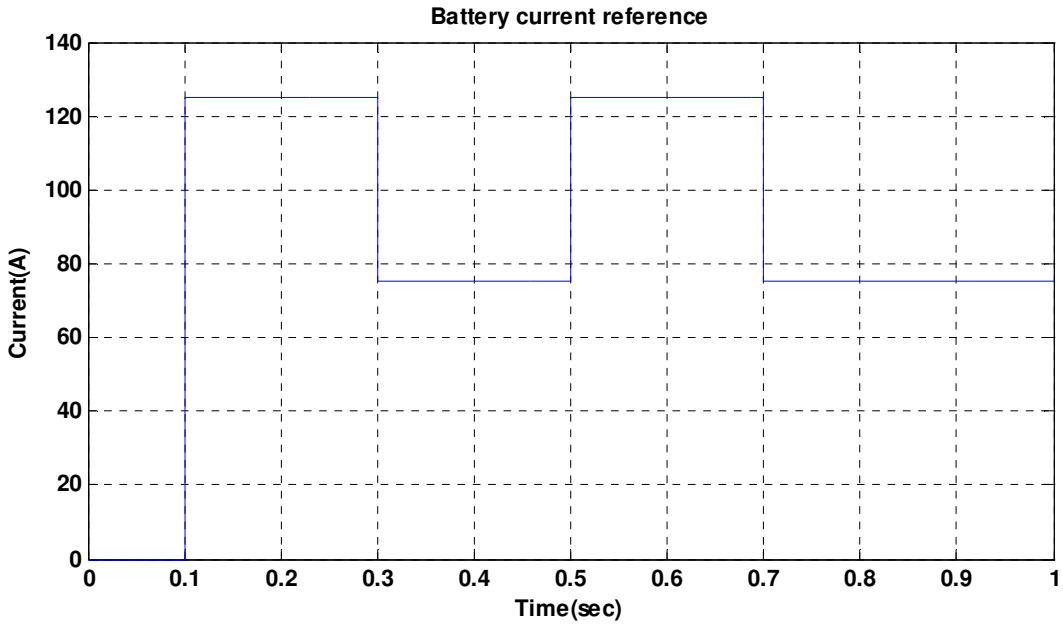

Figure 5-5 Battery current reference used for the simulation

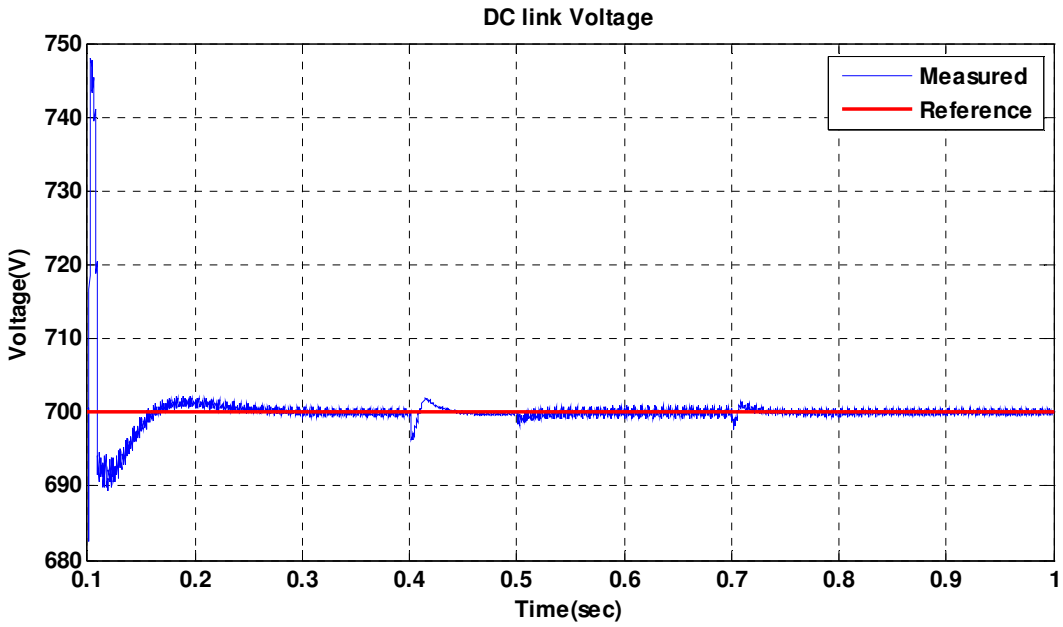

Figure 5-6 The DC link response for step changes in battery reference current

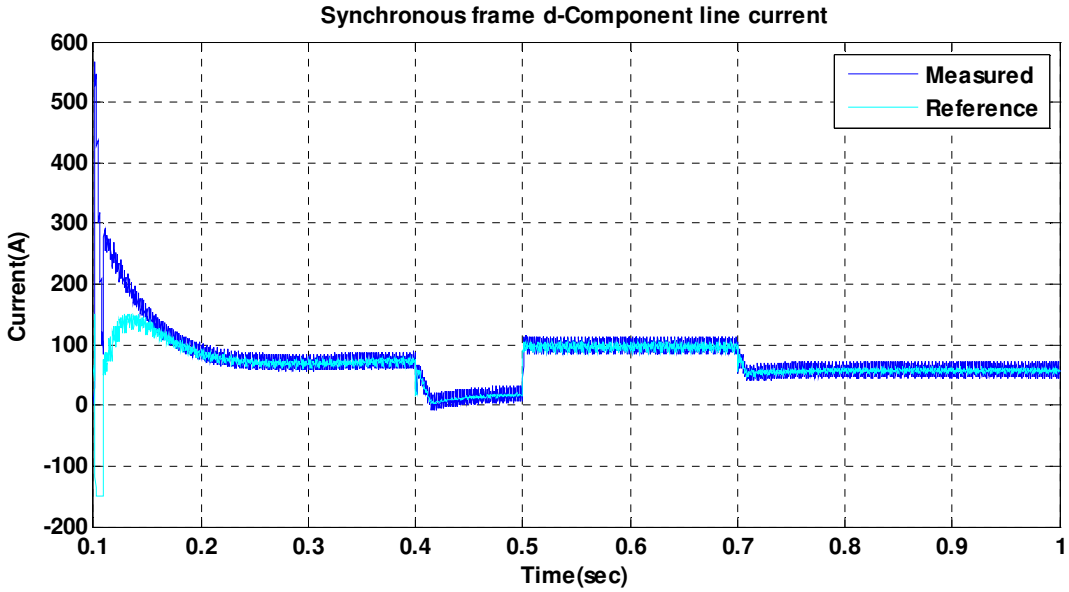

Figure 5-7 Response Synchronous d component current

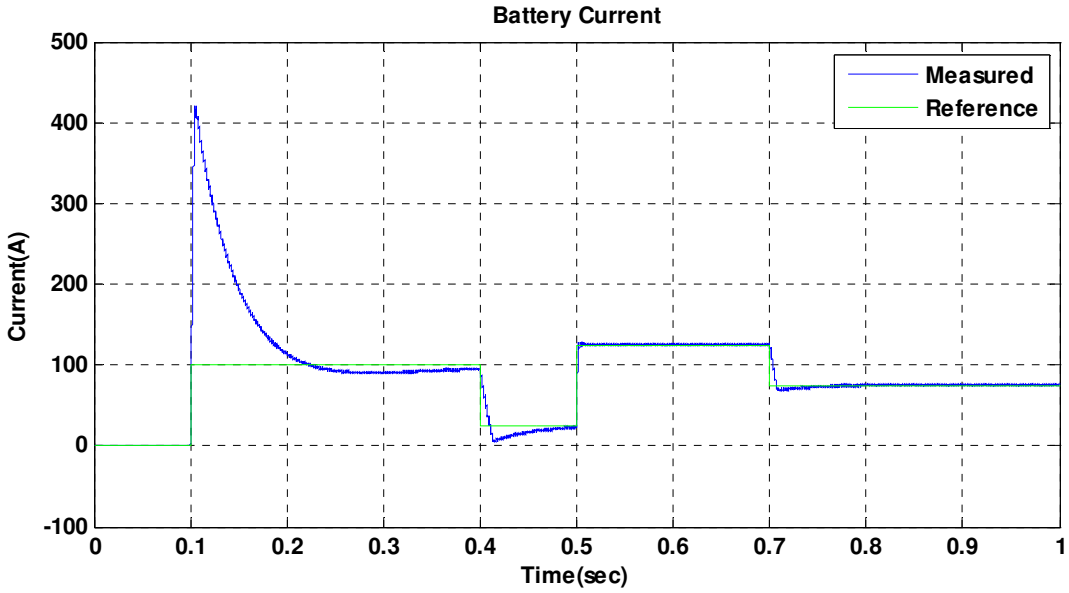

Figure 5-8 battery current response for step changes in reference current

The above shocking simulation results can be dealt with easily just by low pass filtering the battery reference current. The results below show the response of the battery current, the grid current and the Dc link voltage response when the same is done. The same step changes in battery reference current as in **Fel! Hittar inte referenskälla.** are used.

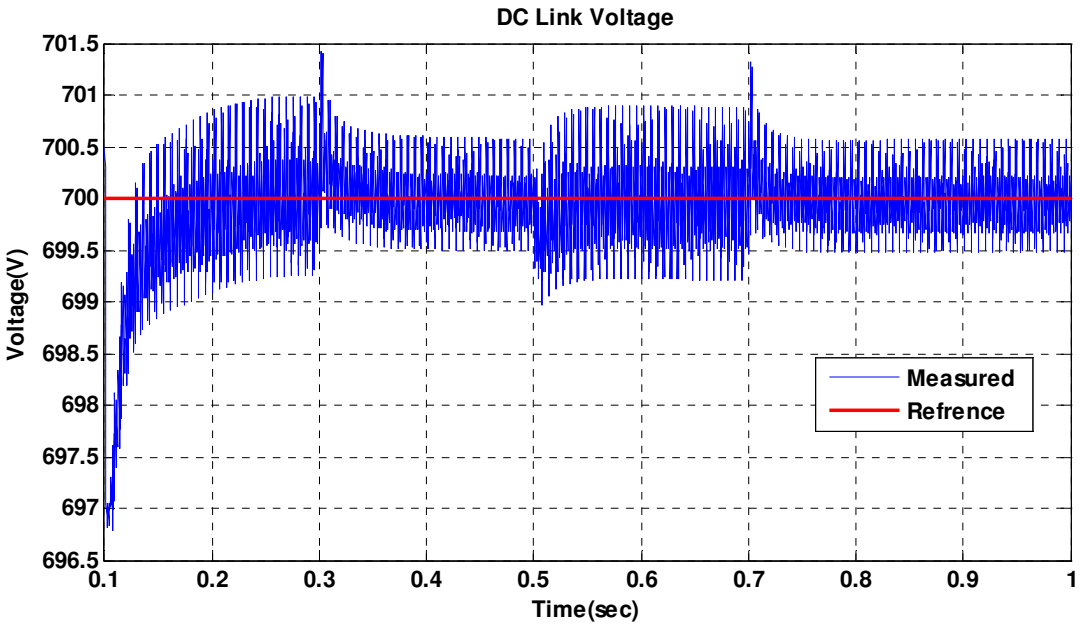

Figure 5-9 the DC link response for step changes in battery reference current

From the figure above we can see that the controller has managed to maintain the DC link voltage almost constant while the battery draws highly variable current. This is just the worst case scenario of the actual charging cycle. Moreover the ripple is higher for higher current levels as can be expected.

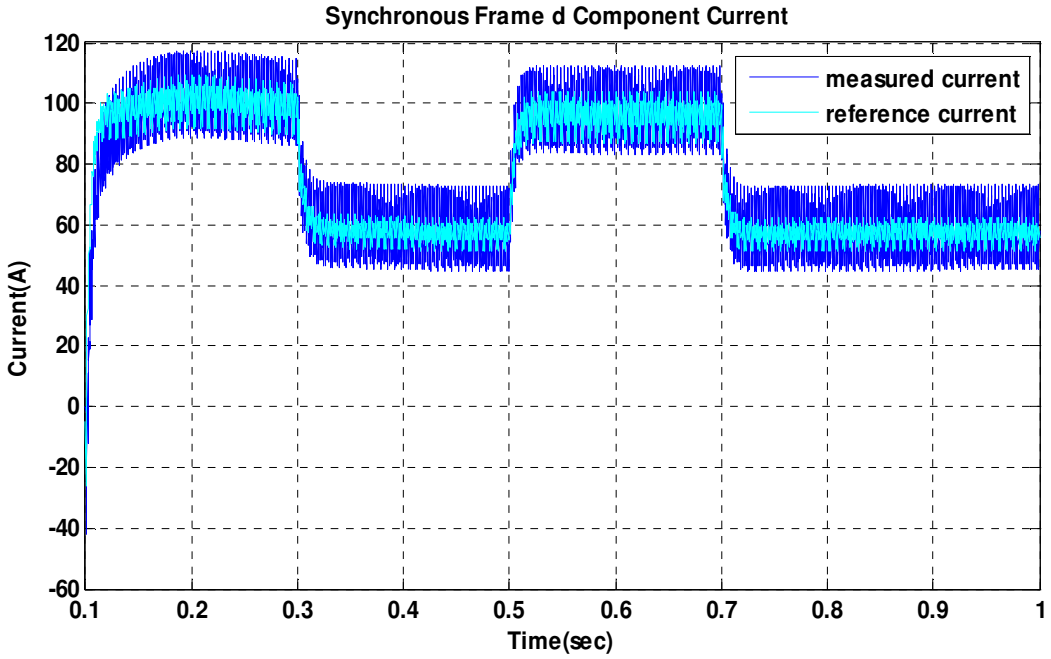

Figure 5-10 Response Synchronous d component current

Contrary to the previous case the grid current drawn follows the reference current and there is no overshot.

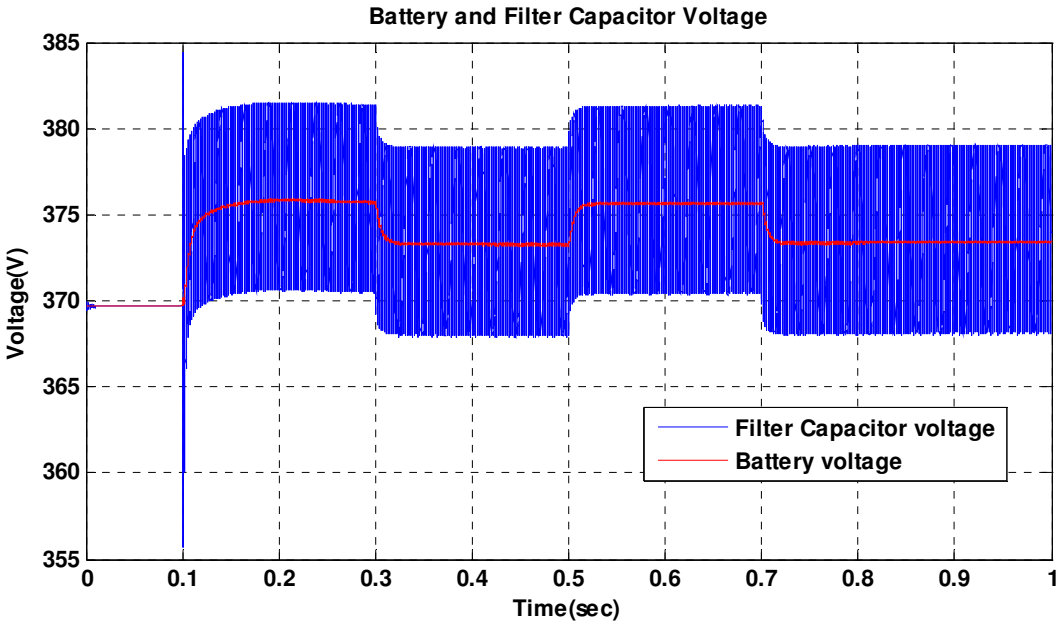

Figure 5-11 Battery voltage response for step changes in input voltage

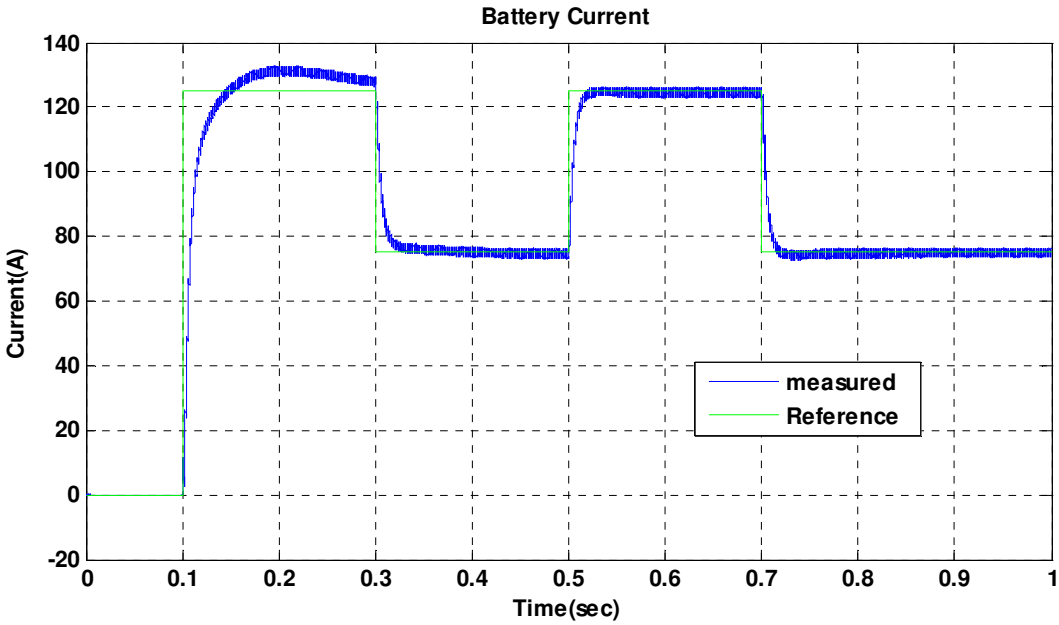

Figure 5-12 battery current response for step changes in reference current

Here we have small overshoot (+5A) on battery current and only for short period of time and in the beginning only. If required, this can totally be eliminated by taking reasonably lower steps in battery reference current.

5.5.2 Pre-charging the DC link and the DC filter capacitors

It is stressed above that pre-charging of the capacitor is essential; indeed it is a disaster for the grid if not done. The simulation result in Figure 5-13 shows what happens to the grid

current when the DC link voltage is initially 300V. Here one should note that the controller circuit is not activated it is just the diode rectifier which is charging the capacitor. It can be seen that the current drawn from the grid is huge and the same current flows through the capacitor. This may even damage circuit components involved; even though it is for short period of time.

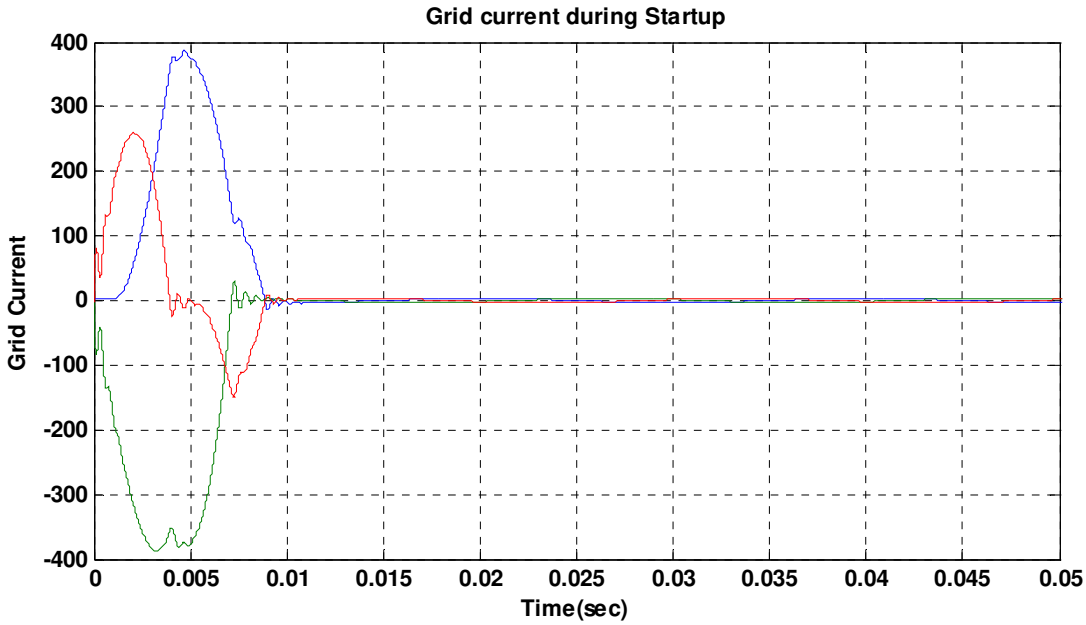

Figure 5-13 Start up Grid Current with Low DC link voltage

But how low should the DC link voltage be to require pre-charging? Well, as far as the grid current is concerned it is safe to work with a DC link voltage above 500V without pre-charging. But to avoid over modulation thereby compromise the controller performance, Pre-charging is recommended whenever the DC link capacitor voltage falls below 650V.

On other hand the filter capacitors on the DC side also need some pre-charging to the battery voltage or limiting/damping the inrush current from the battery to the filter capacitor before the charging process starts. If charging starts before this is done, the controller will malfunction as there is uncontrollable current oscillation between the battery and the filter. If not damped the current oscillation peak is very high. The following simulation result shows the battery current when the connection is not assisted by damping resistors.

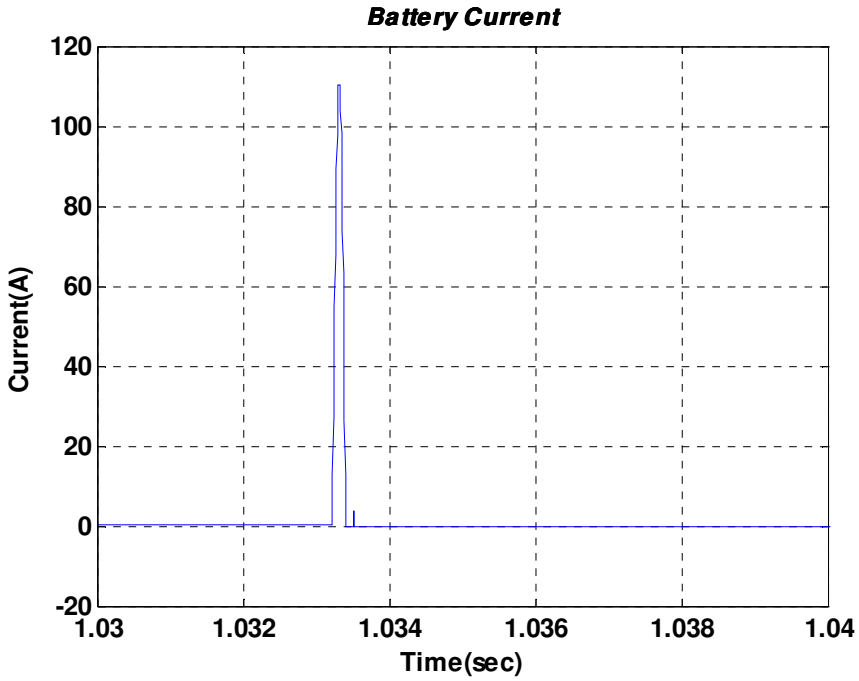

Figure 5-14 Overshoot in battery current

This overshoot in current is from the battery to the filter capacitor which is not welcomed by a battery which needs to be charged.

Then how to charge the capacitors? The DC link voltage can easily be charged to the peak line to line voltage using the already available diodes rectifier bridges in the VSC [34]. Using the appropriate series resistors, we can control the current level drawn from the grid. These series resistors are to be bypassed when the circuit starts supplying power.

Alternatively, the DC link capacitor could be charged to the required level using the same diode bridge rectifiers supplying the DC voltage through the DC/DC buck/boost converter. Here the appropriate switching mechanism should be used to make it work as per desired.

The first approach is best in limiting the current from the grid but it falls short of compromising the controller in the beginning for large current steps. Of course which ever approach is used the damping series resistor is necessary; and this results in power loss. But it is very low as it lasts for a short period of time.

The following simulation results provide the comparison of the two approaches. In the first approach the grid supply is connected to the VSC through the series resistors and left to charge the capacitor to the peak of line to line voltage. Then the resistors are bypassed where there is an extra inrush current. Meanwhile the DC filter capacitor is charged to half of the DC link voltage. Next the battery is connected with the DC/DC converter and synchronized with the filter capacitor.

In the second approach first the grid is switched in the DC/DC converter Battery side and it charges the DC link capacitor to 700V using boost strategy (shown in Figure 5-17). When it is done it is switched back on DC link side ready for operation. Then the battery

is connected to appropriate terminals of the DC/DC converter where, similar to the previous case, it is synchronized with the filter capacitor, then charging starts.

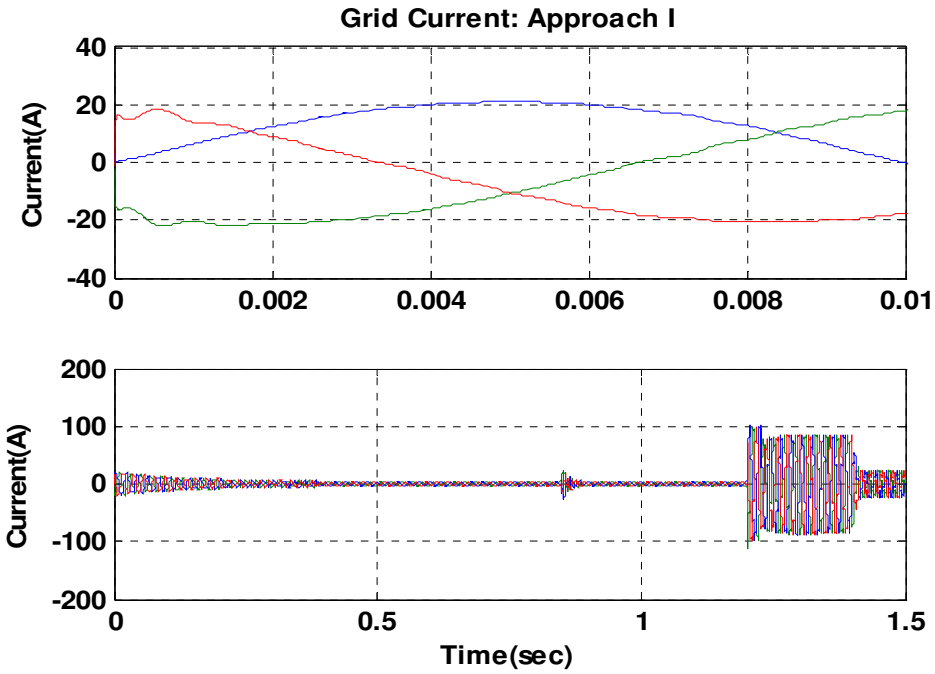

Figure 5-15 Comparison of Current from the Grid

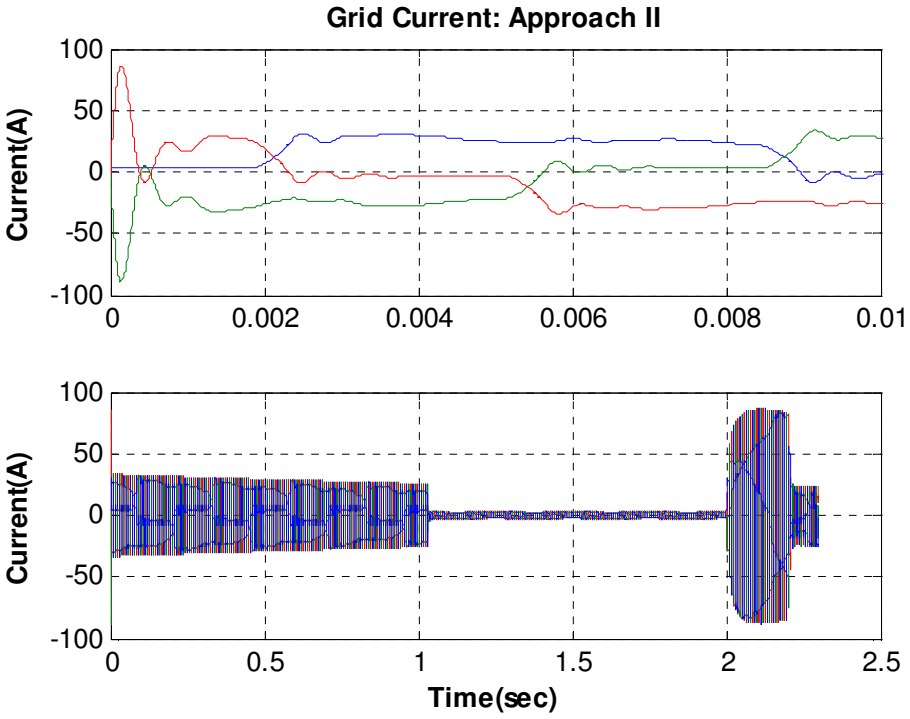

Figure 5-16 Comparison of Current from the Grid

It can be clearly seen the first approach is better in limiting the current in the beginning and results in less distorted waveforms. However, when charging starts there is an over-shoot, if the step current is of high value, as in the simulation.

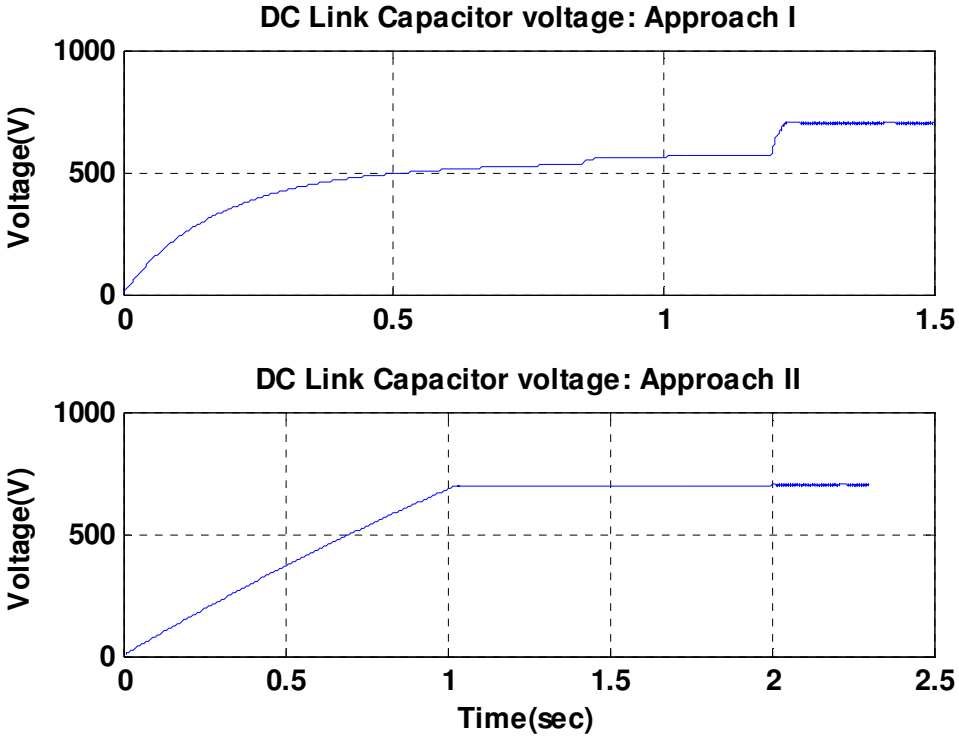

Figure 5-17 Charging the DC link Capacitor

This figure shows the process of charging the DC link Capacitor.

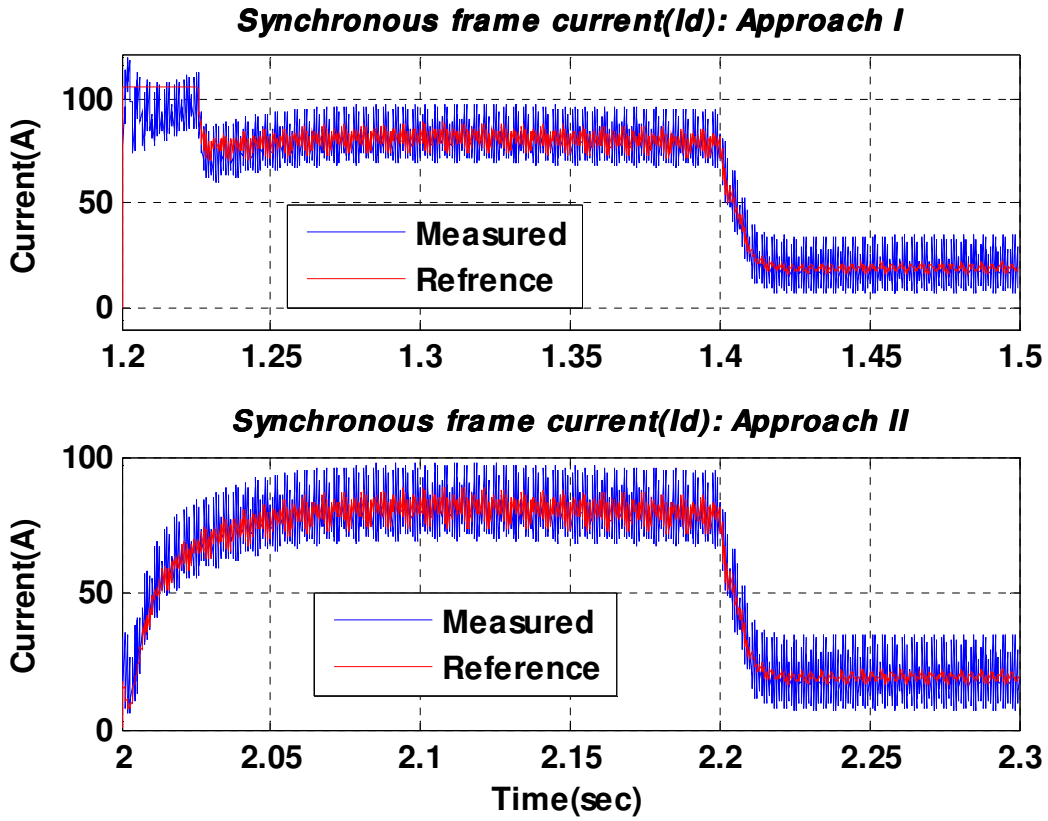

Figure 5-18 synchronous frame current

This is another view of the line current in synchronous frame. Here the current hits the limit and the controller goes for over modulation for the time the current is saturated. It is clear that the second approach is better in maintaining the current as desired by the reference value and there is no over modulation.

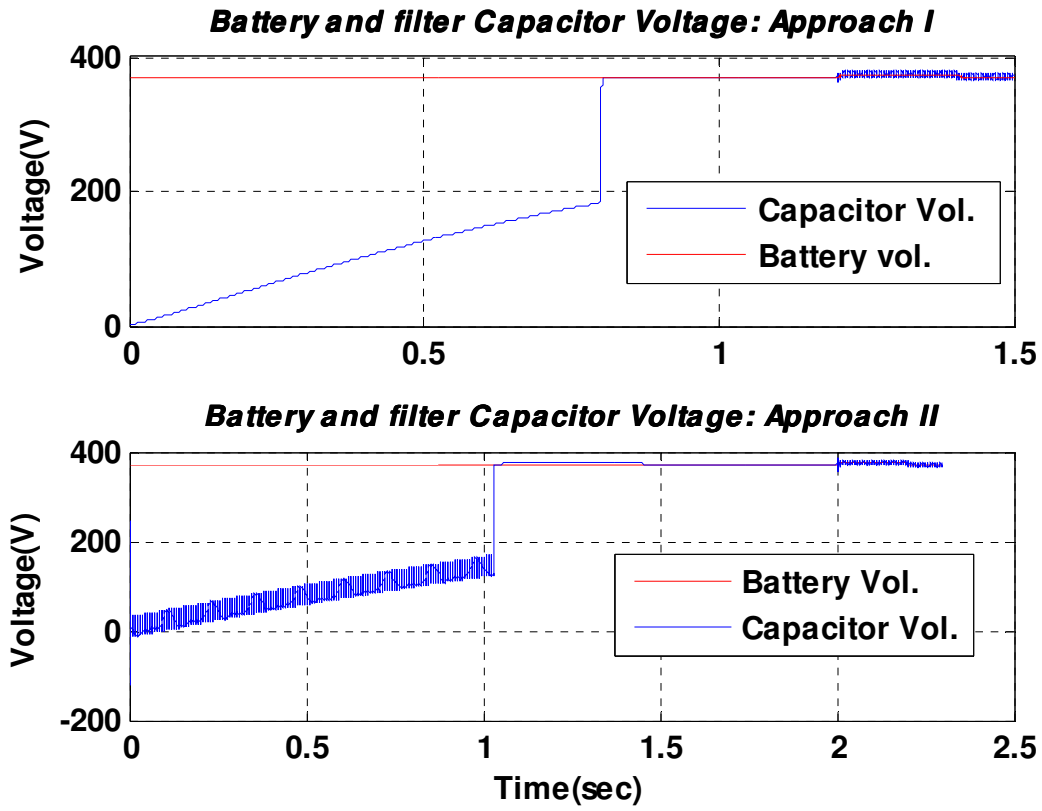

Figure 5-19 Filter Capacitor and battery voltage

In the first approached the filter capacitor is charged to half the DC link voltage though leakage currents owing to the voltage felt due to its position in the circuit. This of course should be facilitated for two reasons one the filter capacitor needs to be charged anyway. The second reason is that it will relieve the stress from the upper IGBT in DC/DC converter.

In the second approach the filter capacitor is directly charged. Also in the beginning the there is an inrush current which is safe relative to the rating of the capacitor.

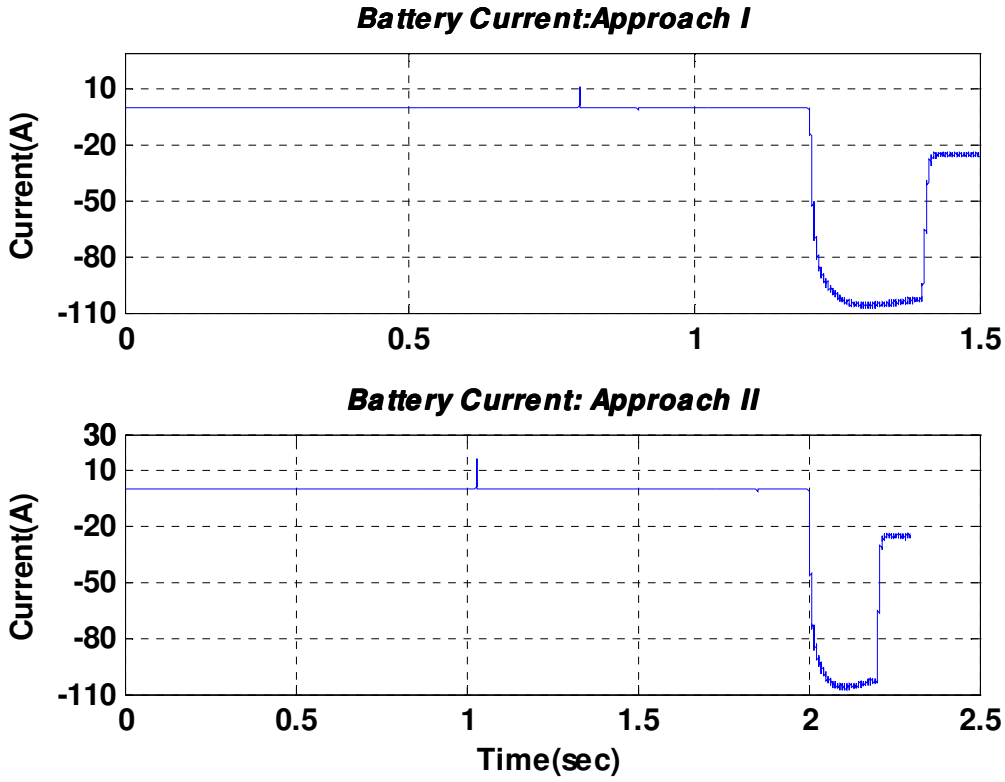

Here we see that when the battery is connected to the filter capacitor there is a current flow (at time 0.7(I) and 1.01(II)) from the battery to the filter capacitor owing to the voltage difference existing there. This phase is assisted by a damping resistor in both approaches. Comparatively this current is low magnitude and highly damped. Both approaches almost result in the same performance.

In the meantime, whenever the DC link voltage is not at its set value, it is vital that we low pass the Step from the measured Dc link voltage value to the set level to lower the overshoot that could occur.

At the end, which approach to use is dependent on the suitability of the implementation and the cost of the components to be used. The first approach requires a three phase series resistors and one three phase by pass breaker while one DC breaker and one IGBT and a resistor are enough for the second approach. The rest component requirements are similar.

5.5.3 Reference current generation for the q component of the grid current

There is a phase difference between the grid voltage and the capacitor voltage owing the voltage drop over the filter inductance. And maintaining a zero angle difference between the capacitor voltage and line current does not guarantee unity power factor from the grid. Therefore to draw a load at unity power factor form the grid, the q-reference current should be different from zero. Here the simple relation between the grid side current (I2),

capacitor voltage (Uc) and converter side current (I1) is exploited. This is written as follows- considering steady state

$$I_{2d} = I_{1d}$$
$$I_{2q} = I_{1q} + \omega C U_{cd}$$

5-1

The philosophy is the ratio of synchronous frame grid current and synchronous frame grid voltage should be equal. To maintain equality in the ratios the equation above is used without the need to measure the grid current. The Simulink diagram of the implementation is provided below.

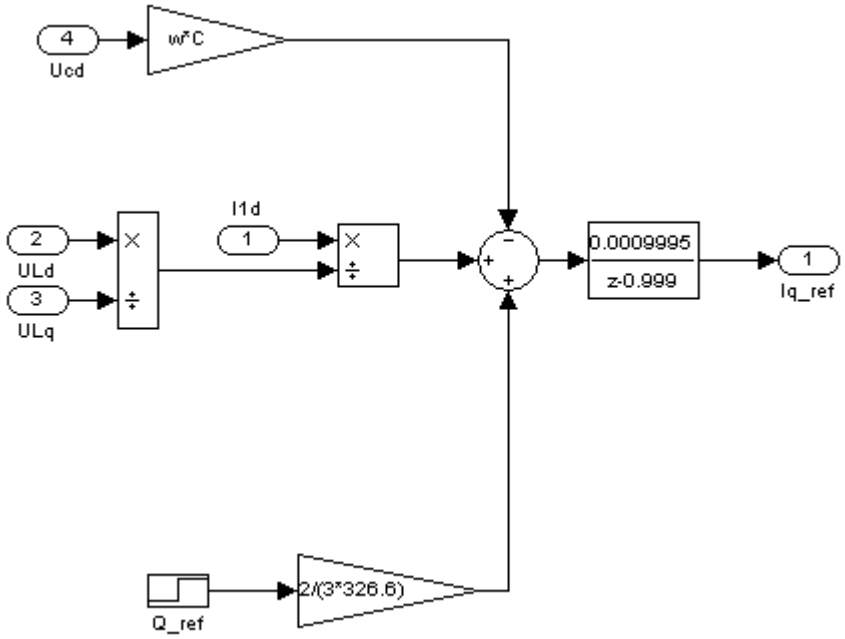

Figure 5-20 Simulink diagram for Iqref generating

A low pass filter is used to remove the high frequency ac component which inherent in the measured signals.

The approach is more pronounced when low power is drawn from the grid where the reactive power is higher at zero q-reference current. The following simulation result shows the same when the power drawn from the grid is 10Kw. In the simulation after the charging is started in the first 0.2 sec the q-reference is set to zero then the above algorithm takes over.

From the simulation the algorithm is good as producing the reference current. The reactive power drawn from the grid decreases but it does not assure zero reactive power. This is due to the approximation inherent in the above equation.

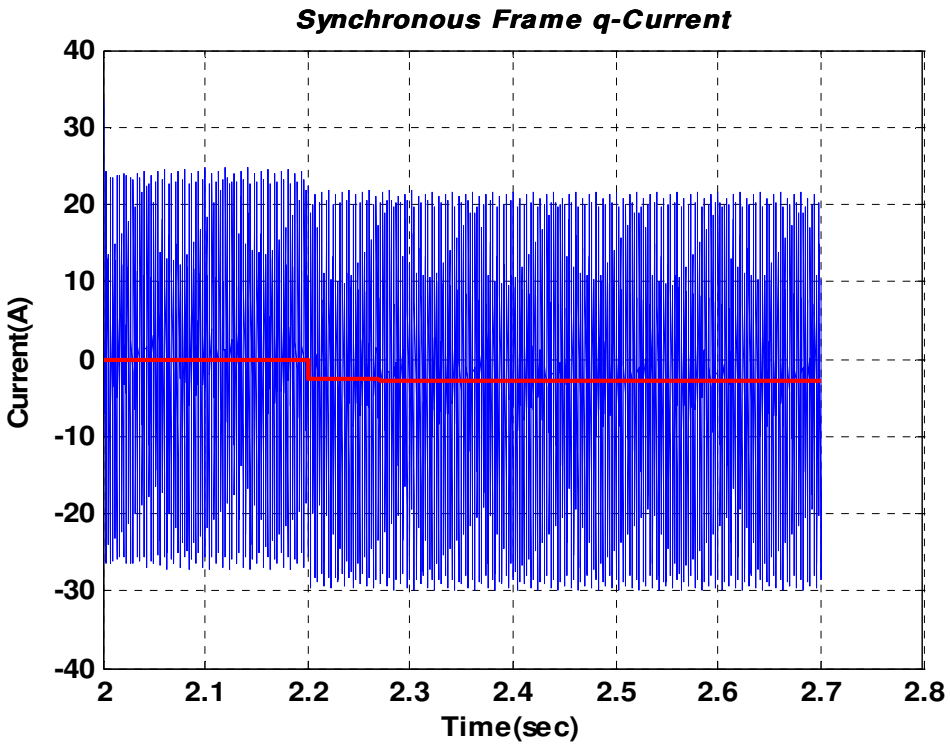

Figure 5-21 Synchronous frame q current

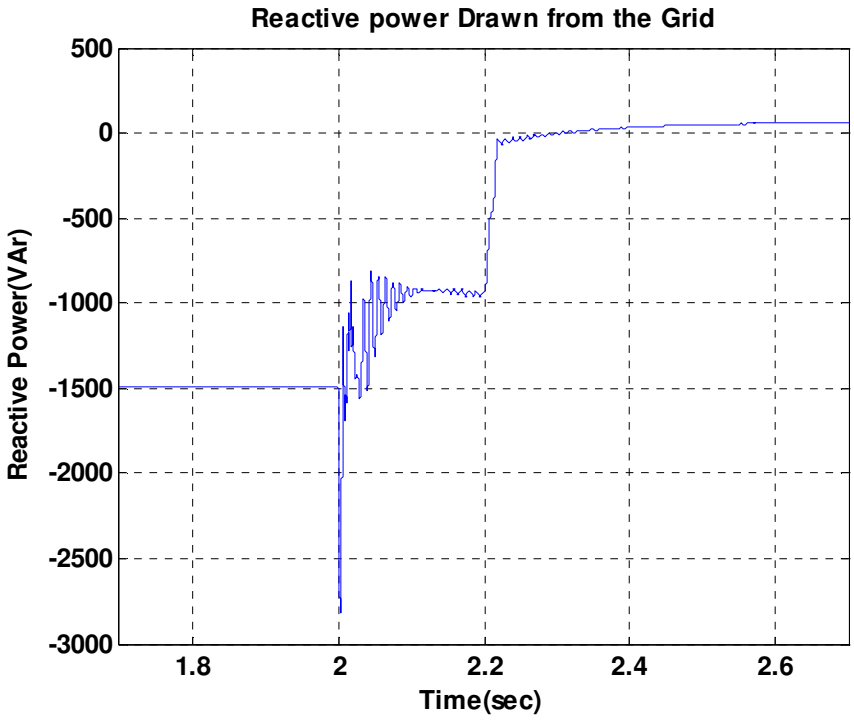

Figure 5-22 Reactive Power from the grid

6 THE SOLUTION: THE CHARGE SUPERVISORY ALGORITHM (CSA)

As mentioned in the introduction, the main aim of the thesis is to insure safe and reliable charging in case the BMS malfunctions. In another way the work in thesis enables the charging system to be aware of what is going on. It enables the charging system to take decision on whether the BMS working properly or not, if not, it will take over the charging process all in all and ensure safe charging.

Thus this section, taking inputs from previous sections, describes how this is accomplished. However, due to versatility xEV battery system, it was necessary to make some simplifying assumptions. Hence the section starts by stating these simplifying assumptions. It also explains how practical these assumptions are.

6.1 Assumptions made in the algorithm

Assumption I: this assumption deals with the maximum allowable battery terminal voltage. That is, there is standardized maximum voltage limit for all batteries used in xEVs. Or the maximum voltage limit for each vehicle type is available from the BMS.

Reasons for the assumption: To avoid damage to the battery the voltage limit of the battery should not be violated. However, in battery charging, especially fast charging environment it is possible for battery voltage to reach the limit while the battery is not fully charged. If an off board battery charger should participate in supervision of the battery it is important that it should have this knowledge. Moreover it is impossible for the off board battery charger to decide this limit in any way if it is not provided.

Practicality of the assumption: Almost every equipment has standard working voltage but EV Batteries due to the early stages in development, standard voltages are not yet decided. Thus it is possible for standard voltage limits to be set for xEV batteries. When this is not available, it is possible to make this information available from the BMS. Such information is already available in the so called intelligent batteries [43, 45]; however it is not clear if they are there in all xEV batteries.

Assumption II: This assumption comes into play to validate the charging current demanded by the BMS. That is, the current demanded by the BMS is correct unless it results in abnormal temperature increase; like if it is found that the temperature will hit the limit in a short period of time. Also if the BMS should demand comparatively low current, an appropriate current will be provided keeping in check the temperature increase.

Reasons for the assumption: this is a must assumption based on the information available to the author presently. As such there is no information available to relate the battery capacity or internal resistance to specific current revel. Someone may raise the question 'How then are the manufacturers determining the charging capability of a given battery?' well manufactures do specify the current rating or current capability of a battery based on:

- Electrochemical characteristic consideration: such as the battery electrolyte concentration, electrode geometry and many other microscopic considerations. Dif-

ferent values are given for short term and long term ratings of a battery. This appears in manufacturer's datasheet as a pulse current of specified duration or continuous current.

- Practical consideration: such as how long should the battery be used? For example you can use a battery rated 10A for 15A provided that it conforms to condition 1 above, but it will have shorter cycle life. Moreover the limit for cycle life also depends how we interpret it. For example the usual trend is the battery is at the end of life it is 80% of the original capacity. And of course there is no a mathematical relation which some body can use to relate cycle life with a charge or discharge current.

Batteries are optimized for energy or power, and they could be different chemistry. Even if they are assumed to be ,say, energy optimized and are specific chemistry, say Li-ion, there is no information available to the author on how to determine the charging current of the battery on the basis of information that could be available online while charging.

However there could be another way into the problem by monitoring the charging efficiency; considering the inefficiency due to voltage drop over the internal resistance alone. Consumer electronics battery charging typically results in charging efficiency of 99.9% [44]; usually slow charging. However it clear that fast charging will be less efficient. But presently there is no information to the author what the limiting efficiency on fast charging is.

Practicality of the assumption: Even though this assumption does not result in optimum charging, as optimality depends on how we specify it as described earlier, it does insure a safe charging strategy.

Assumption III: this assumption is concerned with thermal related issues. Here the assumption is that there is same maximum charging temperature limit for all batteries or they are available from the BMS. And all temperature rises while charging should be limited below certain value; and this is the same for all battery types.

Reasons for the assumption: almost all batteries for xEVs release heat during charging process. Depending on the heat released and the cooling system, this results in temperature rise. All xEV batteries do have a maximum charging temperature, if this limit should be violated, the battery performance will deteriorate. However not only should we consider the temperature limit, but also the temperature increment during charging as discussed in section 2. This temperature limit and increments could vary from battery to battery. Unless we are supported by 'assumption III' it is not possible to determine them in anyway.

Practicality of the assumption: as mentioned above the temperature limits do vary from battery to battery. As long as our concern is safe charging if we could take the safest temperature limit. That is, among available battery types we take lowest temperature limit available. For example for Li-ion batteries investigated in this report this temperature limit is 40^0C (refer to Table 2.3 the performance characteristics of lithium-ion cells of different chemistries from various battery developers **[6]Table 2.3**). Moreover it is possible that this information is available from the BMS as in intelligent batteries [43, 45].

Assumption IV: this assumption has already been mentioned on section three in relation thermal modeling. Here we only mention the assumption for the sake of completeness. It is assumed that thermal generation less cooling system is constant i.e. the net heat generation is constant.

Assumption V: this of course could be considered more of an approach. Presently most manufacturers recommend constant current/constant voltage (CC/CV) charging. However there could be also another better way of charging the battery as in [46]. But in this thesis CC/CV is charging strategy is followed. That is CC/CV from the BMS for all vehicles are assumed.

Now based on these simplifying assumptions, the different optimization routines will be discussed.

6.2 Implementation

The overall supervisory algorithm has six main routines. These are

- Model Parameter Identification Routine (MPIR):-this includes every process and procedure involved in the parameter identification, state adjustment though Kalman filter and so on. This is discussed in section four.
- Battery Voltage Monitoring Routine(BVMR)
- SOC Monitoring Routine(SOCMR)
- Temperature Monitoring Routine(TMR)
- Minimum Current Generating Routine(MCGR)
- Reference current Generating Routine(RCGR)

The last five routines are discussed below. Before that Figure 6-1 gives the clear picture on how the overall structure works and how the different routines interact to each other.

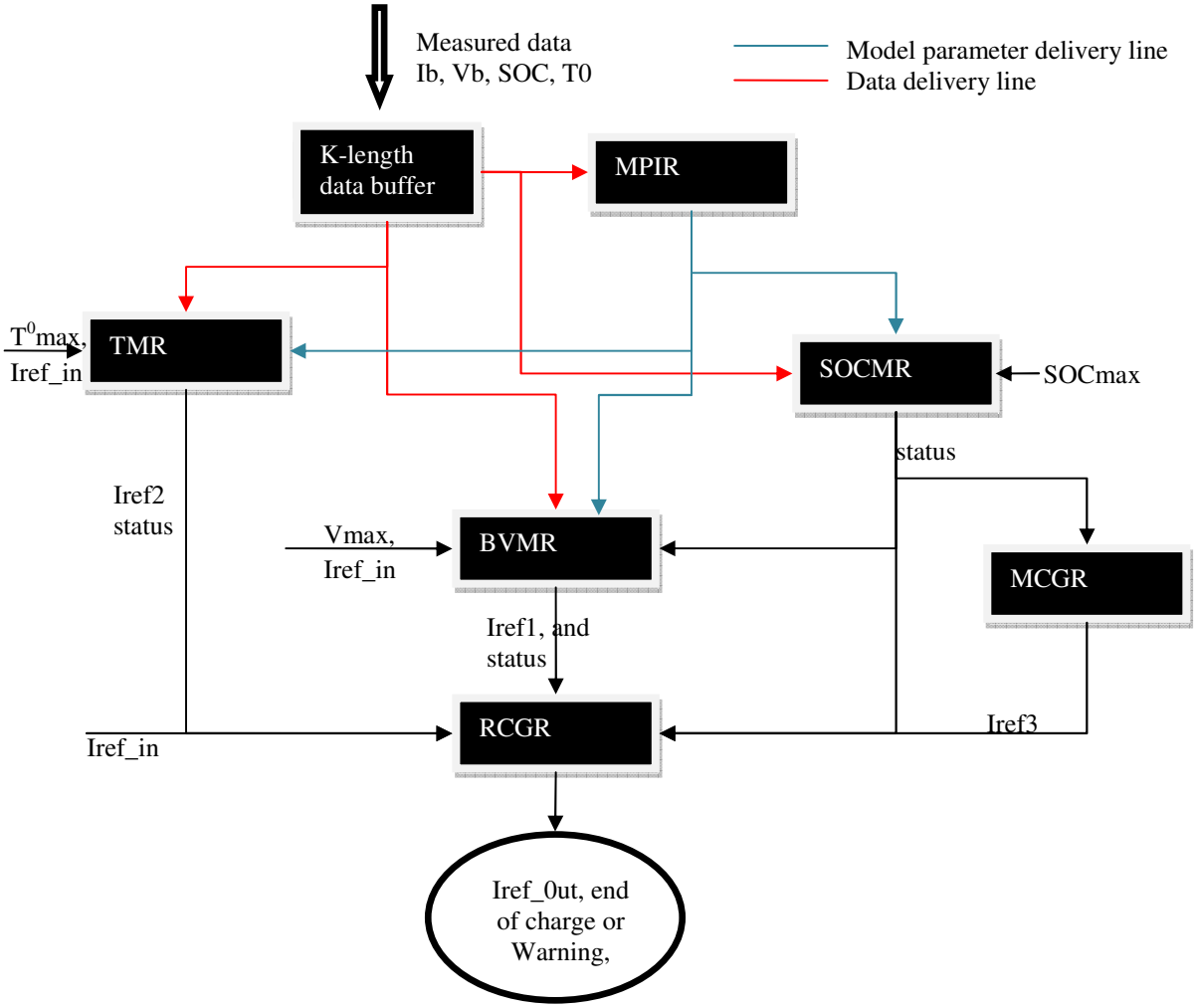

Figure 6-1 the overall charge supervisory algorithm

As can be seen on Figure 6-1 the overall aim of the routine is calculating safe value for reference current or issue warning. The system gets input about the battery current (Ib), voltage (Vb), temperature (T^0), SOC, current reference (Iref_in) from the BMS. Using this data the supervisory algorithms executes the different routines shown in the flow chart (see Figure 6-1) each time step. However within each routine some computation demanding executions are done after predetermined sample intervals. These will be mentioned in corresponding sections.

6.2.1 State of charge Monitoring routine

As discussed earlier in section four, we have to rely on the BMS to get information about the SOC of the battery. However these readings should be validated to check if, for some reason, the BMS is malfunctioning. If they are found to be valid they are used for charge monitoring purpose.

Figure 6-2 shows the SOC reading validation and monitoring routine. The routine starts by initializing the different status report values. It also gets most recent current and SOC reading from the data buffer and model information from the MPIR. It calculates the error between the model predicted values and the reading. Then the necessary decisions are taken as given in the flow chart.

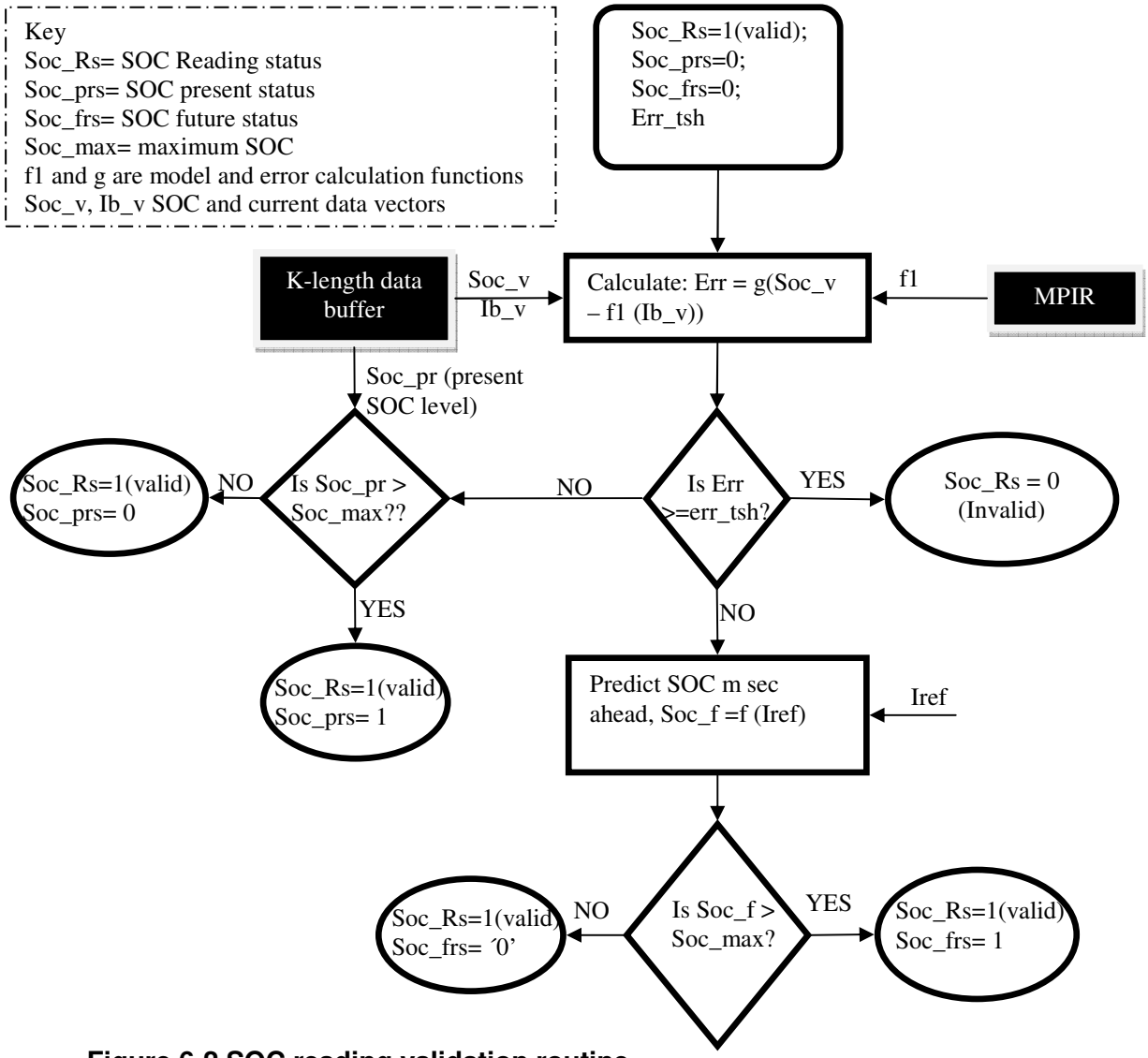

Figure 6-2 SOC reading validation routine

The actual implementation is not exactly as it appears. SOC reading validation routine is done only every 5 sec while the rest are done each sampling interval where the sampling interval is 0.2 sec.

6.2.2 Battery Voltage Monitoring Routine (BVMR)

This routine is entitled to make sure the maximum voltage of the battery is not violated. The following flowchart in Figure 6-33 provides an over view of how this routine

works

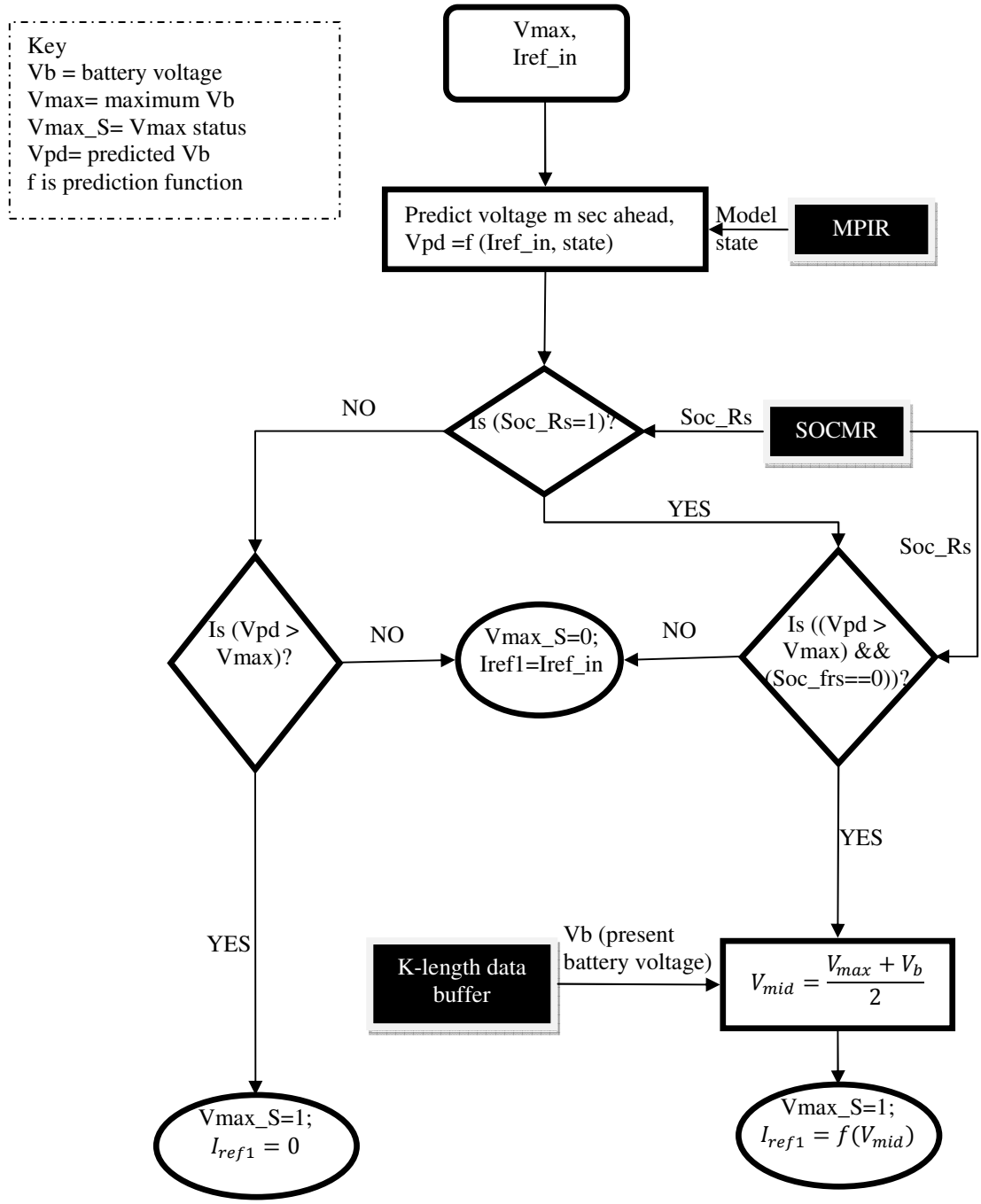

Figure 6-3 flow chart for battery voltage monitoring routine

The input to this routine is the battery model and current state from the optimization routine and the current reference from the BMS. It predicts the voltage steps ahead and if the predicted voltage is found to be equal to or greater than the limit voltage and the maximum soc level is not attained in the meantime, the current which results in the mid voltage between the current battery voltage and the maximum voltage is calculated. This current is taken as a reference. Otherwise the same reference current as given by the BMS is taken as reference current in this routine. Finally this current level is passed to MPIR for

further decision making. Moreover some more issues like what if the BMS changes the current reference a bit later is also included which is not shown in the flow chart.

6.2.3 Temperature Monitoring Routine

The overall temperature monitoring routine is shown in **Fel! Hittar inte referenskälla.**. The basic procedure for validation is the same as SOC reading validation routine, the difference is only the inputs i.e. the model and the data (temperature). The temperature is predicted steps ahead and if it is going to be on or above the limit the reference current is halved, provided the reference current is not changed from the previous step (not shown in the flow chart). The routine also considers the BMS reference current reduction if it happens in the next steps which are not shown as well.

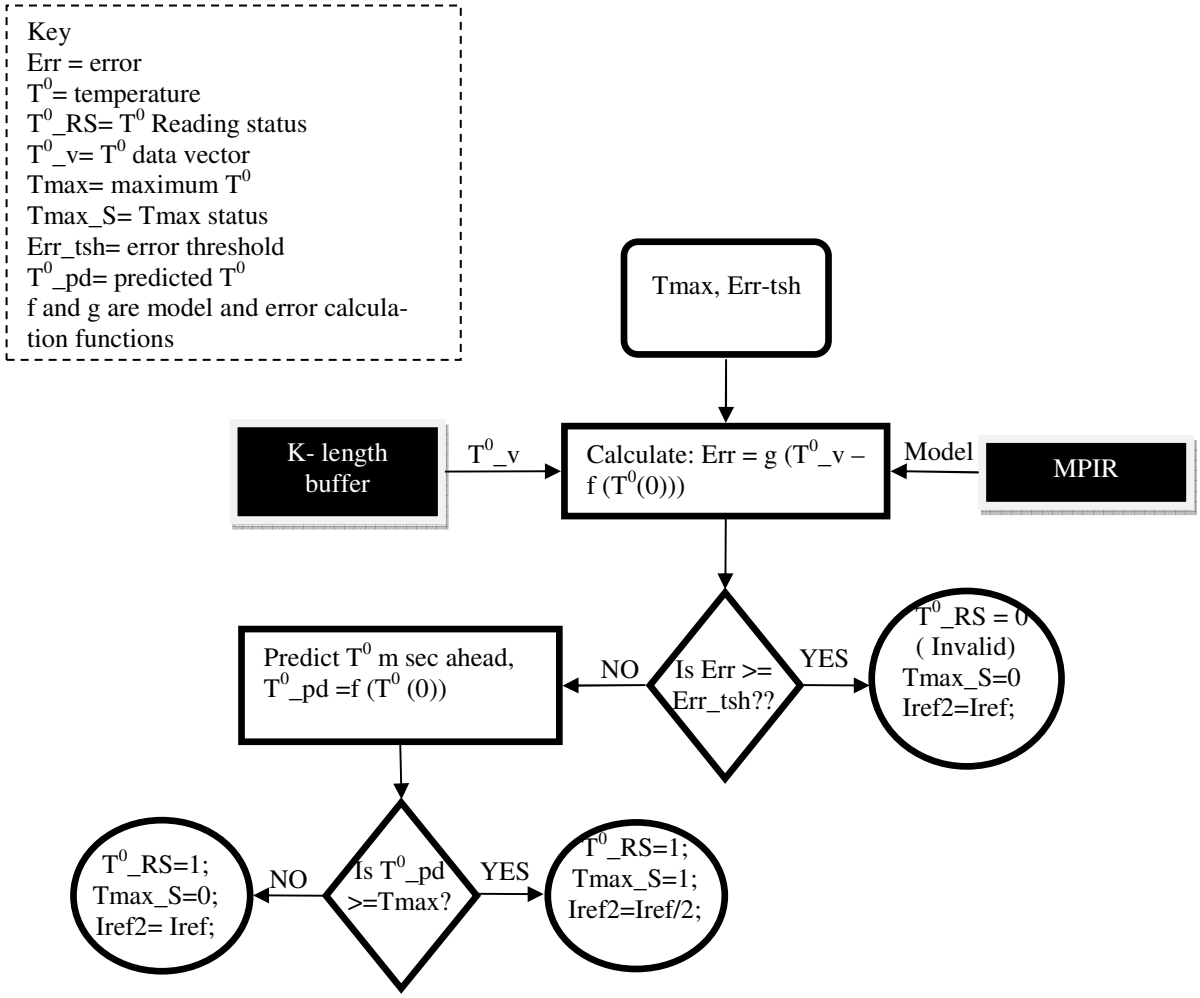

Figure 6-4 Temperature Monitoring Routine

6.2.4 Minimum Current Generating Routine (MCGR)

This routine intended to give the minimum current incase the BMS provides very low current reference for some reason. This current value is calculated based on the time it takes to charge the battery to the desired level. Figure 6-6 shows the flow chart for MCRG routine.

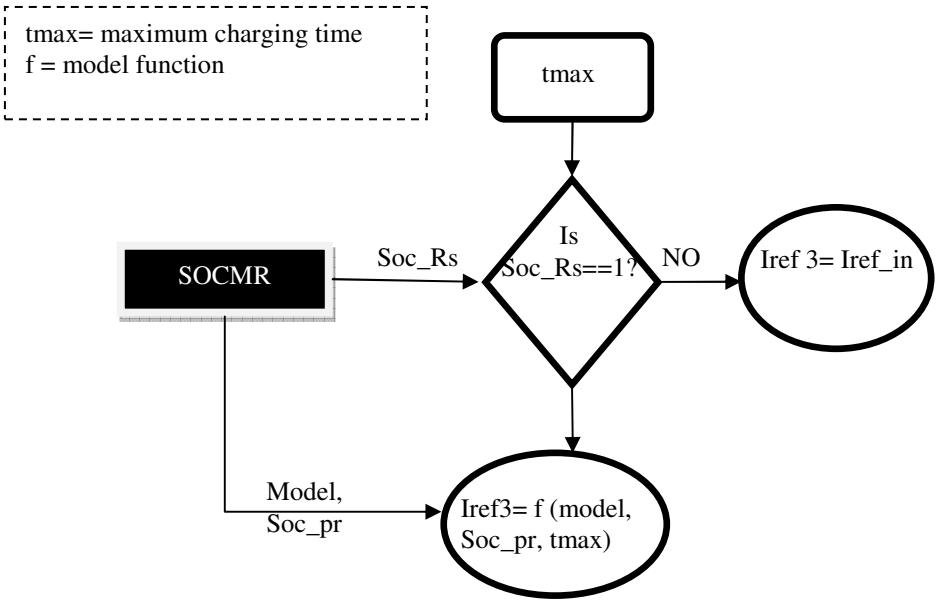

Figure 6-6 MCGR routine flow chart

6.2.5 Reference current Generating Routine (RCGR)

This routine takes current references from different routines above makes the appropriate decision on current reference based on the available status information.

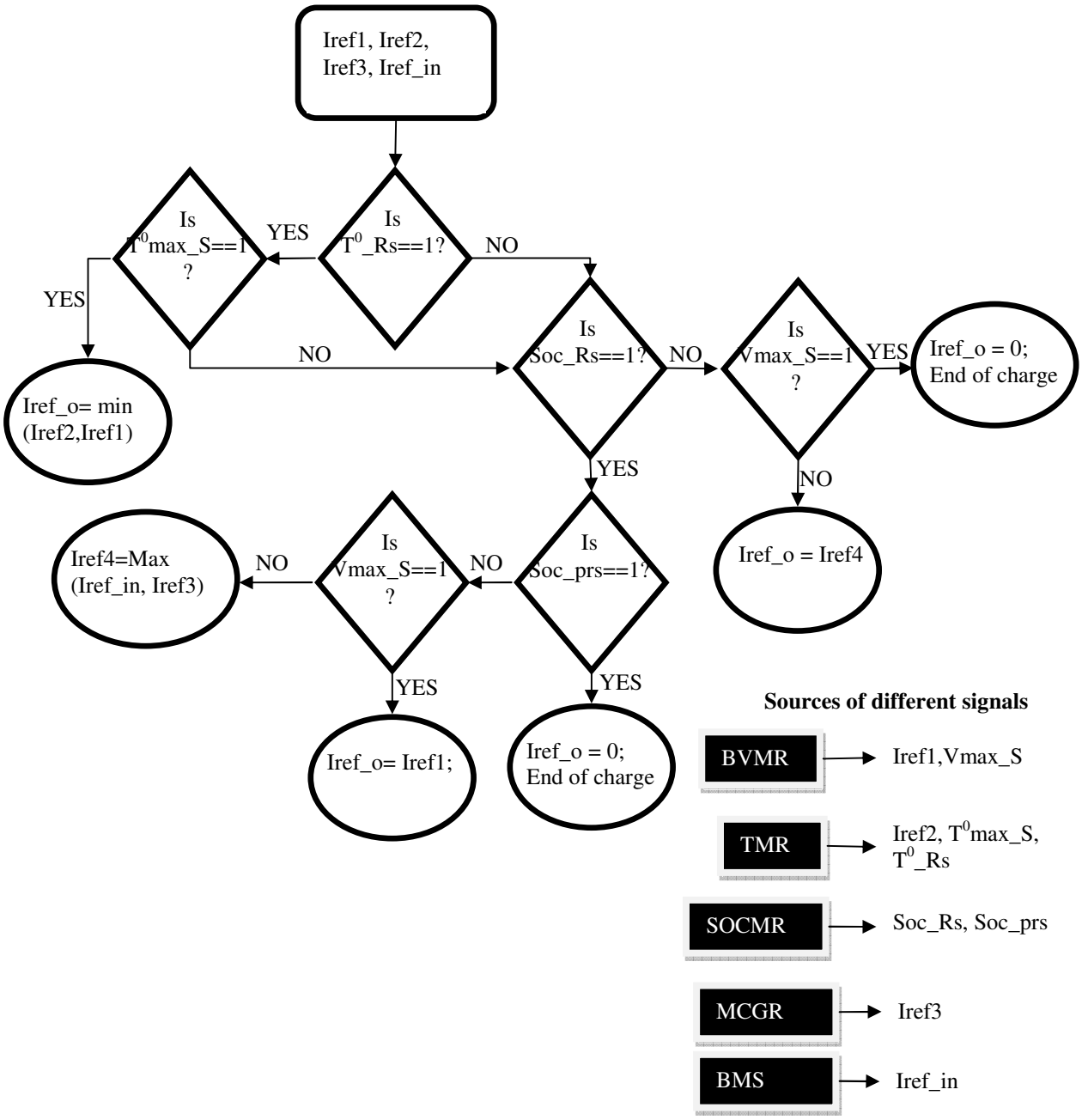

Figure 6-7 Reference Current Generation Routine

The above flow chart clearly depicts how the right current reference is chosen. In the figure 'Iref_in' is the reference current from the BMS and the rest signals come from the respective routine shown in the Figure 6-7.

7 RESULTS AND ANALYSIS

This section provides an analysis of the different routines discussed in section 6 creating some scenarios. The aim of this section then is to show the performance of the routines and how well coordinated their response is. However, before that the following subsection provides how the simulation is setup.

7.1 Simulation set up

Figure 7-1 shows the Matlab model of the simulation

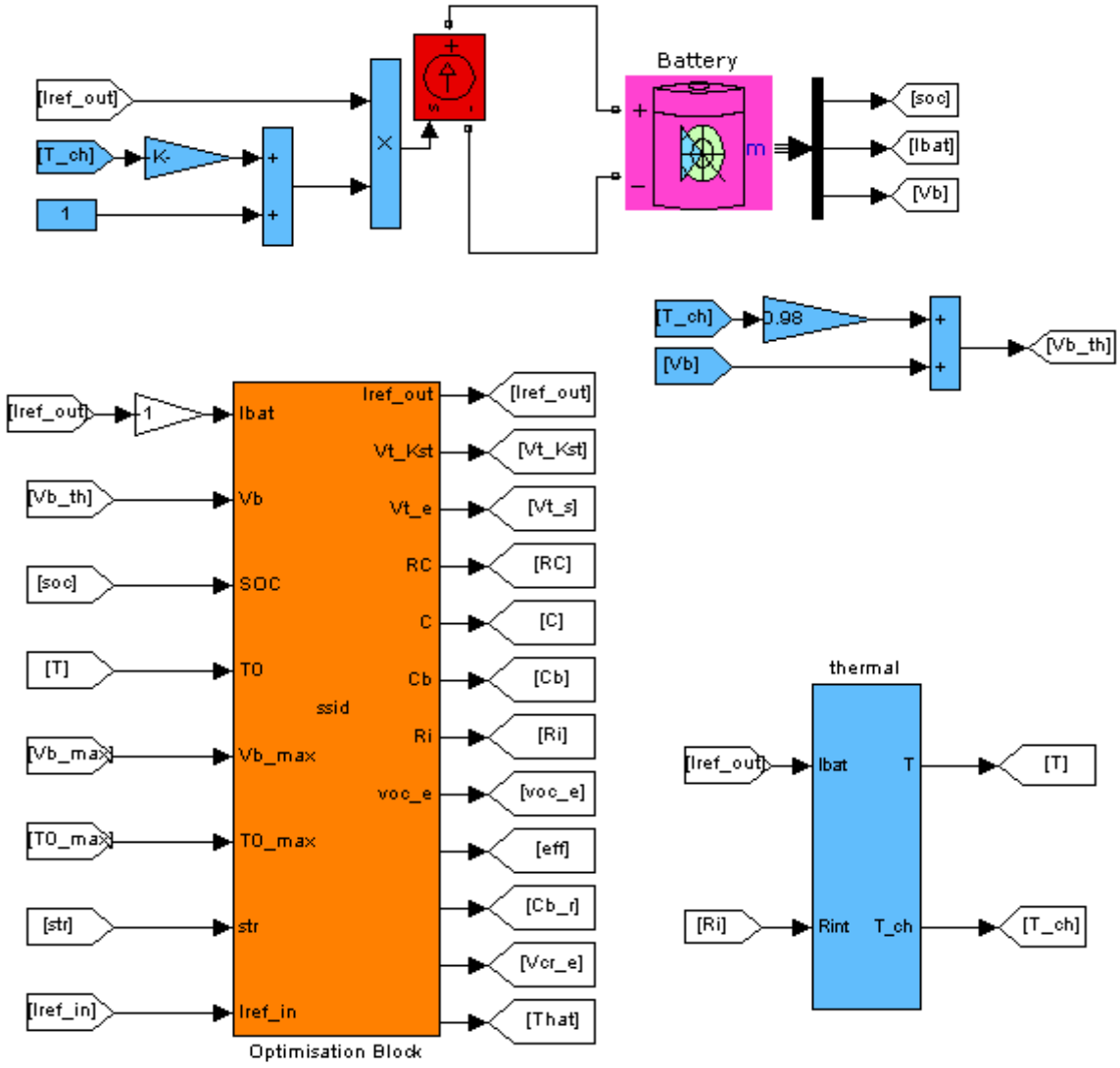

Figure 7-1 Matlab model of the simulation setup

There are four main blocks shown in fig 7-1,

- The battery model (Magenta)
- The thermal model (Light blue blocks)
- The controlled current source (Red)
- The Optimization block (Orange)

7.1.1 Simulation model for battery including thermal model

The battery model used is the model that comes with Matlab in SimPowerSystems toolbox. This model is implemented using the model highlighted at the end of section 3.2.3; but it does not include thermal model. Thus there is a need to include thermal model.

At the end of section 3 we have discussed thermal related issues of a battery. Here we have applied the same principle to include thermal model to the given battery model. Here is how it is done: the block in Figure 7-2 calculates the temperature rise for a given charging current. Given the initial temperature of the battery, the change in temperature is calculated. Some representative model parameters are given in Table 7.1.

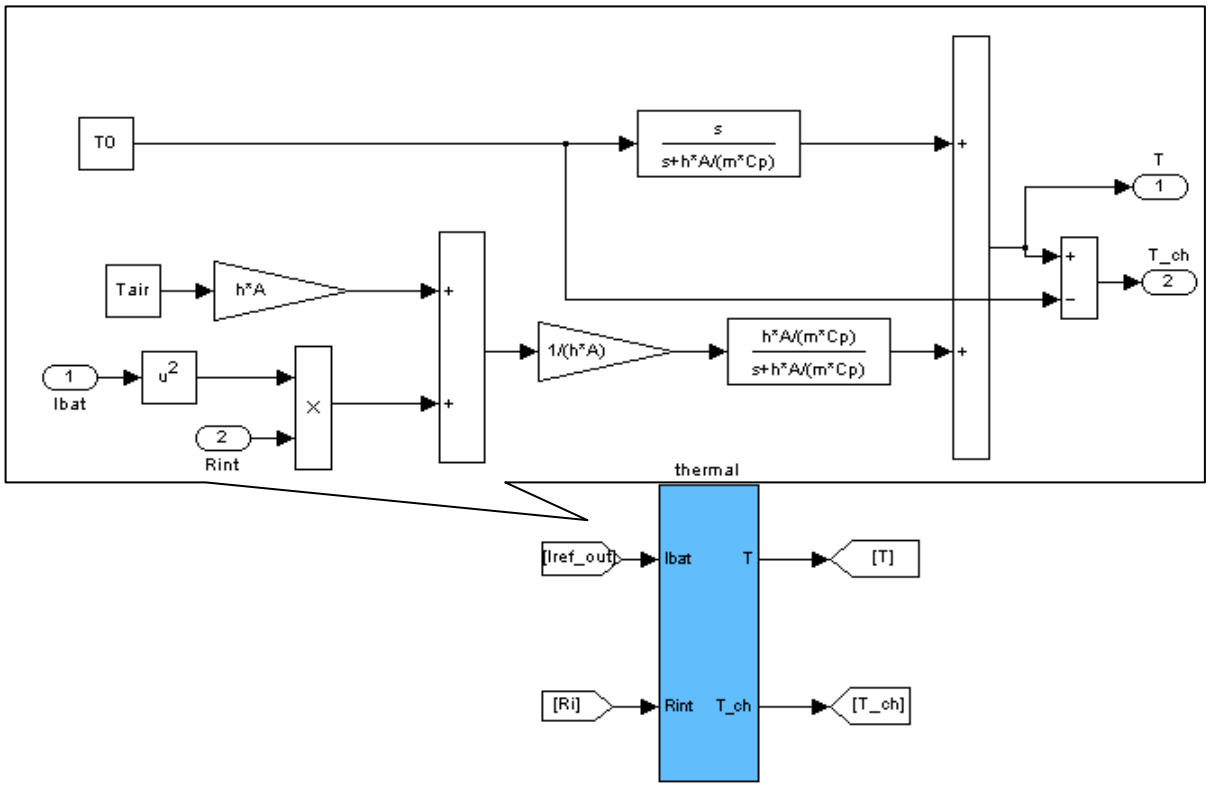

Figure 7-2 Simulink model for calculating the temperature rise in a battery during charging

Table 7.1 Thermal model parameter values

Parameter	definition	Value
h (W m^{-2} K^{-1})	The heat transfer coefficient for forced convection	5
A(m^2)	Battery surface area exposed to the convective cooling medium (typically air)	2.0755
M(Kg)	Mass of the battery	250 [7]

Parameter	definition	Value
Volume(m^3)	Volume of the battery	0.15 [7]
Cp(KJ $Kg^{-1}K^{-1}$)	Specific capacity of the battery	1.0118 **Fel! Hittar inte referenskälla.**
T0(^{0}C)	Initial battery temperature	25
Tair(^{0}C)	Ambient temperature	25

The heat transfer coefficient is something which is dependent on the battery cooling system and there is no information to the author what the typical value is. But here its value is chosen to have the effect that is required. The mass and volume of the battery is taken from [7] (USABC battery goals for EVs). And If we take one of the Li-ion batteries in **Table 2.3** (say the one in [48]) and dimension it according to EV requirements in [7], then we get the surface area of the battery exposed to air approximately as in Table 7.1. It is assumed that the ambient temperature is 25^{0}C and the battery temperature initially is the same as the ambient temperature. One can assume whatever initial battery temperature as long as it is in the operating range of the battery. The specific heat capacity of lithium ion battery is taken from reference **Fel! Hittar inte referenskälla.** which is the specific heat capacity for a typical Li-ion polymer battery used for EV application.

However these are just representative parameters for fictitious battery and not actual battery; such information is hard to find for a given battery. Moreover what is needed to see is if the temperature monitoring system predicts future temperature correctly and how it reacts whenever triggering events occur. In that respect the given parameters fulfill the objective of the simulation.

As it is specified in section 3, to simplify things, it is assumed that the change in charge acceptance and open circuit voltage are linearly related to the change in temperature. The change in open circuit voltage (see eq. 3-16) is evaluated as shown in Figure 7-3.

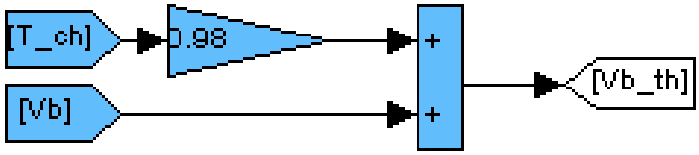

Figure 7-3 Modeling effect of temperature on battery voltage

Here the gain is taken by linearizing the curve given for temperature-dependent potential-correction term in Ref [9].

The input to optimization algorithm is 'Vb_th' which is considered as the measured battery terminal voltage.

The change in charge acceptance (see eq. 3-15) is incorporated by manipulating the current flowing into battery (see Figure 7-4).

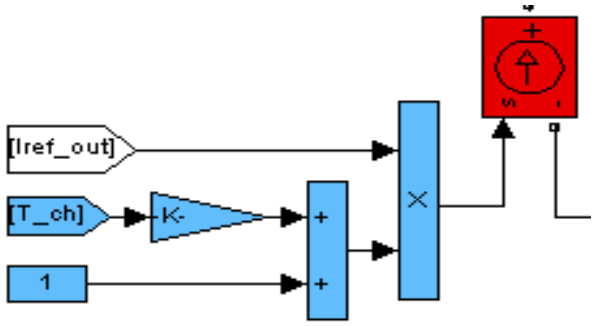

Figure 7-4 Modeling effect of temperature on charge acceptance

Here once again the gain term is taken from reference [9] in similar procedure as mentioned above.

From Figure 7-4 Modeling effect of temperature on charge acceptance, for a given reference current 'Iref_out' the rate of change of SOC will be different depending on the temperature of the battery. It is achieved by manipulating the actual current flowing into the battery. However what the optimization algorithm knows is that the current flowing into the battery is the same as the reference current provided by itself in the previous routine.

The approach used in the simulation set up to model the change in charge acceptance is not completely genuine as there will a difference between the current that is assumed to flow into the battery and what actually flows. Even though this properly models the change in charge acceptance it could affect the current-voltage (V-I) relation of the model. The proper modeling would have been a allowing all current to flow in and then manipulating the capacity of the battery depending on the change in temperature. It is used here this way as there is no way to manipulate the capacity once the simulation is started with given simulation set up. But since the temperature change is very slow it has negligible effect on the V-I relationship of the battery.

7.1.2 The converter simulation model

Using the actual converter model in the simulation is very computation intensive and time consuming. In section 5 we have discussed the converter and it is seen that, except for starting process, it can be considered as a controlled current source. Therefore all of the simulation results provided below use a simple controlled current source as shown in Figure 7-1. It is controlled by the reference current provided by the optimization block.

7.1.3 The optimization routine

Finally the optimization routine includes all model identification and decision making processes discussed in section 4. It is implemented In S-function.

7.2 Results and Analysis

7.2.1 Identification

Before looking at the results, let us ask our self the question: 'what do we want to see in identification?' One answer is the identified parameters must be able to predict correctly.

The other is the identified parameter values should be nearly constant for time invariant models, or slowly varying for time varying models. Here we have a battery model with time varying characteristic. But the thermal model and the SOC models are nearly constant. This can easily be understood from the way the model is formulated and is setup for simulation. Let us see first their prediction capability.

7.2.1.1 Identified model prediction capability

Model for terminal voltage prediction

Figure 7-5 shows the prediction performance of the V-I relationship Battery model. It can easily be seen that the prediction performance very good. The prediction is started once the optimization routine has collected enough data to optimize the battery model parameters. In this simulation the time it takes is 5 sec with sampling interval of 0.2sec. That is the minimum data length used for optimization is 25 sample data.

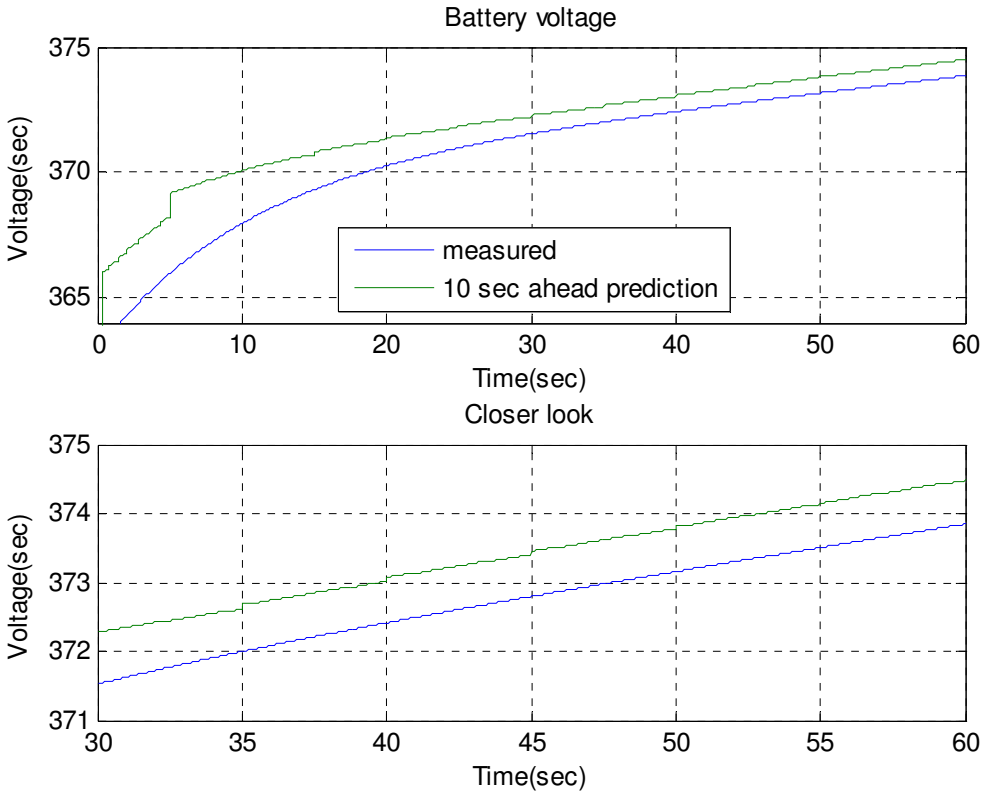

Figure 7-5 measured and predicted voltage

Model for State of charge prediction

Similarly Figure 7-6 shows the prediction performance of the SOC model.

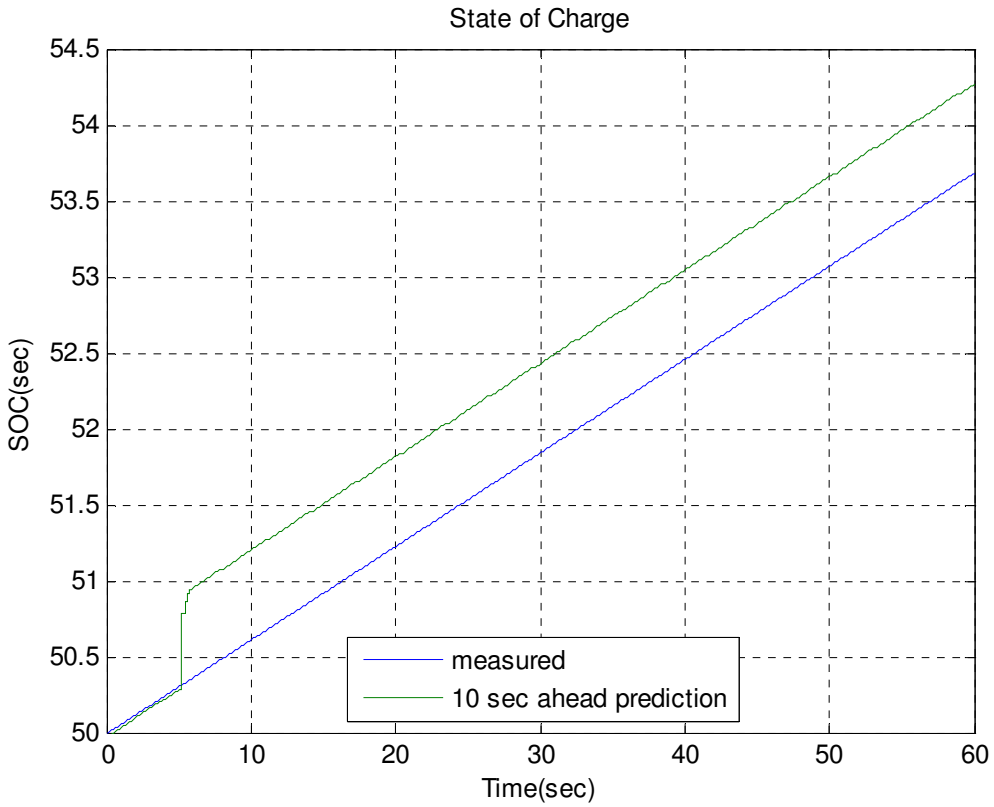

Figure 7-6 Measured and predicted SOC

Model for temperature prediction

If the exact parameter values as in Table 7.1 are used, the thermal constant of the battery will be around 6hr and 45 min; this is usually the case for battery thermal time constants. However, the simulation will not show any visible result for thermal behavior of batteries and predicting the temperature after 10 sec or even 10 minutes will give no benefit as the temperature change is very small. Thus for batteries working under normal condition such prediction is not necessary and the battery thermal model can be approximated by linear model which then can be used for validating the temperature reading. However if something goes wrong and if the temperature starts to increase rapidly, assuming this temperature rise follows the model developed in section 3, the same model can be used to take action in time. Therefore to simulate such effects and to see more clearly the prediction capability of the temperature monitoring routines the specific heat capacity of the battery is reduced to 100. The following figure shows the same. The remaining simulation results on temperature monitoring use the same value.

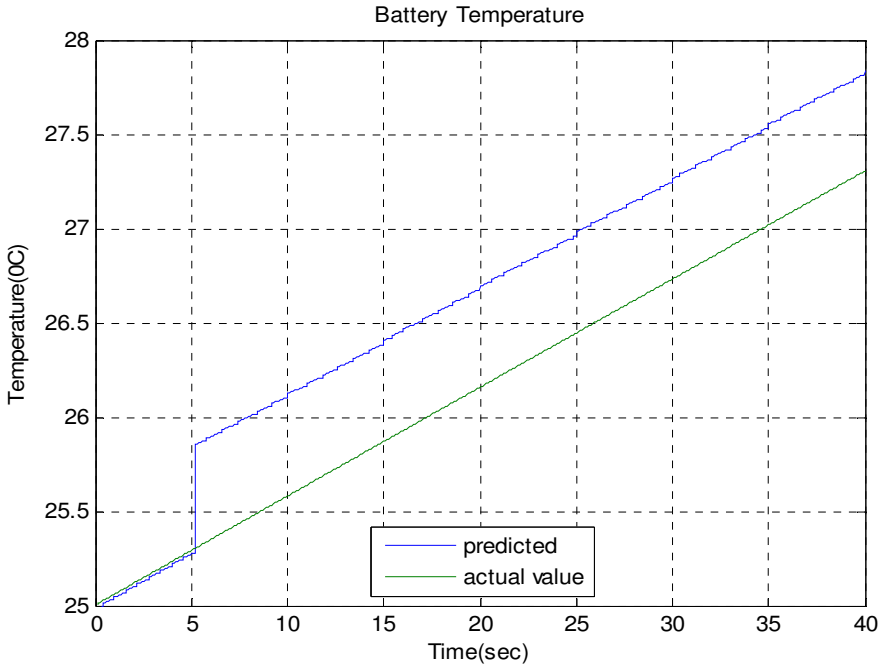

Figure 7-7 Measured and Predicted Temperature

In all of the figures above we see one fact: they all show good performance in predicting 10 sec ahead.

Before concluding this subsection let us see the effect of the converter on the prediction performance of the different models. **Figure 7-8** shows prediction performance of the different models when they work with the actual converter circuit instead of the controlled current source. It can be seen that the performance is not compromised and the decision to replace it with controlled current source is validated.

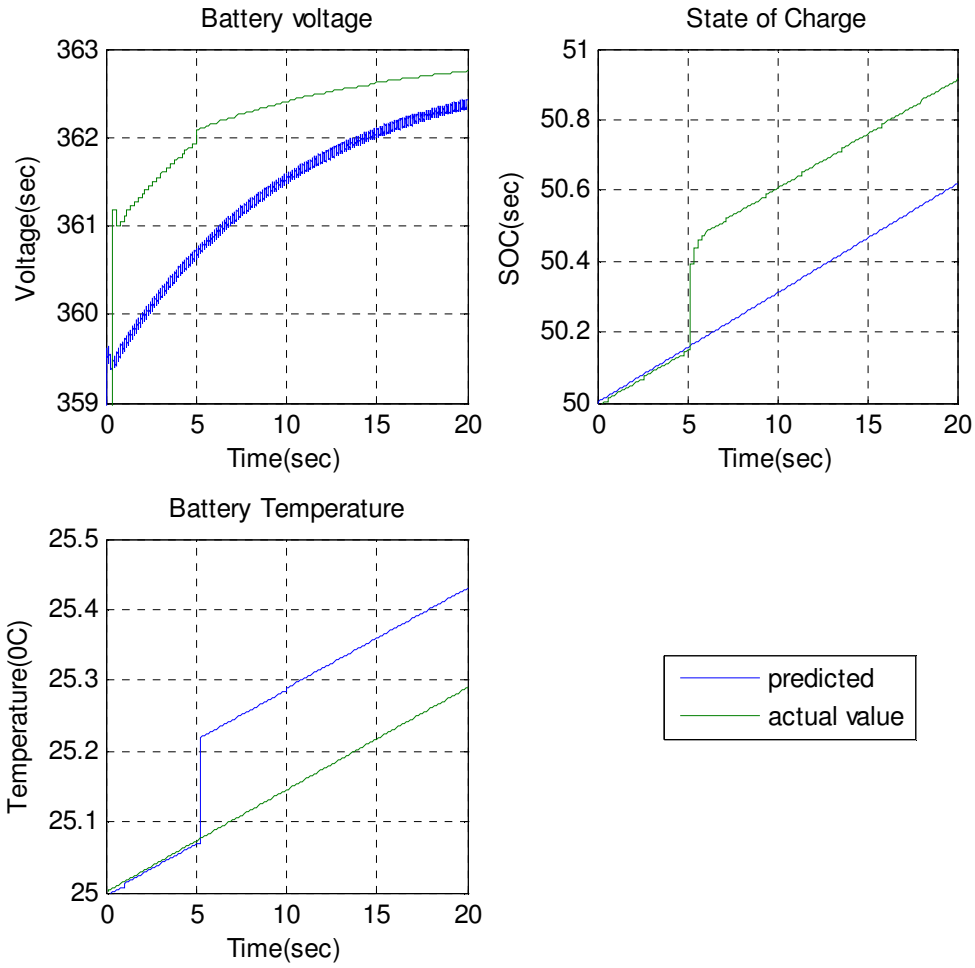

Figure 7-8 prediction performance of the different models when working with the charging circuit

7.2.1.2 Identified parameter consistency

- Parameters for voltage current relation:

  In parameter estimation, as specified previously, initial parameters affect the ultimate result if the objective function happens to have several local minima. Moreover the larger the number of parameter the greater is the possibility to have several local minima. In parameter estimation for V-I battery model the parameters are relatively many. Therefore there we see parameter variation. This most visibly seen in parameter which have less effect on V-I relation in time range we are working in, that is Cb. The rest are comparatively constant. This is enough as far as our aim is concerned. We only need to be able to predict the voltage correctly that is all. Moreover there are no real capacitors or resistors in a battery to whose value we can check.

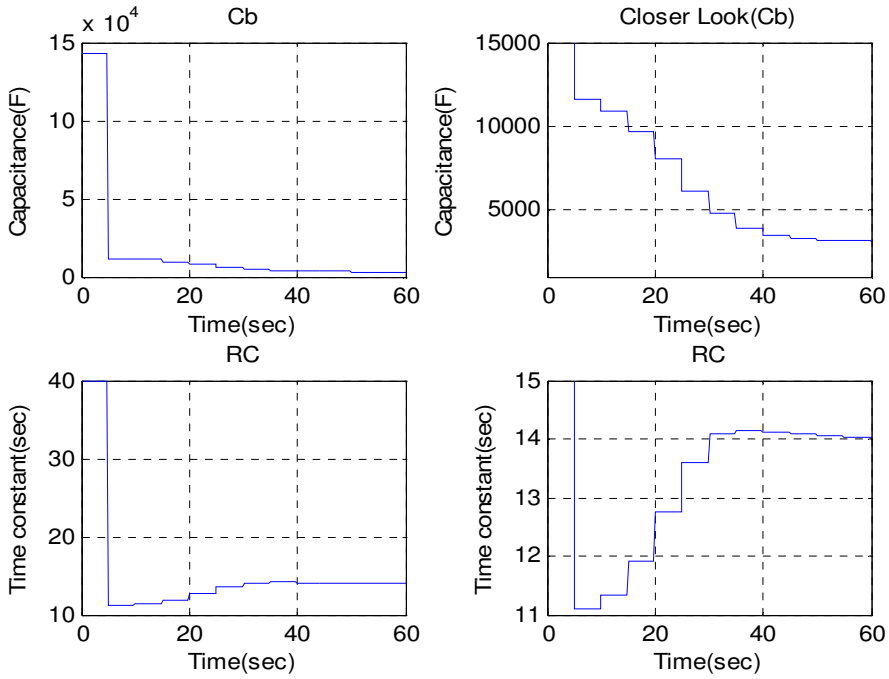

Figure 7-9 battery V-I model parameters

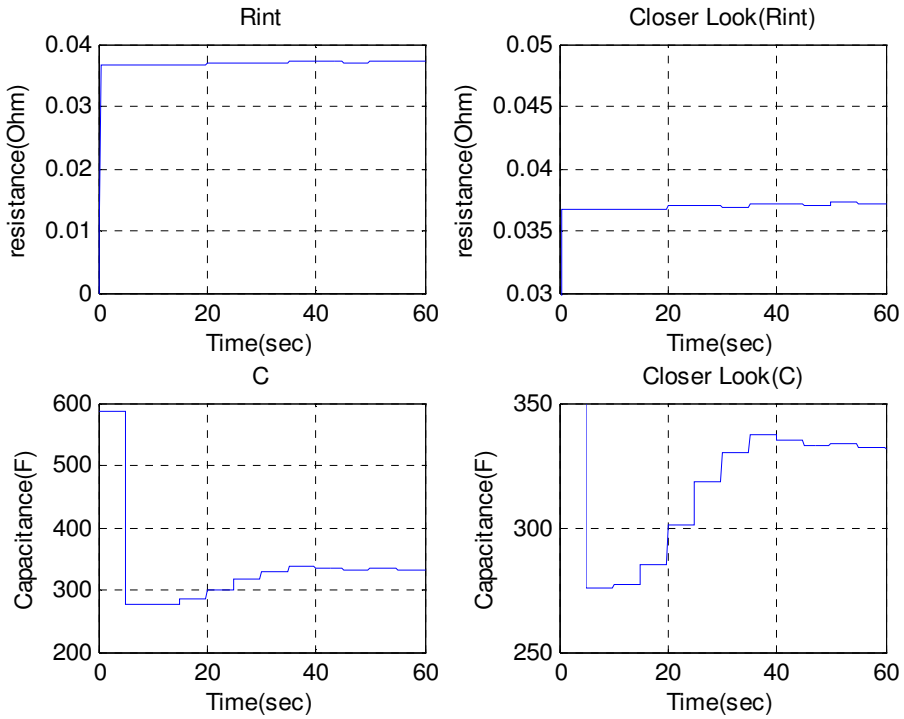

Figure 7-10 Battery V-I model parameters (continued)

- Parameters for SOC monitoring: - here although the model parameters are two: columbic efficiency and capacity, as seen in section 3 they are numerically indistinguishable. Therefore one parameter is fixed at a given value the other is optimized. Thus we fix efficiency at 1 (that is 100%) and optimize the capacity of the

battery C_b. Moreover since this is a linear model, linear solver is used to optimize the parameter.

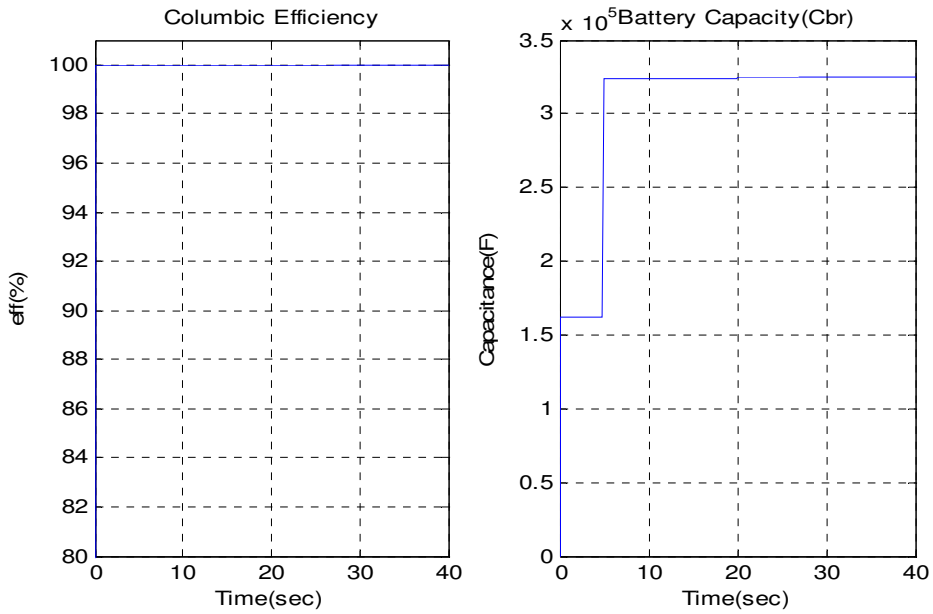

Figure 7-11 SOC model parameters

- Parameters for temperature monitoring

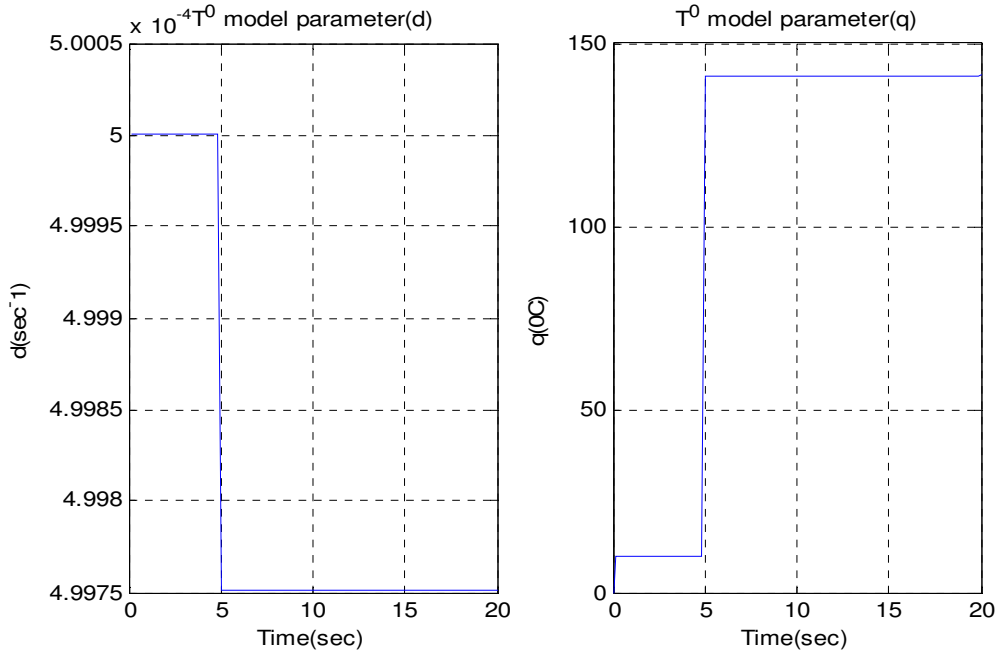

Figure 7-12 Thermal Model Parameters

From the above figures the overall impression is the parameters are well identified. Besides, lower number of parameters will result in a more or less constant value for the identified parameters.

Next an analysis of the performance each routine will be presented.

7.2.2 SOC Validation and monitoring

The first task of this routine is validating the SOC measurement values. It uses the error between model-predicted values and measurement values to accomplish its task. The error threshold is selected based on our expectation of the noise level. However the prediction performance is only good at much lower noise levels. Here it has to be noted that the time range we are working in affects the noise rejection capability of the routine. In longer time ranges, it easier to see how the SOC trajectory is moving better than in shorter time ranges. ´

To see the noise rejection capability of the routine a white noise is added to the measured SOC level. Then error for various noise power levels calculated and the prediction capability of the routine is checked. Based on the way the error is calculated in the routine an error value beyond 0.1% indicates that the routine is not appropriately predicting. The following figure shows the different signals for error level of around 1% (left) and 0.1% (right).

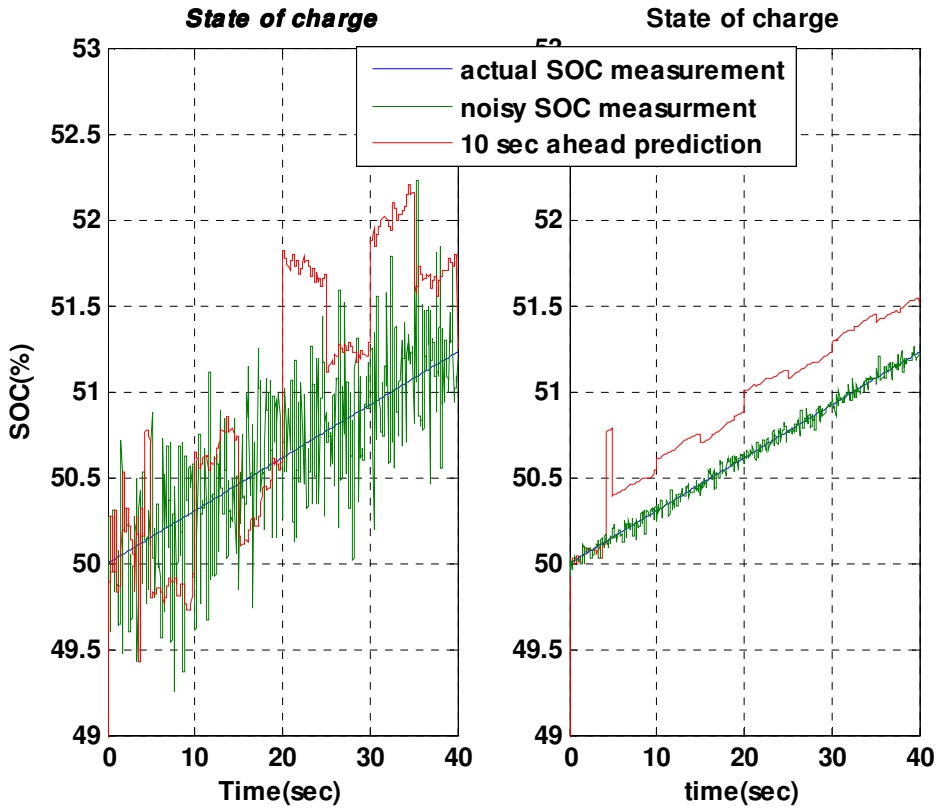

Figure 7-13 state of charge prediction

From the figure in the left it can be seen that in a sample data taken for 5 sec or 10 sec it is difficult to anticipate the trajectory of the SOC but in longer time ranges it could be done. Therefore for better noise rejection capability of the routine, besides using filters, it is recommended to increase the time window which is used by the routine.

The rest of the routines task is providing the status signals therefore it discussed in the next subsections by creating scenarios.

7.2.3 Terminal voltage monitoring

This routine is responsible for keeping in check of the battery voltage limit. For the model we working with the voltage limit is 385V.

Scenario I: SOC measurement is correct and the voltage limit reaches while the BMS does not take action (the BMS malfunctions)!

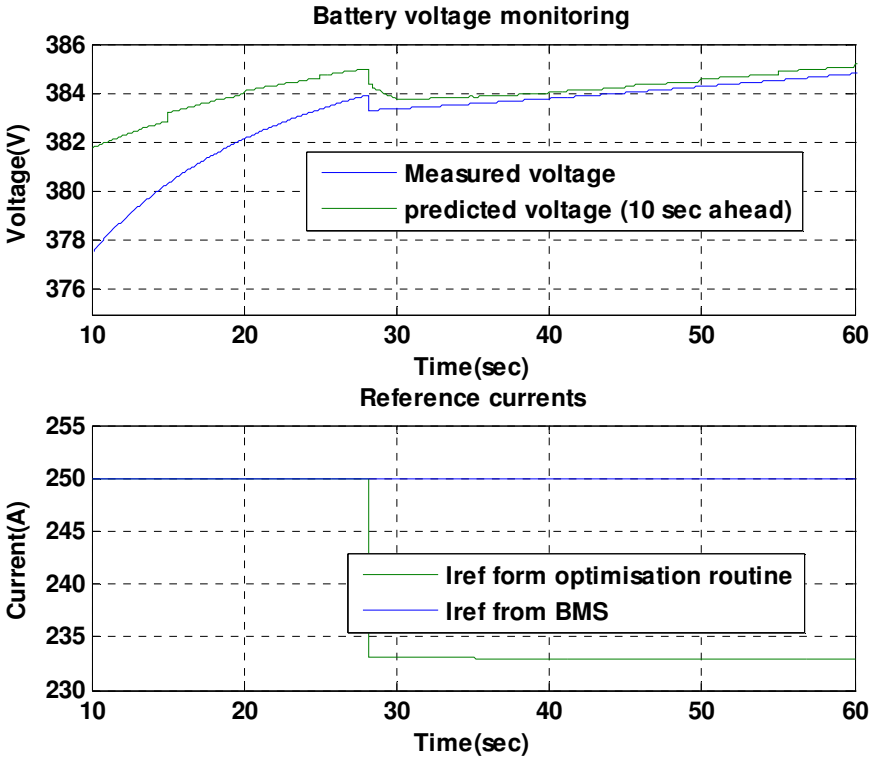

Figure 7-14 voltage monitoring, Scenario I

Scenario II: SOC measurement is correct and the voltage limit reaches while the BMS does take action!

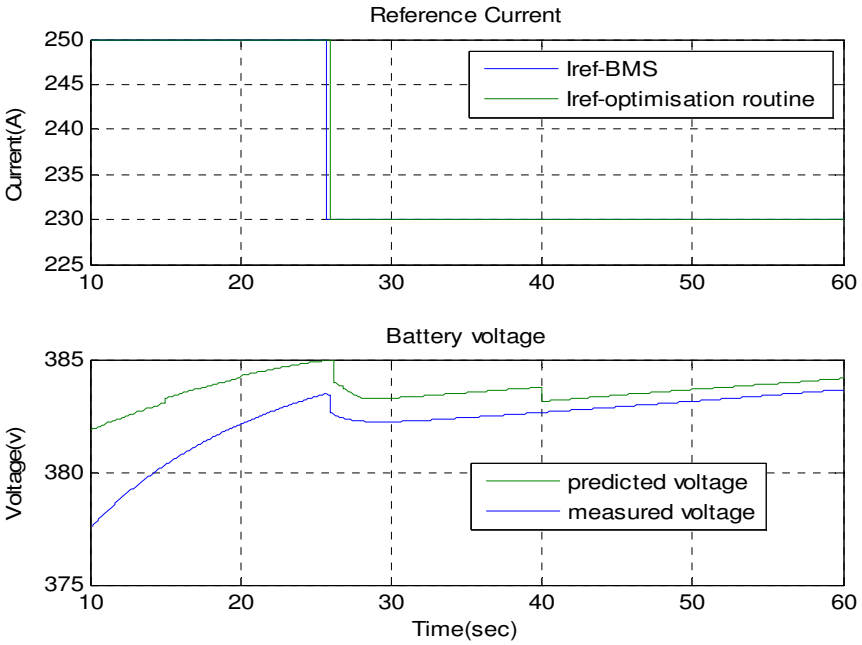

Figure 7-15 voltage monitoring, Scenario II

Scenario III: SOC measurement is correct and the voltage limit reaches while the BMS does take action but it is a bit late!

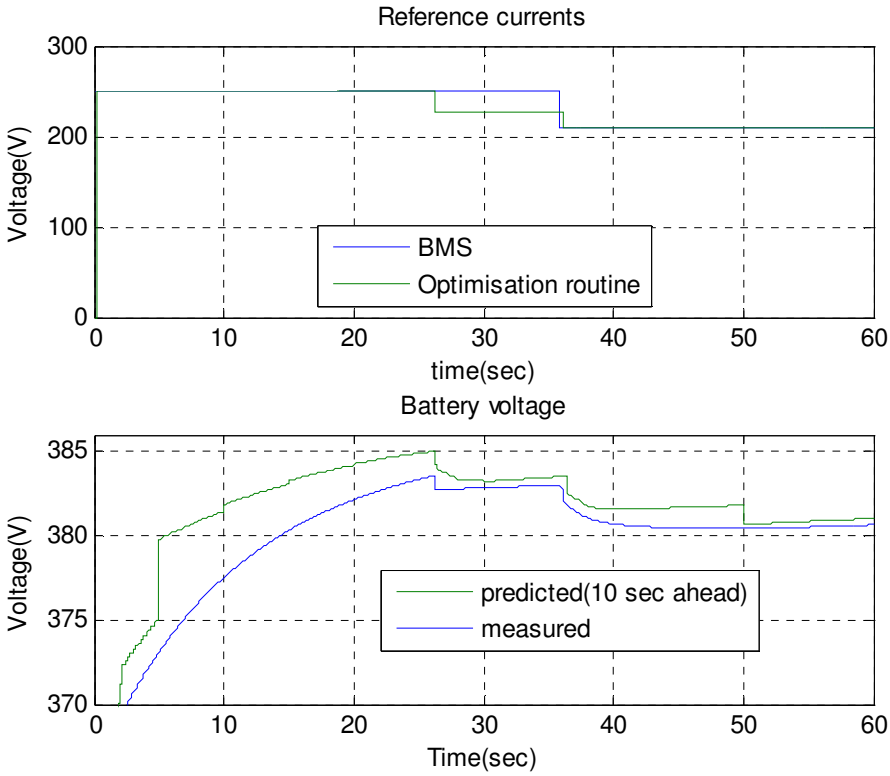

Figure 7-16 voltage monitoring, Scenario III

In Figure 7-16 the optimization routine acts in time and reduces the current to avoid voltage limit violation then the BMS reduces the reference current, then we take the minimum of the two from safety consideration point of view.

Scenario IV: SOC measurement is incorrect and the voltage limit reaches: in this work it is decided that the charging process should be ended; as there is no way to tell when the required level of SOC is reached. Of course this more probably results in premature charge interruption. But it is a necessary measure to avoid possible battery overcharging and damage.

7.2.4 Temperature validation and monitoring

Similar to the SOC validation and monitoring, the prediction is reliable in almost noise free environment. It also depends on the thermal time constant the battery system and the time window we are working with. Figure 7-17 shows the result for noisy environment. As it can be seen the noise level is very low but if the noise level is increased it could result in unacceptable results. Moreover the initial parameter values for the optimization will affect the actual performance. The parameters values should be as much as possible close to their actual value. At least we need to have an Idea on what the thermal time constant could be. In addition, we can see that in length of time window we are working in a

linear model with one parameter could work as accurately as the nonlinear model; and even better, since we have to optimize only one parameter.

On the other hand, as far as validation is concerned we can decide the error threshold based on our expectation of the noise level there, and use Kalman filter to get better temperature readings.

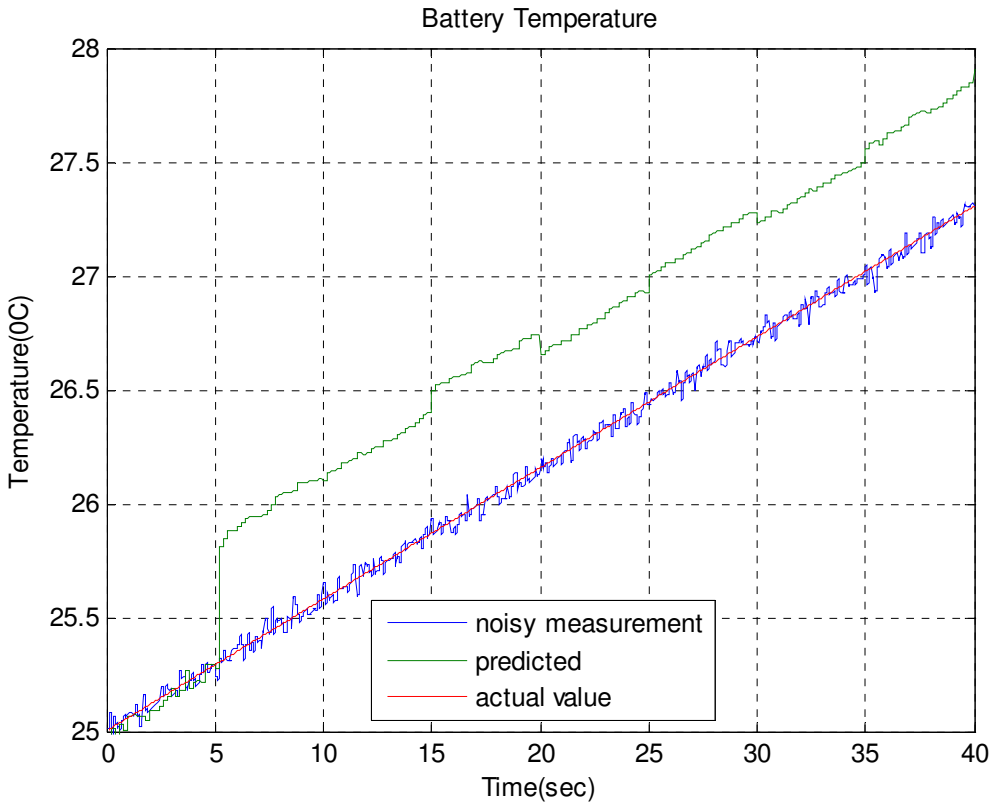

Figure 7-17 Temperature Reading Validation

Now let us see how the routine reacts when temperature limit is reached. The temperature limit is 45^0C. We take the battery and ambient temperature to be initially at 42^0C to reduce the simulation time.

The routine takes action based on its predicted temperature 10 sec ahead if it happens that after 10 seconds the temperature limit will be reached the routine takes action in time; making the charging process more safer. In this report, what is done is to halve the charging reference current to culminate the temperature rise. But if the BMS happens to reduce the current reference, then the charging current reference will follow that of the BMS's.

Scenario I: when temperature limit is reached and the BMS did not take action (the BMS malfunctions)!

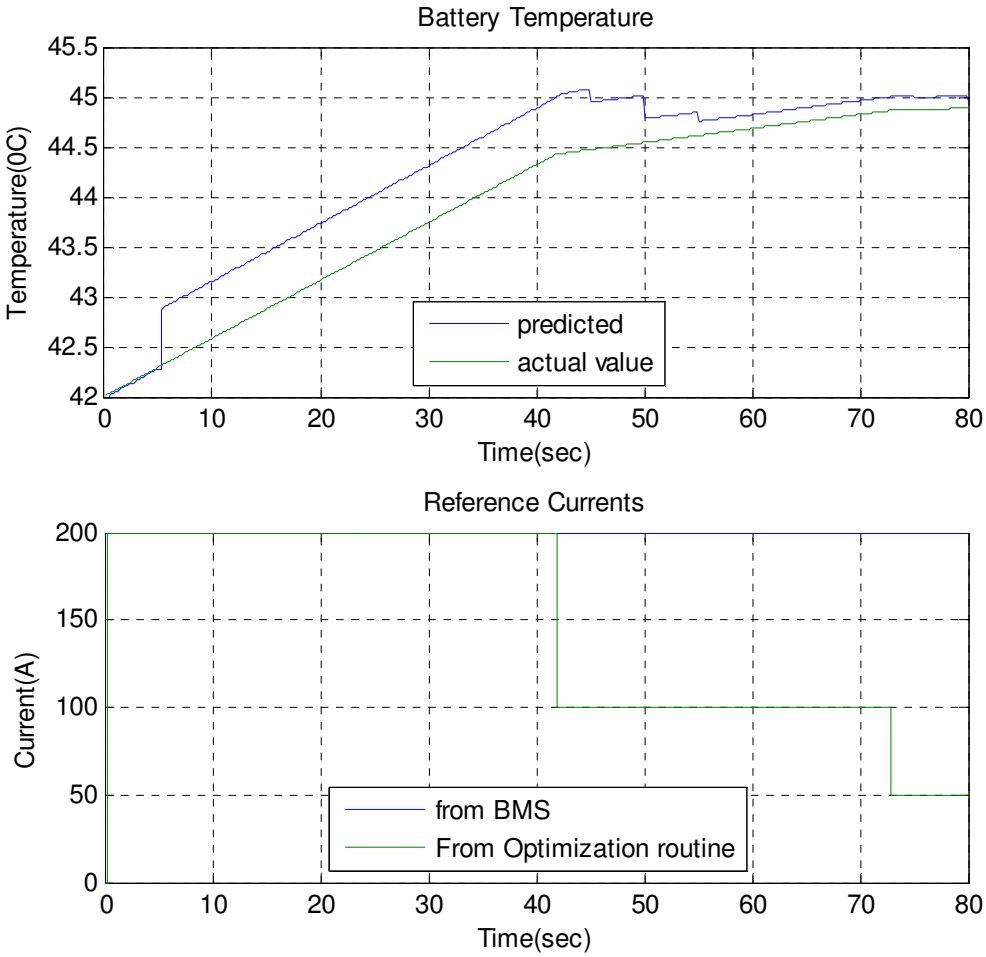

Figure 7-18 Temperature monitoring, Scenario I

We see the limit reaches twice consecutively as the result the current reference is halved twice.

Scenario II: when temperature limit is reached and the BMS did take action a bit latter

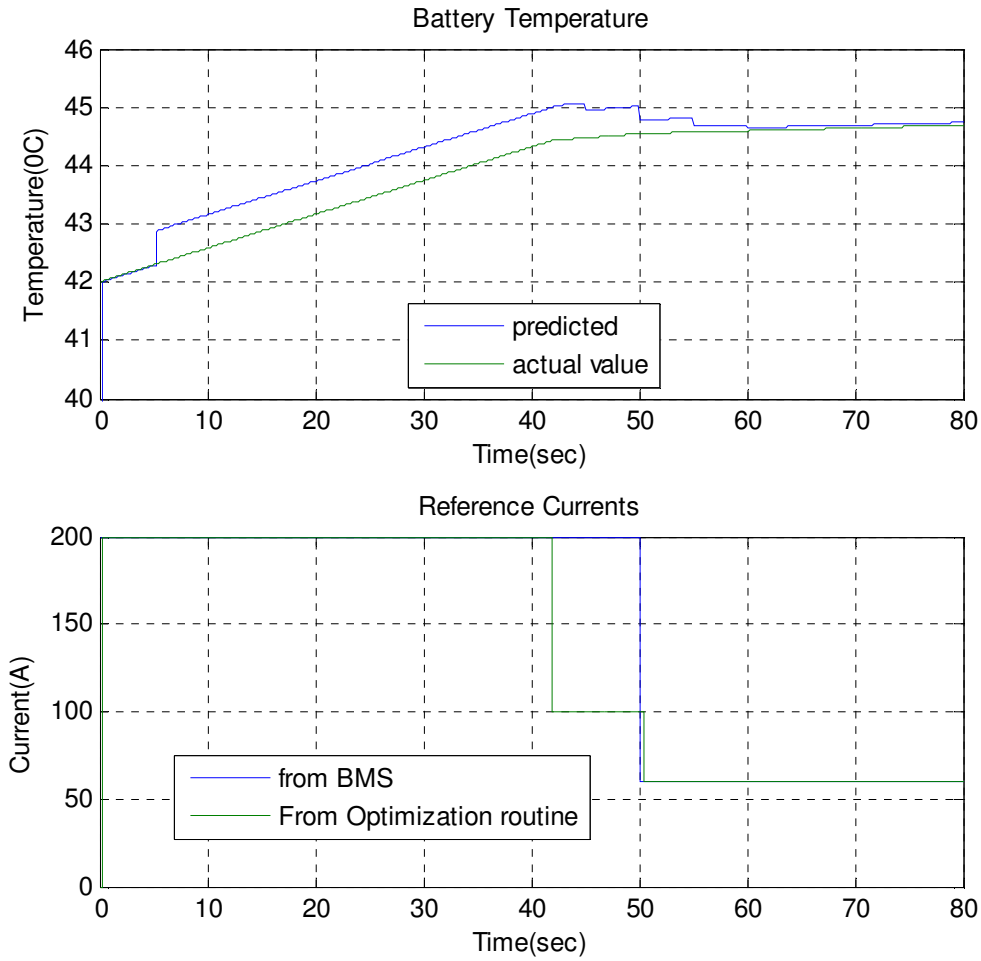

Figure 7-19 Temperature monitoring, Scenario II

Here the temperature is reached the BMS have not taken action; the TMR decreases the reference current. Then the BMS takes action and reduces the reference current and the TMR follows.

Scenario III: when temperature limit is reached and the BMS did take action in time.

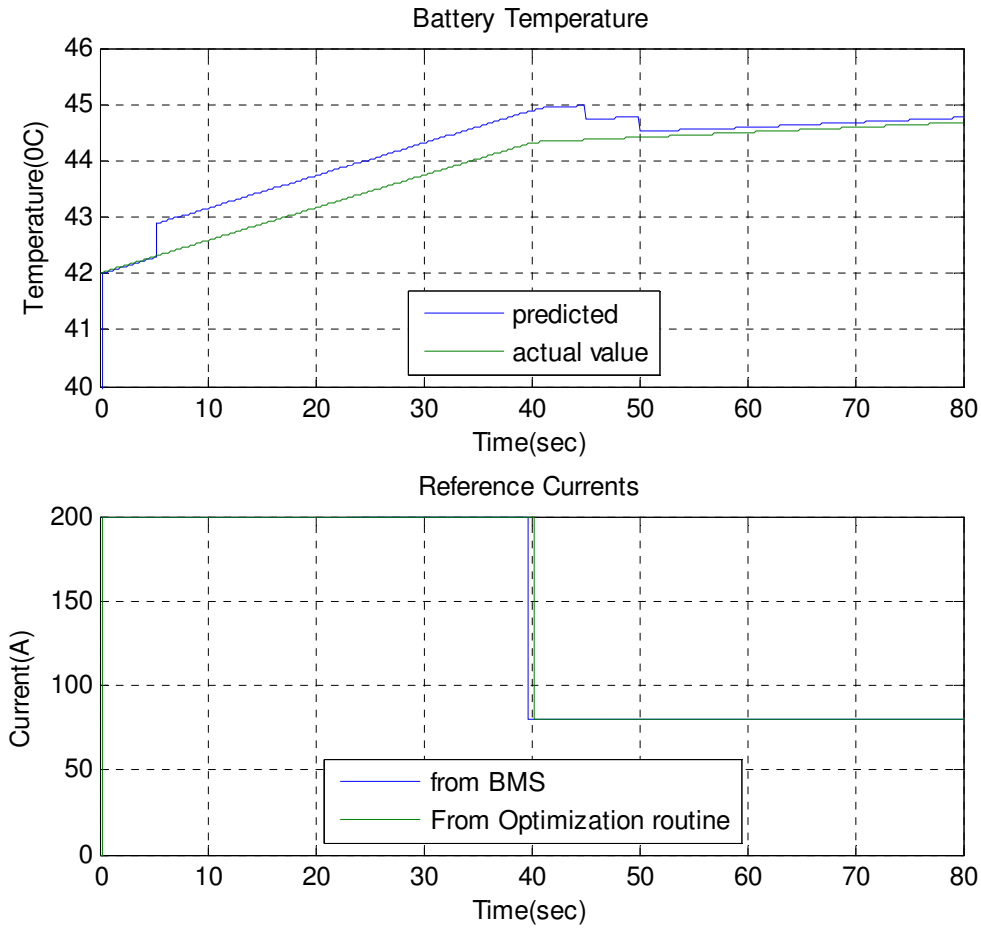

Figure 7-20 Temperature monitoring, Scenario III

7.2.5 Minimum current Generation Routine

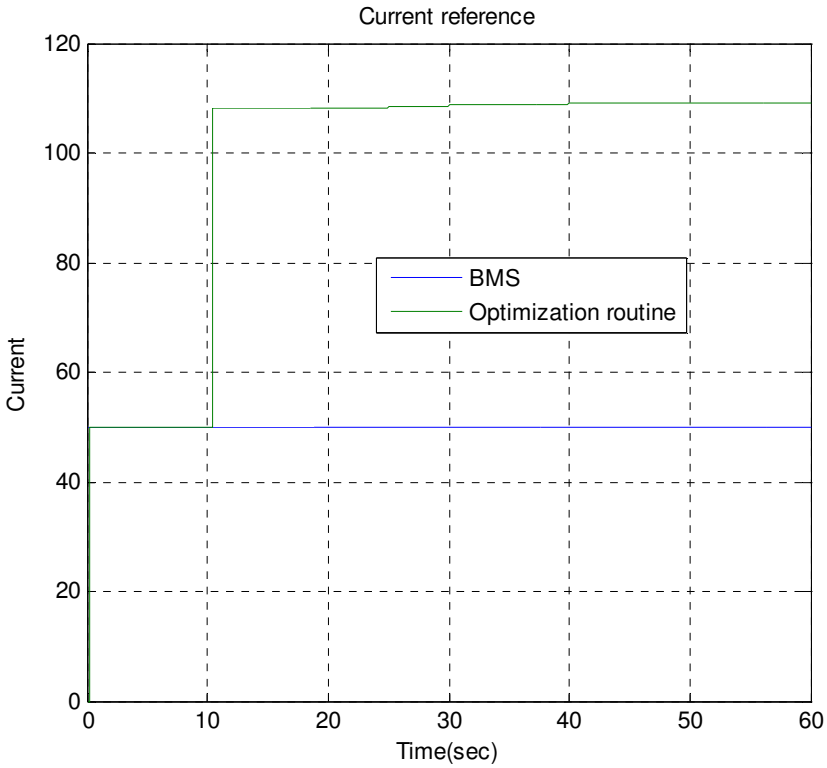

Figure 7-21 Minimum Current calculation

Here the charging current from the BMS is low compared to the capacity of the battery. And it takes unreasonably long time when fast charging is considered. Therefore the routine calculates the minimum current which results in the required charge level within the time slot of fast charging.

7.2.6 Output reference current coordination

In this section we will see how the reference current generation routine (RCGR) will end the charging process. It is seen above how well RCGR has coordinated the orders from the different routines. Let us see how it handles the double event: reaching voltage limit and end of charge. The end of charge is reached when SOC is 85%.

Figure 7-22 shows the case when first the voltage limit is reached where by the current is reduced then the maximum SOC level is reached which ends the charging process.

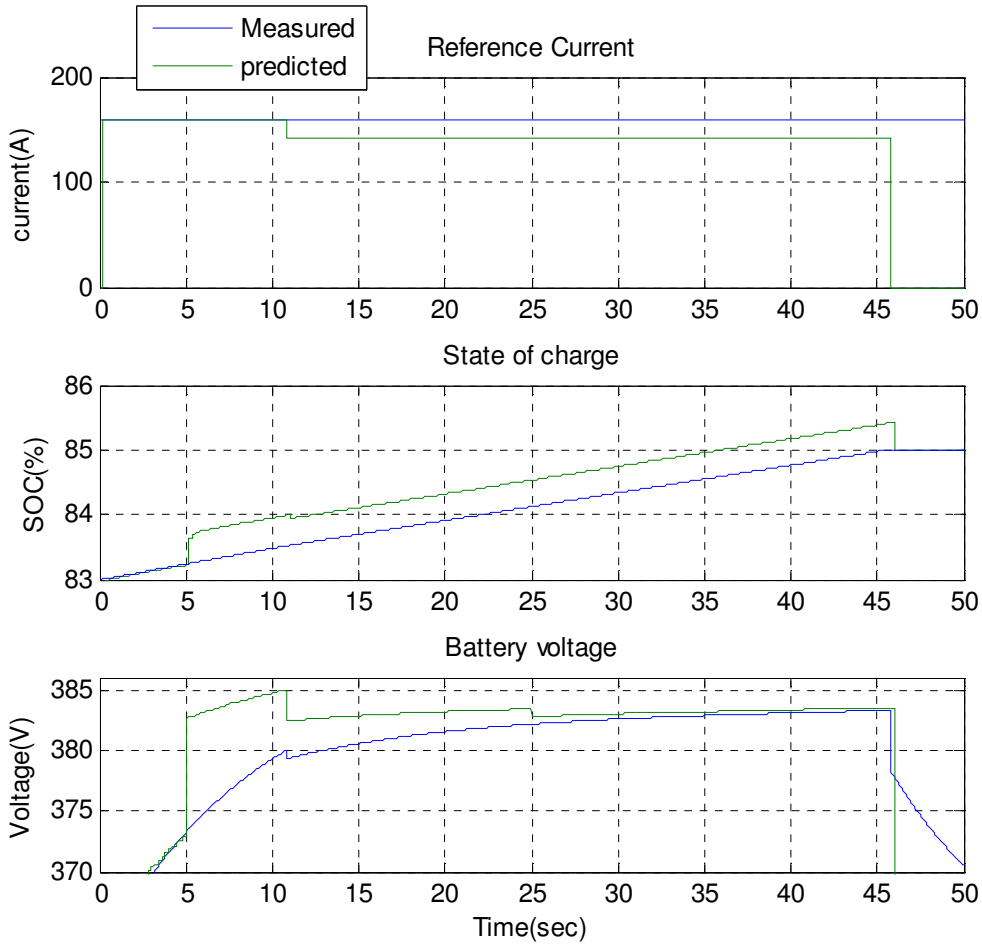

Figure 7-22 Voltage limit and end of Charging

8 CONCLUSIONS

In this thesis a charge supervisory algorithm has been developed for an off-board battery charger. Unlike many off-board battery chargers, a charger which is equipped with this algorithm will be able to take some crucial decisions independent of the BMS whenever it is necessary. This results in safe and reliable charging process.

The algorithm uses three important models to facilitate its decision making:

- Battery V-I characteristic model
- Battery SOC model
- Battery thermal model

The model parameters are identified using the data collected during the charging process. The identification process uses for nonlinear models the LM method and linear solvers for linear models. In case of nonlinear models, it is found that using constrained optimization provides a better result in terms of prediction performance and consistency of the parameters. The optimization routine is executed after a specified time of interval. Executing the routine every sample interval is both computationally intensive and unnecessary as only slow parameter variation is expected. However for better accuracy we have to make use of each sampled data. This is accomplished through the use of the recursive Kalman filter which is executed during each sampling interval. This will counteract errors that occur due to modeling and measurement.

On the other hand before accepting the new optimized parameters the error of the objective function is checked and if it is above a given threshold the old parameters are maintained until the next routine. The convergence problem occurs when the collected data are not well conditioned.

The supervisory algorithm works well provided that the simplifying assumptions given in section 6 holds true. These assumptions are necessary due to the versatility of the battery system and without those assumptions it is difficult to carry out the objective of the thesis.

All in all, the algorithm is composed of six main routines which carry out specific tasks and communicate to each other through parameters and status information. These routines are

- Model Identification routine (MIR)
- Battery Voltage Monitoring Routine(BVMR)
- SOC Monitoring Routine(SOCMR)
- Temperature Monitoring Routine(TMR)
- Minimum Current Generating Routine(MCGR)
- Reference current Generating Routine(RCGR)

MIR is the routine which optimizes the model parameters as mentioned above. BVMR takes care of the battery voltage limit. It ensures in no time during the charging process the battery voltage limit is violated. It predicts the future value of battery voltage based on the current states and battery V-I model. A Kalman filter is used to get correct current states which will result in a correct future battery voltage prediction. During the work it is found that the accurate parameter tuning of the Kalman filter is very important to get satisfactory battery voltage prediction.

SOCMR checks the SOC readings for correctness or consistency and predicts the future value of SOC if they are found to be correct. Then it provides information to other routines about the present and future status of the SOC. The SOCMR checks the readings for correctness based the error between model predicted value and measured value. If the error is found to be above a given threshold the SOC readings are said be incorrect. The error threshold is selected based on our expectation of the noise level which the algorithm is expected to encounter.

However the SOC prediction could be corrupted in an environment where the noise level could be considered reasonable. This happens if the time window during which the algorithm is working on is short or the rate of change of SOC is relatively slow. Thus there are two possible solutions in dealing with this problem. Filters and longer time windows could be used to suppress noises. On the other hand predicting SOC unlike battery voltage and temperature is less important. Thus it can be avoided without having any effect on the performance of the overall algorithm. Hence the most important task of this routine is checking if the readings are correct or not and providing the present status of the SOC to other routines.

TMR is entitled to make sure that the temperature readings are correct and predict the temperature a specific time ahead to avoid any possibility of reaching temperature limit. If it is found that the temperature limit will be reached after a given time, then the charging current is reduced in time to reduce the temperature rise.

Unlike other models, due to the scarcity of the information on this part, thermal modeling seems to be over simplified. Similar to the SOC prediction, temperature prediction is considerably affected by noise. Similar solutions as for the SOC prediction can apply. However unlike SOC prediction, temperature prediction is important.

On the other hand, in the simulation the thermal time constant of the battery appears to be low, this is because we want to see the prediction capability and the various events more clearly as mentioned above. However the actual time constant is much longer. And this would have been in favor of going for longer time window to get better noise rejection. However, the rate of rise of temperature is usually very low; the noise might make it difficult to predict the temperature trajectory. In that respect, temperature prediction is more important whenever something goes wrong in the battery system the rate rise of the temperature is noticeable. This could be that the charging current is too high or any other reasons that could result in rapid temperature rise in the battery system. However, in normal situations it is enough to validate the readings in which case a linear model with one parameter is preferable as it will have better numerical stability and less computational burden.

MCGR is responsible to for deciding the minimum current that should be delivered to the battery at normal conditions. This routine along with other routines make sure that the charging time will not be unreasonably long. It ensures that all batteries will be charged to the required level in the time frame of fast charging. In this report the time taken is 30 minutes. This time could be decreased as more information on charging capability of actual EV batteries is known.

Finally the RCGR chooses the appropriate reference current from the reference currents generated by the routines mentioned above based on the status information supplied by them.

9 FUTURE WORK

Various future works based on improving this work or using the same concept to apply it for other similar areas could be proposed. To improve this work and to make it practical the following things need to be done.

Carry out Laboratory experiments to understand and decide

- Effect of measurement noise on the algorithm; both in parameter identification, and validation and prediction
- The best prediction horizon, sample time and sample length
- The exact thermal time constant of the battery and the nature of temperature rise.

The routines could be improved and additional features could be added if more practical problems that face the BMS are known. Most of the problems discussed in this thesis are hypothetical, such as incorrect measurements values form the BMS, occurrence of low current references from the BMS. Of course these problems could occur but there is no practical information on them.

It will also be possible to fix the maximum current for a given battery if the worst case charging efficiency of Batteries are known; where the inefficiency is due to the voltage drop on the internal resistance. Or provided that a minimum charging time exists, we can fix the maximum charging current for a particular battery.

In this thesis the optimization routine is executed every 10 sec interval but it is possible to execute it only when the error in the objective function is above a certain value say 1e-2. This could result in a more computationally efficient approach.

Concerning applying the same principle in other areas, for example, for a single battery as in a BMS, actual, meaningful parameters could be determined experimentally and variation in specific parameter can be attributed to specific condition. For example, cold cranking, capacity fading etc. Thus the online optimization algorithm could play an important role in this area. This same principle is used in [10] and [20] for lead acid battery.

10 APPENDIX

Appendix A: The LM method

A.1 How is the initial μ value selected? How is not know in the solution is far from or near to the final solution? Then how is μ updated?

According to [26], the initial value μ_0 is

$$\mu 0 = \tau * max_i\{a_{ii}{}^{(0)}\}$$

10-1

Where

$$a_{ii}{}^{(0)} = diag(A_0 = J(x_0)^T * J(x_0))$$

10-2

Where τ can be any value between 1 and 1e-6 depending on how far the initial parameter values are from the final value. For good initial guess it is 1e-6 [26].

After each iteration μ is updated as follows:

Given f(x+h) as in **Fel! Hittar inte referenskälla.**, where in this case $h = h_{lm}$

$$F\ (x + h_{lm}) \cong L(h) = \frac{1}{2} * l(h_{lm})^T l(h_{lm})$$

$$L(h_{lm}) = \frac{1}{2} * f^T f + h_{lm}{}^T J^T f + \frac{1}{2} h_{lm}{}^T J^T J h_{lm}$$

$$= F(x) + h_{lm}{}^T J^T f + \frac{1}{2} h_{lm}{}^T J^T J h_{lm}$$

10-3

The updating is controlled by the gain ratio which gives us an indication to how far from the final solution we are. This is given by:

$$\varrho = \frac{F(x) - F\ (x + hlm)}{L(0) - L\ (hlm)}$$

10-4

From 4-11 and 10-3

$$L(0) - L\ (hlm) = \frac{1}{2} h_{lm}{}^T (\mu hlm - g)$$

10-5

If ϱ is small (may be even negative), then L (h_{lm}) is a poor approximation, and we should increase μ with the two fold aim of getting closer to the steepest descent direction and reducing the step length. In [26] the following is algorithm is used

$$if\ \varrho > 0, \mu = \mu * max\left\{\frac{1}{3}, 1 - (2\varrho - 1)^3\right\}; v = 2$$

$$else\ \ \mu = \mu * v, v = 2 * v$$

10-6

A.2 Any Iterative process needs stopping criteria. Then what are the stopping criteria for this process?

Well, there are three stopping criteria [26] based on different requirements on involved parameters.

The global minimizer should reflect that F'(x*) =g(x*) =0, therefore it is required that the maximum in norm of g i.e. $\|g\|_\infty$ should as low as a given low value ε_1

$$\left|\left|g\right|\right|_\infty < \varepsilon_1$$

10-7

Another relevant Criterion is to stop if the change in x is small

$$\left|\left|xnew - x\right|\right| \leq \varepsilon_2\left(\left|\left|x\right|\right| + \varepsilon_2\right)$$

10-8

The final stopping criterion is the number of maximum iteration

$$k \geq kmax$$

10-9

More information can be found at reference [26] and its Matlab implementation can be downloaded from the author's website http://www2.imm.dtu.dk/~hbn/Software/.

APPENDIX B: MATLAB FILE DOCUMENTATION: THE INTELLIGENT CHARGER TOOLBOX

All in all this is just a rough introduction to the role of individual functions defined in different M- files, for the actual implementation and further information consult the model files and M-files where the function is defined.

The overall Matlab files can be grouped into two categories

Those involved in with the converters only; without the supervisory algorithm(Converter related files)

Those which deal with the charging circuit along with the supervisory algorithm (SA)(SA related files)

Let us see them one by one.

B.1 Converter Related Files

The user can use this simulation files to study the different characteristic of the converter circuit. The files are only 'mdl' Matlab files, the different parameter values used in them are defined in file > model properties > call backs > InitFcn. The files include

Buck_Boost.mdl:- which is the simulation model of the Buck-Boost converter along with its control circuit.

VSC_BuckBoost_Approach_I.mdl:- this is a simulation model of the whole charger circuit including the VSC, Buck boost converter and their control system. In this simulation model the starting mechanism mentioned as approach I in section 5 is used

VSC_BuckBoost_Approach_II.mdl:- is similar to the above model but the starting mechanism described as approach II in section 5 is implemented in this model

B.2 SA Related Files

These files simulate and can be used to study the performance of the SA algorithm. These contain both 'mdl' and M- Matlab files. These files are comparatively numerous. We have two 'mdl' files from where the simulation is launched:

Intelligent_Charger_CCS.mdl:-Here the controlled current source is used in place of the charging circuit

Intelligent_Charger_Buck_Boost.mdl:- In here the buck-boost DC/DC converter is used to simulate the charging circuit.

From the mdl files the OptMF () S-function is launched.

B.3 The Main Optimization Function (Optmf () Function)

B.3.1 General

This is an S-function from which the different routines are called and coordinated. It samples the measured data at user specified sample interval and stores user specified sample length data. The measured data includes battery current, voltage, temperature and SOC. This data will be used for building the different models and making decisions whenever necessary. It also accepts information and requests related to the battery. The information includes the maximum voltage and temperature, and the start signal while the request is the amount of charging current it should provide. It outputs the optimum reference current to the battery and the different information signals to the user. This information signals include the model parameters for each model, the predicted battery voltage, temperature and SOC level.

Inside the S-function

The main tasks carried out inside the S-function are

Initialization

This initialization can be seen in two ways:

S-function initialization: - this includes determining the number of inputs, output and state variables. This is done in 'mdlInitializeSizes' which usually the case in S-functions.

Simulation variable initialization: this includes initializing model and other parameters. This initialization is done inside mdlUpdate function. The model parameter initialization is carried out by calling prepare_data() function.

Model Parameter Optimization

This part is responsible for calculating the model parameters and is executed at an interval which is set by the user. Different set of functions are involved in parameter identification of each model.

Functions involved in parameter identification of V-I battery model:

A good approximate value of the internal resistance could easily be found whenever a step in current occurs. Using this value, the rest of parameter identification can be done using SMarquardt_M() function.

The 'SMarquardt_M.m' M-file: - this function is taken from http://www2.imm.dtu.dk/~hbn/Software/ is slightly adapted to problem at hand. A call to SMarquardt_M(), provided that enough data is gathered, will optimize the parameter of the battery V-I model. This function gets the measured data, a vector which contains algorithm related values and the initial values of the battery V-I model parameters. The model parameters are passed as structure of matrices. This function uses the help of the following functions to carry out its duty.

The 'extract.m' since the actual optimization works in parameter vectors rather than matrixes. Thus 'extract.m' extracts parameter vectors that need to be optimized from the matrix passed to SMarquardt_M ().

The 'subopt_M.m' M-file: - this is where the objective function for V-I battery model is defined.

'update_mat.m' once the parameters are optimized, the original matrices of the model are updated using the update_mat () function.

Functions involved in parameter identification of SOC of the battery model:

The 'soc_par.m' M-file: - a call to soc_par () with appropriate inputs will optimize the SOC model parameters of the battery.

Functions involved in parameter identification of thermal model of the battery:

The 'Tdq_par.m' M-file: - a call to Tdq_par() with appropriate inputs will optimize the thermal model parameters of the battery. The following two functions are called within this function to carry out the task.

temp_es(), found in temp_es M-file, is the function where the objective function for this model is defined.

SMarquardt, found in SMarquardt M-file, uses the objective function along with other data and algorithm related inputs to solve the problem of optimizing the model parameters.

i) Battery Voltage Monitoring

This part uses Kalman filter to adjust the current states in the model, predicts the battery voltage, and calculates the suitable reference current whenever the predicted voltage is found to be above the voltage limit.

For predicting the future state there by the future battery voltage it uses the function predict_st() found in predict_st.m M-file.

To calculate the suitable reference current whenever the predicted voltage goes above the limit it uses the function cal_Iin() found in cal_Iin.m M-file.

ii) State Of Charge Monitoring

This part of the S-function takes care of SOC related issues; checking the correctness of the SOC provided, predicting the future value, providing the status information to other routines. This all is accomplished by calling the function soc_routine(). Inside the soc_routine function soc_check() is called to calculate the error between the measured and predicted SOC values which then can be used to validate the reading.

iii) Battery Temperature Monitoring

Here a call to temp_routine() function is made to carry out all the tasks necessary for temperature monitoring. Inside the routine temp_es() is called to calculate the error in the objective function which then can be used to validate the temperature readings.

The remaining part of the mdlUpdate function contains calculates the minimum current for a given battery as described in section 6 and produces the appropriate reference current to the converter. Finally the different parameters computed are prepared to be outputted. The outputting is done by mdloutputs function which is usual the case in S-functions.

11 REFERENCES

[1] Charles Botsford. Adam Szczepanek 'Fast Charging vs. Slow Charging: Pros and cons for the New Age of Electric Vehicles' EVS24 International Battery, Hybrid and Fuel Cell Electric Vehicle Symposium, Norway, May 13-16. 2009.

[2] Jonn Axsen, Andrew Burke, Ken Kurani, Batteries for Plug-in Hybrid Electric Vehicles (PHEVs): Goals and the State of Technology circa 2008, Institute of Transportation Studies University of California Davis, CA, may 2008

[3] 'Batteries for Electric Drive Vehicles – –Status 2005 Performance, Durability, and Cost of advanced Batteries for Electric, Hybrid Electric, and Plug-In Hybrid Electric Vehicles,' EPRI technical report 2005

[4] Nickel-Metal Hydride Application Manual-Energizer

[5] NiMH handbook, Panasonic

[6] 'Evaluation of Emerging Battery Technologies for Plug-in Hybrid Vehicles' EPRI final report 2009

[7] USABC Goals for Advanced Batteries for EVs

[8] 'Lithium Ion Technical Manual' Tayloredge electronics services

[9] Lijun Gao, Shengyi Liu, Member, IEEE, and Roger A. Dougal, Senior Member, IEEE, "Dynamic Lithium-Ion Battery Model for System Simulation," IEEE transactions on components and packaging technologies, vol. 25, no. 3, September 2002

[10] Peter in 't panhuis, "Master's Thesis on Li-ion Battery Modeling," Technische Universiteit Eindhoven, Department of Mathematics and Computing Science, January 2005

[11] Min Chen, Student Member, IEEE, and Gabriel A. Rinc´on-Mora, Senior Member, IEEE, "Accurate Electrical Battery Model Capable of Predicting Runtime and I–V Performance," IEEE TRANSACTIONS ON ENERGY CONVERSION, VOL. 21, NO. 2, JUNE 2006

[12] M.R. Jongerden and B.R. Haverkort, "battery modeling"

[13] Daler Rakhmatov, Member, IEEE, Sarma Vrudhula, and Deborah A. Wallach, "A Model for Battery Lifetime Analysis for Organizing Applications on a Pocket Computer

[14] Cun, J.P.; Fiorina, J.N.; Fraisse, M.; Mabboux, H. " the experience of a UPS company in advanced battery monitoring," in Telecommunications Energy Conference, 18th international, pp. 646–653, 6-10 October 1996.

[15] Ryan C. Kroeze, Philip T. Krein, "Electrical Battery Model for Use in Dynamic Electric Vehicle Simulations," University of Illinois ©2008 IEEE

[16] Olivier Tremblay, Member IEEE, Louis-A. Dessaint, Senior Member IEEE, and Abdel-Illah Dekkiche Electrical Engineering Department, Ecole de Technologie

Superieure, "A Generic Battery Model for the Dynamic Simulation of Hybrid Electric Vehicles," 2007 IEEE

[17] Kandler Smith, Chao-Yang Wang 'Power and thermal characterization of a lithium-ion battery Pack for hybrid-electric vehicles', Science direct Journal of Power Sources 160(2006)662–673 Feb. 2006

[18] Siavash Zoroofi, Master's Thesis On "Modeling And Simulation Of Vehicular Power Systems" Chalmers University Of Technology, Göteborg, Sweden, 2008

[19] Lennart ljung (1987), System Identification: Theory for the user, Second edition, prentice-Hall, 1999.

[20] C.R.Gould, C.M.Bingham, Member, IEEE,D.A.Stone, and P.Bentley, New Battery Model and State-of-Health Determination Through Subspace Parameter Estimation and State-Observer Techniques

[21] Michel Verhaegen, Patrick Dewilde, 'Subspace model identification Part 1. The output-error state-space model identification class of algorithms' International Journal of Control, Volume 56, Issue 5 November 1992, pages 1187 – 1210

[22] Mikleš Ján, Fikar Miroslav, 'Process Modelling, Identification, and Control' Springer Berlin Heidelberg, 2007

[23] Tohru Katayama, 'Subspace Methods for System Identification' Springer-Verlag London Limited 2005

[24] Lennart ljung, Torsten Söderstrom, 'Theory and practice of recursive identification' MIT Press (MA), February 1987

[25] Guillaume Mercere, Laurent Bako, Stephane Lecœuche, 'Propagator-based methods for recursive subspace model identification' signal processing page 468–491 science Direct 2008

[26] K.Madsen, H.B.Nielsen, O.Tingleff, Methods for Non-Linear Least Square Problems, 2ndEdition, April 2004, Informatics and Mathematical Modeling Technical University of Denmark

[27] Shidong Shan, A Levenberg-Marquardt Method For Large-Scale Bound-Constrained Nonlinear Least-Squares, Master of Science thesis, The University of British Columbia,2008

[28] Greg Welch, Gary Bishop, 'An Introduction to the Kalman Filter,' Department of Computer Science, University of North Carolina at Chapel Hill, 2006

[29] Sharanya, Jaganathan, Wenzhong Gao, 'Battery Charging Power Electronics Converter and Control for Plug-in Hybrid Electric Vehicle' IEEE, VPPC '09, page 440-447, October 2009

[30] P. Karlsson , M. Bojrup , M. Alaküla , L. Gertmar , 'Efficiency of Off-Board, High Power, Electric Vehicle Battery Chargers With Active Power Line Conditioning Capabilities,' Department of Industrial Electrical Engineering and Automation,

Lund Institute of Technology, Sweden, ABB Corporate Research, Västerås, Sweden, 1997

[31] M. Bojrup, P. Karlsson, M. Alaküla, B. Simonsson, 'A Dual Purpose Battery Charger for Electric Vehicles,' Department of Industrial Electrical Engineering and Automation Lund Institute of Technology, Sweden, 1998

[32] Staffan Norrga, Stephan Meier, Stefan Östlund 'A Three-phase Soft-switched Isolated AC/DC Converter without Auxiliary Circuit,' IEEE Transactions on Industry Applications, Vol. 44, no. 3, May/June 2008

[33] Youssef OUNEJJAR, Kamal AL-HADDAD (IEEE Senior Member), 'New line currents and neutral point balancing technique of three-level three-phase NPC converter,' Industrial Electronics, 2006 IEEE International Symposium, vol,2, page 1436 – 1441, July 2006

[34] J. S. Sivaprasad, Tushar Bhavsar, Rajesh Ghosh And G Narayanan, 'Vector Control Of Three-Phase Ac/Dc Front-End Converter' Indian Academy Of Science, Sãdhanã Vol.33, Part5, pp.591–613, October 2008,

[35] Charles Botsford, Adam Szczepanek 'Fast Charging vs. Slow Charging: Pros and cons for the New Age of Electric Vehicles' EVS24 International Battery, Hybrid and Fuel Cell Electric Vehicle Symposium, Norway, May 13-16, 2009

[36] Michael Lindgren, Jan Svensson, 'Connecting fast switching voltage source converters to the Grid- Harmonic distortion and its reduction,' IEEE/Stockholm power tech Conference proceedings, volume 'power electronics,' page 191-196, June 1995

[37] Marco Liserre, Member IEEE, Frede Blaabjerg, Fellow IEEE, And Steffan Hansen, Member IEEE, 'Design And Control Of An LCL-Filter-Based Three-Phase Active Rectifier,' IEEE Transactions on Industry Applications, VOL.41, NO.5, SEPTEMBER/OCTOBER 2005

[38] Vladimir Blasko, Member, IEEE, and Vikram Kaura, Member, IEEE, 'A Novel Control to Actively Damp Resonance in Input LC Filter of a Three-Phase Voltage Source Converter,' IEEE Transactions On Industry Applications,Vol.33,No.2,March/April1997

[39] Michael Lindgren Jan Svensson, 'Control of a Voltage-source Converter Connected to the Grid through an LCL-filter-Application to Active Filtering,' Power Electronics Specialists Conference, 1998, PESC 98 Record, 29th Annual IEEE

[40] Jong-Woo Choi, Member, IEEE, and Seung-Ki Sul, Member, IEEE, 'Fast Current Controller in Three-Phase AC/DC Boost Converter Using d–q Axis Cross coupling,' IEEE Transactions On Power Electronics, Vol.13, No.1, January1998

[41] Martin Bojrup 'Advanced Control of Active Filters in a Battery Charger Application' Licentiate Theses, Department of Industrial Electrical Engineering and Automation (IEA), Lund Institute of Technology (LTH), 1999

[42] Mohan, Undeland, Robbins, 'Power Electronics Converters, Applications, and Design,' second Edition 1995

[43] Electropaedia: Battery Management Systems (BMS)

[44] Isidor Buchmann, 'Batteries in a portable world: A hand book on rechargeable batteries for non-engineers,' second edition, Cadex Electronics Inc.

[45] Walter A. van Schalkwijk, 'Charging, Monitoring, and Control,' Self CHARGE, Inc Redmond, Washington, Department of Chemical Engineering University of Washington Seattle, Washington, USA

[46] P.-H. Cheng and C.-L. Chen, 'High efficiency and non dissipative fast charging strategy,' IEE Proc. Electr. Power Appl., Vol. 150, No. 5, September 2003

[47] Ahmad A. Pesaran and Matthew Keyser, 'Thermal Characteristics of Selected EV and HEV Batteries' Annual Battery Conference: Advances and Applications, Long Beach, California, January 9-12, 2001

[48] HP 602030 NCA - 45 Ah/ 162 Wh GAIA Cell data sheet